University of Alberta

Phosphatidylethanolamine deficiency in mammalian mitochondria

by

Helin Daniel Bai

A thesis submitted to the Faculty of Graduate Studies and Research
in partial fulfillment of the requirements for the degree of

Master of Science
in
Experimental Medicine

Department of Medicine

Fall 2010
Edmonton, Alberta

Examining Committee

Dr. Jean Vance, Department of Medicine

Dr. Moira Glerum, Department of Medical Genetics

Dr. Thomas Simmen, Department of Cell Biology

DEDICATION

To my parents Barry Bai and Jia Zhu Yang

ABSTRACT

Almost all mammalian cells contain energy-producing organelles called mitochondria. Phosphatidylethanolamine (PE) is a phospholipid which has been implicated to be important for mitochondrial function. The majority of mitochondrial PE is synthesized in mitochondria using the phosphatidylserine decarboxylase (PSD) pathway. To test the hypothesis that PE made from the PSD pathway is required for mitochondrial function, three Chinese Hamster Ovary Cell lines with different PSD-pathway defects were studied. These three cell lines referred to as PSB-2, R-41, and PSD knockdown cells all had ~35% reductions in mitochondrial PE levels compared to the parental cell line. As a result, the mitochondria from all three cell lines have abnormally high sedimentation densities and increased membrane potentials. However, the energy production, motility, and morphologies o

AKNOWLEDGEMENTS

First and foremost, I would like to extend my heartfelt gratitude to Dr. Jean Vance for her mentorship and the opportunity to work in her laboratory. I am very grateful for the wonderful research environment she has worked so hard to have build, it is one where I am able to work on challenging research with independence, one where her door is always open for advice and support, one where I am surrounded by experts in their field willing to offer their advice, and one where I have felt truly at home with our close family of lab members. I also want to thank Dr. Vance for her teachings and the opportunity to learn a variety of different techniques, these are tools which have enriched me and I will carry them with me for the rest of my life.

I want to give thanks to my fellow lab members, Drs. Michinori Matsuo, Jana Strakova, and Guergana Tasseva, and Mr. Russ Watts and Mr. Kyle Peake. You have been, and always will be, my teachers and friends.

I would like offer my deepest gratitude to the members of my graduate committee, Dr. Moira Glerum, and Dr. Simmen. Thank you both for your invaluable insights and contributions to the development of this research project. I am honored for you to critique my thesis and to participate in my defense.

I would also like to give special thanks Dr. Evangelos Michelakis and all of the members of his laboratory for their help and expertise, without whom, many of the experiments in this investigation would not have been possible.

TABLE OF CONTENTS

LIST OF TABLES

LIST OF FIGURES AND ILLUSTRATIONS

LIST OF SYMBOLS, ABBREVATIONS, AND NOMENCLATURE

ATP……..……..adenosine triphosphates
CHO ……...……....Chinese Hamster Ovary
COX……..…..……..….cytochrome c oxidase
Dnf1p and Dnf2p…….…..……aminophospholipid translocases
EMS…….……endomembrane targeting sequences
EPT1…….CDP-ethanolamine:1,2-DG ethanolaminephosphotransferase
ER……..endoplasmic reticulum
ETNK1 and ETNK2…….ethanolamine kinase
FMN……..flavin mononucleotide
GPI ……..……..glycosylphosphatidylinositol
IP3 ……..…..… inositol trisphosphate
IM ……intermembrane targeting sequence
Ip……..…..iron-protein
LS……..……..……..Leigh syndrome
MAM……mitochondrial associated membranes
MEFs……..mouse embryonic fibroblasts
MF……..……..……..microfilaments
Mfn1 and Mfn2……..……..……..mitofusin
MIM ……..……mitochondrial inner membrane
MIT ……..……..…mitochondrial targeting sequence
MPTP…….....mitochondria permeability transition pore
MT……..……..microtubules
MTP……..……mitochondrial transition pore
PC ……..……..…Phosphatidylcholine
PE ……..……..….phosphatidylethanolamine
PET……..…….positron emission tomography
PDH……pyruvate dehydrogenase
PHYLIP……phylogeny inference package analysis
PKC ……protein kinase C
PS ……..……...phosphatidylserine
PSD ……..……..……phosphatidylserine decarboxylase
PSS I…….……..phosphatidylserine synthase I
PSS II……..….phosphatidylserine synthase II
qPCR ……...quantitative real time polymerase chain reaction
VDAC……...……voltage-dependent anion channel
$(\Delta\mu_H)$……..……..……..proton motor force
(ΔpH)……..……pH gradient
$(\Delta\Psi)$……..……mitochondrial membrane potential

CHAPTER 1:

INTRODUCTION

1.1 Introduction

Mitochondria are membrane enclosed organelles that are present in most eukaryotic cells and are known to participate in a wide range of cellular functions [1]. In humans, mitochondrial defects are known to cause degeneration of the brain, heart, liver, skeletal muscles, kidneys and the endocrine and respiratory systems [2]. Although the worldwide epidemiology of mitochondrial diseases is unknown, it has been estimated that 1 in 5,000 individuals in the Western World are born with a serious mitochondrial genetic disease [3].

One of the most prominent roles of mitochondria is the production of high energy adenosine triphosphates (ATPs), a process which generates approximately 90% of the body's energy needs [4]. Mitochondria are also involved in the regulation of numerous other cellular processes including: apoptosis [5], cellular proliferation [6], cellular metabolism [4], and calcium storage and signaling [7]. Furthermore, mitochondria participate in the synthesis of complex hydrophobic molecules such as porphyrins and steroids [4]. Some of these hydrophobic molecules include membrane phospholipids such as cardiolipin [8], phosphatidylglycerol [9], and phosphatidylethanolamine [10].

The primary focus of this thesis is on mitochondrial abnormalities which result from defects in a phospholipid biosynthetic pathway called the phosphatidylserine decarboxylase (PSD) pathway. Phospholipids are the primary building blocks of all biological membranes. The correct concentrations of phospholipids are crucial to the formation and function of lipid bilayers in eukaryotic cells and their organelles [11]. In mammalian cells, mitochondrial

phospholipids comprise a significant proportion of the entire cellular phospholipid content [12]. In particular, phosphatidylethanolamine (PE) is a phospholipid which is known to be enriched in mitochondria [10]. In mammals, PE on average makes up ~20% of cellular phospholipids and ~25-30% of mitochondrial phospholipids (Table 1.1) [12]. The synthesis of PE in mammals occurs via two major pathways which are spatially separated, thereby generating two distinct pools of PE (Fig.1.1 and Fig.1.2). The CDP-ethanolamine pathway which uses CDP-ethanolamine and 1,2-diacylglycerol to generate PE has its last biosynthetic step in the endoplasmic reticulum (ER) [13]. The PSD pathway which generates PE through the decarboxylation of phosphatidylserine (PS) occurs on the inner membrane of mitochondria [14]. Although the relative contribution of PE biosynthetic pathways to cellular PE content appears to vary across tissues and cell types, it is known that in some cells such as Chinese Hamster Ovary (CHO) cells, the majority of mitochondrial PE is synthesized via the PSD pathway [15-18].

Since mitochondria perform a wide variety of functions, and the phospholipid biosynthetic pathways involving these organelles are rather complex, a detailed discussion of these topics will be reviewed in the subsequent chapters. In chapter two, a discussion of the known functions PS and PE will be offered. Chapters three and four will contain a detailed discussion of the two types enzymes involved in mitochondrial PE synthesis, namely the PS synthases and PSD. Lastly, in chapter five, a brief introduction to mitochondrial physiology and the current understanding of mitochondrial phospholipid deficiencies will be

provided. Thus, this chapter will provide a context and a foundation for the later in-depth discussions that follow.

Membrane Lipid Composition (% total)			
	CHO Cell	Mitochondria	
		Outer	Inner
PE	21	33	24
PC	51	46	38
PS	7	1	4
CL	2.3	6	16
PG	1	N.D.	N.D.
Cholest	-	N.D.	N.D.
PI	8	10	16

Table 1.1
A table showing the relative lipid compositions of CHO cells and CHO mitochondria. N.D. represents non-detectable lipid levels. (Adapted from Vance, D.E. and Vance, J.E., 2008) [12].

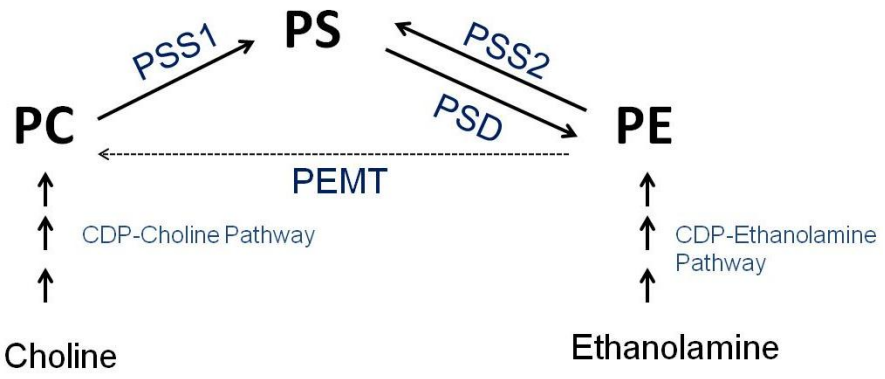

Fig. 1.1
A figure showing the metabolic relationship between PS, PE, and PC. The phospholipids and their precursors are shown in black. The phospholipid biosynthetic pathways are shown in blue. PS, PE, and PC stand for phosphatidylserine, phosphatidylethanolamine, and phosphatidylcholine respectively. PSS, PSD, and PEMT stand for PS synthase, phosphatidylserine decarboxylase, and phosphatidylethanolamine N-methyltransferase respectively. (Adapted from Vance, D.E. and Vance, J.E., 2008) [12].

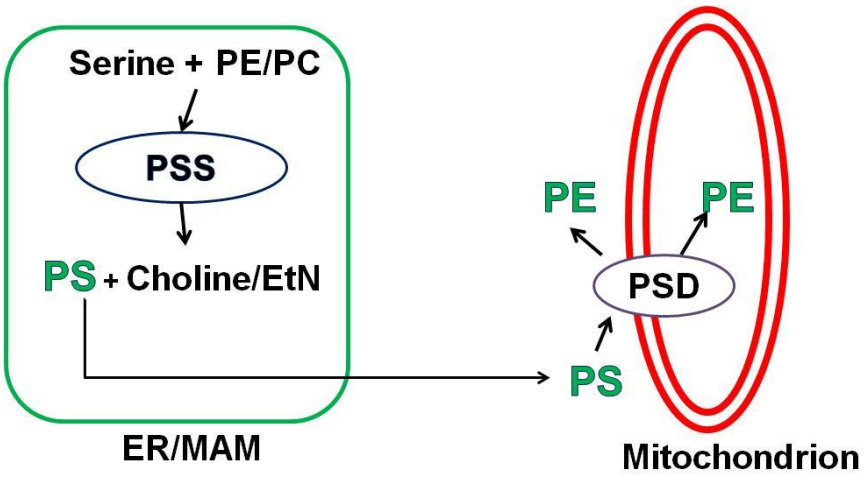

Fig. 1.2
A cartoon showing the subcellular locations involved in PE biosynthesis in the PSD pathway. The phospholipids and their precursors are shown in black. The ER is shown in green and the mitochondrion is shown in red. EtN, PS, PE, and PC stand for ethanolamine, phosphatidylserine, phosphatidylethanolamine, and phosphatidylcholine respectively. ER and MAM stand for endoplasmic reticulum and mitochondrial associated membrane repesctively.

1.2 Rationale

The foundation of this investigation is largely based upon a previous study from our laboratory in which the *Pisd* gene was knocked out in mice [19]. Through breeding $Pisd^{+/-}$ mice, it was determined that an elimination of the PSD enzyme resulted in embryonic lethality between days eight and ten after conception. Through histological analyses, it was found that $Pisd^{-/-}$ embryos lacked germ layer differentiation and extra-embryonic components. Thus, it is believed that between days eight and ten after conception, these undifferentiated embryos were reabsorbed back into the uterine walls [19]. Furthermore, electron microscopy experiments were also performed upon the mitochondria of $Pisd^{-/-}$ embryos isolated at day eight. When 2-dimensional morphologies of $Pisd^{-/-}$ embryo mitochondria were compared to that of the $Pisd^{+/+}$ and $Pisd^{+/-}$ embryo mitochondria, it was determined that they were much more punctate in morphology (Fig. 1.3) [19]. When mouse embryonic fibroblasts (MEFs) were subsequently generated from these embryos, large numbers of aberrantly shaped and mislocalized mitochondria were also observed via confocal microscopy (Fig. 1.4). The growth of these MEFs was also very limited, such that lipid analyses were not possible. However, $Pisd^{+/-}$ MEFs with 50% of normal *Pisd* mRNA appeared normal and had normal growth rates [19]. Thus, these results suggest that there is a minimum level of PSD activity which is required for mammalian development and function.

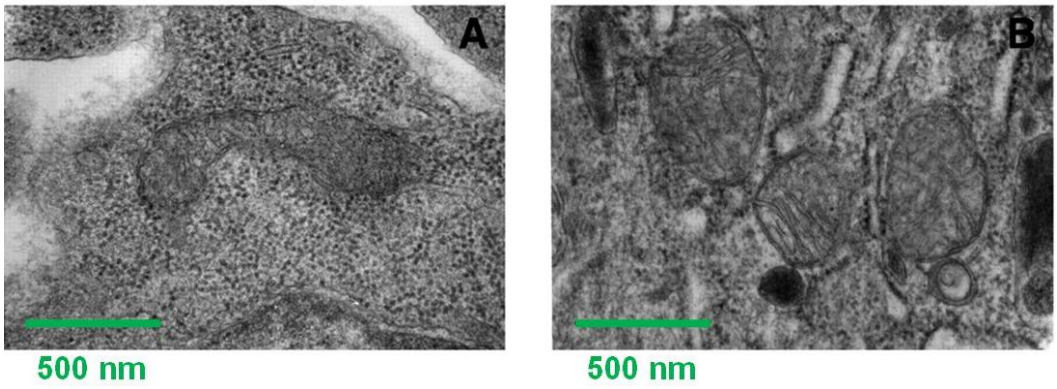

Fig. 1.3
Electron microscopy images comparing the morphology of mitochondria from *Pisd*$^{+/+}$ (Panel A) and *Pisd*$^{-/-}$ (Panel B) mouse embryos. (Adapted from Steenbergen et al, 2005) [19]

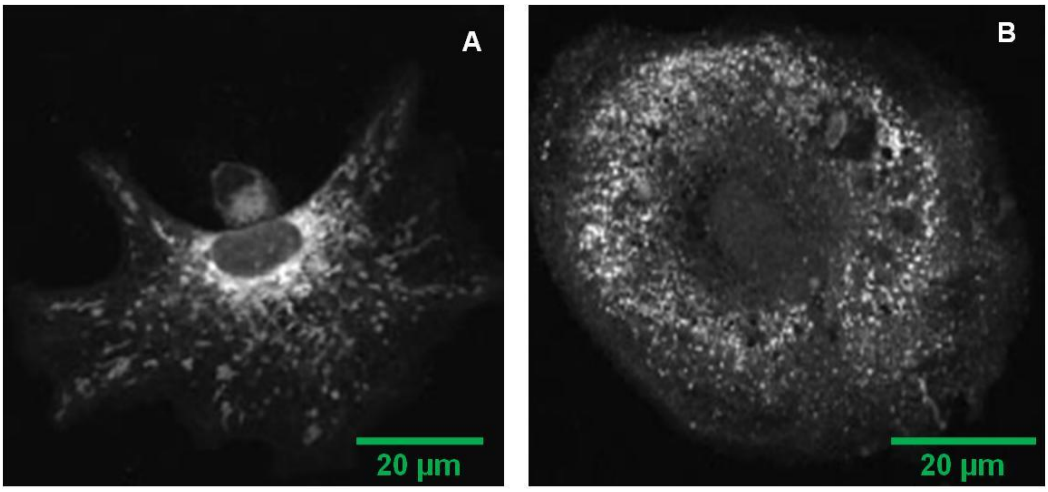

Fig. 1.4
A comparison of *Pisd*$^{+/+}$ (Panel A) and *Pisd*$^{-/-}$ (Panel B) mitochondria in MEF cells stained with Mitotracker Red CMX-ROS. (Adapted from Steenbergen et al, 2005) [19]

1.3 Hypothesis and Research Goals

Since the elimination of PSD in mice resulted in mitochondrial abnormalities and embryonic lethality, we hypothesized that a decrease in PE synthesized via the PSD pathway would cause mitochondrial dysfunction. To test this hypothesis, three Chinese Hamster Ovary (CHO) cell-lines were used, each with a different defect in the PSD pathway. The PSB-2 cell line has a defect in the synthesis of PS, a substrate for the PE decarboxylation [20], the R-41 cells have a defect in the transport of PS to the mitochondrion for decarboxylation by PSD [21], and the PSD KD cells have a decreased expression of PSD via dsiRNA knockdown. Through studying these three cell lines, we hope to gain an understanding of the relationship between mitochondrial PE levels and mitochondrial dysfunction. Moreover, it is also the aim of this investigation to determine the minimum level of PSD activity that is required for mammalian survival.

CHAPTER 2:

THE PHYSIOLOGICAL IMPORTANCE OF PHOSPHATIDYLSERINE AND PHOSPHATIDYLETHANOLAMINE TO MAMMAILAN CELLS

2.1 Phosphatidylserine and Phosphatidylethanolamine

PS and PE are two metabolically related phospholipids (Fig. 1.1). Here, the biophysical and physiological importance of these phospholipids will be reviewed in detail.

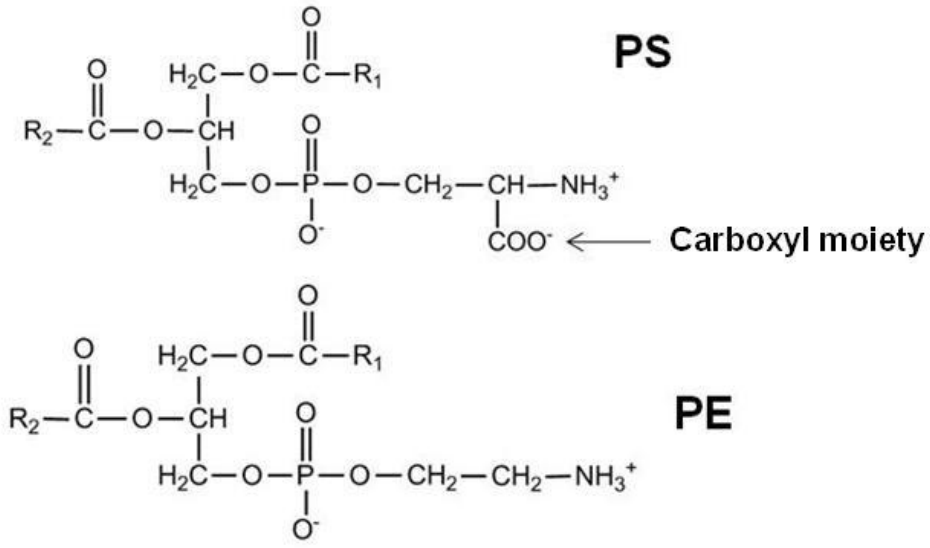

Fig. 2.1
The chemical structures of PS and PE. R_1 and R_2 represent the fatty acid substituents of PS and PE. Note: PS contains a carboxyl moiety which is decarboxylated to form PE.

2.2 Biophysical Importance of Phosphatidylserine and Phosphatidylethanolamine

In mammalian cells, PS and PE are normally found on the inner-leaflet of plasma membranes. This localization of PS and PE can be explained by their biophysical properties. Firstly, PS and PE have small head groups relative to their large hydrophobic domains which give them a cone like molecular structure. This molecular shape favors the formation of inward curving structures such as inverted micelles, which when mixed with cylindrical phospholipids such as PC

will generate curved lipid bilayers [22]. Thus, the stacking properties of curved phospholipid bilayers necessitate molecules like PS and PE to be maintained on the inner leaflet of biological membranes. Secondly, the presence of cone-shaped lipids in phospholipid bilayers allows for membrane flexibility and the accommodation of trans-membrane proteins. Through ^{31}P NMR and microcalorimetry experiments, it was demonstrated that the insertion of non-bilayer forming phospholipids like PS and PE into biological membranes is important for decreasing potential energies within membranes [22]. This metastability that results from the insertion of PE into membranes, as we shall see later, is the key to membrane fusion, fission, and contractile ring disassembly during cytokinesis [22, 23].

The localization of cone-shaped phospholipids to the inner-leaflet of membranes is also important for the maintenance of membrane integrity. In 2006, *Li et al* studied a strain of choline deficient phosphatidylethanolamine N-methyltransferase (CD-*Pemt*$^{-/-}$) mice which had decreased levels of PC in the liver. As a result of a decreased molar ratio of PC to PE, the livers of the CD-*Pemt*$^{-/-}$ mice leaked liver-enzymes and developed steatohepatitis which ultimately progressed into liver failure [24]. It was proposed that the decreased PC to PE ratio caused PE, which is normally enriched on the inner-leaflet of the plasma membrane, to take the place PC on the outer-leaflet of the plasma membrane, causing abnormal lipid packing. Furthermore, when the PC to PE ratio was normalized, the mice were able to escape liver failure, suggesting that membrane integrity is dependent on phospholipid composition and topology [24].

2.3 Physiological Importance of Phosphatidylserine

Phosphatidylserine (PS), which makes up 3 to 10% of mammalian membranes is an important phospholipid for a number of cellular processes [25].

Although PS is normally highly enriched on the inner leaflet of plasma membranes, there are several processes in which PS becomes exposed on the external surface of cells. For example, during the early stages of the apoptosis cascade, PS becomes externalized on apoptotic cells to signal for their removal by lymphocytes [26]. It is believed that a receptor on macrophages recognizes the externalized PS, which upon binding, promotes the phagocytosis of apoptotic cells [26]. This process is thought to occur through an apoptosis-meditated increase in intracellular calcium. Increases in calcium levels firstly deactivate aminophospholipid translocases which maintain the normal membrane phospholipid distribution, and secondly, the higher calcium levels also activate a number lipid scramblases which increase membrane entropy, thus resulting in PS equilibration on both leaflets of the plasma membrane [27, 28].

The blood coagulation process is another example in which PS is externalized. PS exposure on the surface of platelets is one of the early steps of the blood clotting cascade, as it stimulates the activation of a number of clotting factors such as Xa and Va [29, 30]. Thrombin is a serine protease that converts soluble fibrinogen into insoluble strands of fibrin to assist in the closure of injured blood vessels. As PS becomes exposed on activated platelets, factors such as Xa and Va convert prothrombin to thrombin to begin coagulation [31, 32]. Thus, PS

is considered to be a ligand which can induce the allosteric activation of proteins involved in blood clotting.

In addition to being a ligand, PS is also a known cofactor for a number of enzymes. One of the most notable examples is protein kinase C, a class of proteins which participates in a wide range of signal transduction pathways [33, 34]. Other known enzymes that are activated by PS include: Raf-1 kinase [35], Na/K ATPase [36], dynamin-1[37], neutral sphingomyelinase[38], and Hsp70[39].

2.4 Physiological Importance of PE

In mammalian cells, PE is generally the second most abundant phospholipid, making up approximately 20% of total phospholipids. It should be noted however, that the distribution of PE differs in different subcellular membranes and even across tissues (Table 1.1).

In addition to playing a key role in the membrane structure and integrity, PE is also involved in a large number of cellular processes. In the following, we shall discuss some the most notable processes.

The role of PE in membrane fusion events has been well established. Through *in vitro* studies with unilamellar vesicles comprised of PE and various other cellular phospholipids, *Hope et al*. in 1986 first showed that membrane fusion in physiological conditions is dependent on calcium and PE [40]. Later, studies by Morris et al. elucidated the mechanism of this fusion through simulating the interaction between PE, PS, and calcium *in vitro[41]*. It is believed that calcium neutralizes the negative charge of PS to destabilize its interaction

with PE in the inner leaflet of membranes. Thus, this subsequent metastability of PE is believed to be the key for membrane interaction and fusion. [41]

Studies using fluorescently-tagged PE molecules in apoptotic cytotoxic T cells have shown that PE is externalized during apoptosis [42]. Interestingly, the loading of apoptotic cells with unilamellar vesicles containing PE decreased fluorescent PE externalization, which suggests that the amount of PE externalized may be a regulated process [42]. Since the mechanism underlying this event is still unclear, further investigation is required.

Glycosylphosphatidylinositol (GPI) is a glycolipid that can be attached to the C-terminus of proteins during posttranslational modification. In biological membranes, GPI anchors are used to attach a wide variety of signalling proteins to external cellular surfaces. The ethanolamine moieties of GPI anchors are derived from PE as there are no known pathways for de novo ethanolamine synthesis [43, 44]. Thus, it is possible that decreases in cellular PE levels may affect the availability of ethanolamine for the synthesis of GPI anchors.

During the cytokinesis stage of cell division, the plasma membrane is constricted and then sealed between the two daughter cells. During this process, a rearrangement of the phospholipid bilayers occurs. In 2001, *Emoto et al*. showed PE molecules on the inner-leaflets of plasma membranes are exposed on the external-leaflets of cleavage furrow sites during cytokinesis [23]. Through manipulation of cell-surface-PE using a PE-binding peptide and establishing a mutant cell line defective in PE biosynthesis, it was demonstrated that cytokinesis requires PE [23]. Thus, trans-bilayer redistribution of PE plays a critical role in

mediating movements between the contractile ring and the plasma membrane during cytokinesis.

Recently, PE has been demonstrated to be involved in cellular autophagy. The first evidence of this was brought forth in 2007 by *Neubauer et al*. using a yeast model. In yeast, the Vps4p and Vps36p proteins are involved in the formation autophagosomes. Interestingly, in Vps4p and Vps36p mutant cells, which have impaired autophagosome formation, PE supplementation rescues them of their defect. The defect in autophagosome formation was also observed in PE-deficient cells. When the PE levels were restored to normal in PE-deficient cells, it was observed that the cells regained their ability to generate autophagosmes. Thus, these results strongly suggest that PE is a limiting molecule in the autophagy process [45].

In 2010, *Hailey et al.* studied the formation of autophagosomes in a line of rat kidney cells. Through observing starvation induced autophagocytic cells, it was found that mitochondrial membranes labeled with fluorescent tags co-localized with autophagosomes more than any other subcellular membrane. Furthermore, it was observed that fluorescently tagged autophagosomal markers such as Atg5 and LC3 co-localized with mitochondria, and mitochondrial markers such as Fis1 co-localized with autophagosomes. The highlight of this study was the intracellular tracking of fluorescence-labeled PS (NBD-PS). NBD-PS was observed traveling from the MAM to mitochondria, where it was decarboxylated to NBD-PE. The NBD-PE in mitochondria was subsequently found to be

transferred to autophagosomes, which demonstrated that PE made from the PSD pathway specifically, is involved in the formation of autophagosomes [46].

CHAPTER 3:

PHOSPHATIDYLSERINE SYNTHASES

3.1 Phosphatidylserine Synthases

In the PSD pathway, the biosynthesis of PS precedes that of PE (Fig. 1.1). In this chapter, I shall review the enzymes responsible for the biosynthesis of PS in terms of their structure, regulation, and physiological importance. In mammals, PS is synthesized via an exchange of L-serine with the base moieties of two phospholipids, either PC or PE. Studies using CHO cells have identified two mammalian PS synthases named phosphatidylserine synthase I (PSS I) and phosphatidylserine synthase II (PSS II). *In vitro*, PSS I uses PC and PE as phosphatidyl donors for serine-base-exchange and PSS II utilizes only PE [47].

3.2 The Discovery and Classification of Phosphatidylserine Synthases

PS synthase activity was first documented by *Hübscher et al.* in 1959 when they found that rat liver homogenates had the ability to incorporate [^{14}C] L-serine into PC to generate PS in a calcium stimulated, energy independent reaction [48]. Later, in 1961, when experiments by *Borkenhagen at al*. also showed that [^{14}C] L-serine was incorporated into PE to yield PS in a similar manner, the existence of a PS synthase which used both PC and PE as phosphatidyl donors was proposed [49]. The first insight into the localization of PS synthase activity was brought forth with the subcellular fractionation of rat liver, which revealed that PS synthase activity was most enriched in the ER or microsome fraction [50]. The precise subcellular localization of PS synthase activity was later elucidated by researchers in our laboratory through the isolation of a unique ER-mitochondria associated membrane called mitochondrial associated membranes (MAM). Through fractionation of crude rat liver

mitochondria via Percoll gradient centrifugation, it was found that MAM fractions contained two-fold higher serine base-exchange activities than microsomal fractions [51]. The reports that rat liver mitochondria also contained PS synthase activity were eventually proven false mainly through two experiments *by Stone, et al., Saito et al., and Kuge et al* [47, 50, 52]. Through immunoprecipitating PSS I from the nuclei, mitochondria, ER, Golgi, plasma membrane and cytosol fractions of CHO cells, *Saito et al*. demonstrated that PSS I is only localized on the ER and MAM and not on any other organelle membranes [53]. A similar experiment was performed using a CHO cell line which lacked PSS I activity. The remaining PSS II activity, as expected, was found to be enriched in only the microsomal and MAM fractions of CHO cell homogenates[47]. Over the course of the next twenty years, PS synthase activity was documented in a variety of mammalian tissues including brain, heart, lung, and liver. Interestingly, however, this activity was not found in bacteria [54].

The existence of two distinct PS synthases was first proposed in the mid 1980s when an enzyme which synthesized PS from only PE but not from PC was partially purified from rat brain microsomes [55]. This result was further supported when *Voelker et al.* and *Nishijima et al*. independently generated mutant PS synthase CHO cell lines via chemical mutagenesis. These similar mutant cell lines referred to as M9.1.1 and PSA-3 cells respectively, lacked the enzymatic activity for PS synthesis from PC but retained PS synthesis activity from PE [56, 57]. Through radiolabeling and *in vitro* experiments, it was shown that the rates of PS synthesis in the mutant cells were indeed ~35-55% lower than

in parental cells. Thus, these results demonstrated that there were two PS synthases. One enzyme, which synthesized PS from both PE and PC, was named serine-exchange enzyme I (later renamed PSS I), and the other which used only PE, was named serine-exchange enzyme II (later renamed PSS II) [56, 57].

3.3 Nucleotide Sequence and Structure

Information about the protein sequences of mammalian PSS I and PSS II was made available through the successful cloning and overexpression of their CHO cell cDNAs (referred to as *PssA* and *PssB* respectively) [58, 59]. The cDNA encoding PSS I was first cloned through using PSA-3 cells, which are a line of PSS I deficient and PS autotrophic CHO cells. Through the complementation cloning of PSA-3 cells with cDNAs from the parental CHO K1 cell line, a cDNA encoding a 473 amino acid peptide was cloned. When this cDNA was expressed in PSA-3 cells, the choline-exchange activity was restored and the PS and PE levels were also normalized, confirming that the cDNA indeed encoded the PSS I enzyme [60].

The PSS I cDNA was also cloned from rat liver and human myeloblasts [61]. When the hamster, rat, and human sequences were compared, the homology between the three species was greater than 90%. In all three species, the PSS I gene contains 13 exons that span 12 introns. Interestingly, however, the hamster and rat PSS I genes are located on chromosome 13 whereas the human ortholog is located on chromosome 8 [61].

A 2004 mutagenesis study by *Oshawa et al.* provided information about the catalytic residues of PSS I [62]. Through the replacement of 66 candidate

polar residues with hydrophobic alanine residues, it was found that eight residues (His-172, Glu-197, Glu-200, Asn-209, Glu-212, Asp-216, Asp-221 and Asn-226) were required for the catalytic activity of PSS I. In particular Asn-209 was responsible for L-serine binding. Furthermore, six amino acids (Arg-95, His-97, Cys-189, Arg-262, Gln-266 and Arg-336) were found to be important for the regulation of PSS I activity [62].

The cDNA sequence encoding PSS II was found through homology searches of human expressed sequence tags which had similarities to the PSS I gene. The uncovered PSS II cDNA sequence shared a 32% homology with PSS I and was predicted to encode a 55 kDa 474 amino acid protein [59]. Although the amino acid sequences of PSS I and II are only 32% homologous, the overexpression and purification of the enzymes revealed that the 3-dimensional structures of the two enzymes are highly similar. Through hydrophobicity analyses via the Kyte and Doolittle method, it was found that the two enzymes shared identical solvent sequestered regions and membrane spanning domains [63]. A CHO cDNA ortholog of human PSS II was subsequently cloned and over-expressed in CHO K1 cells to study the regulation of its activity. In these cells, the ethanolamine-serine exchange activity was increased by 10-fold, which corresponded to a 6-fold increase in total PS synthase activity. Furthermore, the choline-serine exchange activity was unchanged, which demonstrated that the cDNA cloned was indeed that of PSS II [59]. Finally, when PSS II was expressed in M9.1.1 cells which lacked PSS I activity, the cells were rescued of their need for PS supplementation, which suggested that PSS II has the capacity to

complement PSS I [64]. Thus, these results demonstrated that there are indeed two PS synthases which are encoded by different genes and that they have the ability to independently modulate cellular PS levels.

3.4 Regulation

The transcriptional and post-translational regulations of mammalian PS synthases are currently not fully understood. Recent studies, however, from our laboratory have suggested that zinc finger and basic helix-loop-helix family transcription factors (specifically, Sp1, Sp2, and nMyc factors) are involved in the transcriptional regulation of PSS I enzyme levels (*Tasseva et al.*, unpublished results).

At present, the feedback mechanisms of PSS I and II are thought to be the major method by which PS synthase activity is regulated. Indeed, studies by *Nishijima et al.* have demonstrated that at micromolar concentrations, PS supplementation can linearly down-regulate L-serine incorporation into PS in CHO cells [65]. *In vitro*, the addition of 80μM PS to CHO cells decreased PSS I and II activity by three and five-folds respectively [65]. Thus, these results suggest that PS is a negative regulator of PS synthase activity.

The feedback regulation of the individual PS synthases was elucidated through the generation of a mutant CHO cell line via chemical mutagenesis (named mutant-29). This mutant cell line was resistant to inhibition of PS synthase activity by exogenous PS [66]. Through sequencing the cDNA of mutant-29 cells, it was found that these cells had a point mutation in the PSS I Arg-95 residue which was replaced with a Lys. As a result of this mutation,

mutant-29 cells had a 3-fold increase in PSS I activity which led to a two-fold increase in PS levels. However, when this mutant PSS I was over-expressed in wildtype cells, PSS I activity was not increased, suggesting that PSS I may also be post-translationally regulated [67]. Thus, feedback inhibition of PSS I by PS is required for the maintenance of mammalian PS levels, and Arg-95 on PSS I is critical for this inhibition.

The feedback inhibition of PSS II by PS was also observed based upon similar earlier findings with PSS I. The first evidence for PSS II inhibition by PS was found through the supplementation of PSA-3 cells (which lack PSS I activity) with PS [68]. When L-serine incorporation into PS was inhibited in these cells by PS, it was hypothesized that a similar Arg-97-Lys mutation would prevent PSS II end-product-inhibition as well. When a PSS II containing the latter mutation was stably expressed in wildtype CHO cells, PS synthesis increased by 4-fold, suggesting that both PSS I and II are highly sensitive to inhibition by PS [68]. In 2003, *Kuge et al.* provided evidence that PS synthase inhibition was caused by PS alone, and not by any other metabolically related phospholipids. This was done through the purification PSS II to near homogeneity, followed by the addition of PS, PE, and PC. When it was observed that neither PE nor PC negatively regulated PSS II, it became clear that PS alone was responsible for the inhibition of PSS II via an interaction with Arg-97 [69].

3.5 Physiological Importance of Phosphatidylserine Synthases

To understand the mammalian PSS I and II enzymes in terms of why they exist and their relative contributions to cellular PS levels, a number of

mutagenesis and knockout experiments have been performed. In following, we shall discuss these studies as they pertain to the consequences mammalian PSSI and II defects *in vitro* and *in vivo*.

The generation of PSS I, PSS II, and PSS I and II deficient CHO cells has elucidated the cellular requirements for PS synthesis from the two PS synthase pathways. As previously mentioned, two PSS I-deficient lines of CHO cells have been generated (named PSA-3 and M9.1.1) [56, 57]. Although both cell lines have defective PS synthesis from PC and normal PS synthesis activity from PE, they however, have somewhat different phenotypes. The M9.1.1 cells require ethanolamine and PS supplementation for survival, whereas, PSA-3 cells require either PS or PE but not ethanolamine. Furthermore, whereas the PSS II activity of M9.1.1 cells was increased by 85% compared to the wildtype cells, it was decreased by 55% in PSA-3 cells. At present, the reason for these different phenotypes is not fully understood [56, 57].

When the PSS I defective PSA-3 cells were further mutagenized to generate a defect in PSS II, a new cell line called PSB-2 cells were cloned [70]. The difference between PSB-2 cells and the parental PSA-3 cells is that PSB-2 cells require PS supplementation for survival as opposed to either PS or PE, which strongly suggests that they have a defect in the synthesis of PS from PE. As a result of mutations in both PSS I and II, PSB-2 cells transcribe missense PSS I mRNA and have significantly reduced (80%) PSS II mRNA. These mutations translate to a complete elimination of PSS I activity and a 95% reduction of PSS II activity in PSB-2 cells compared to that of the wildtype. The PS and PE levels

of PSB-2 were also reduced by 66% and 49% respectively compared to that of the wildtype cells (Fig. 3). Therefore, the PS synthase activity in PSB-2 cells was only 5% that of wildtype cells [70].

To understand the relative contributions of each PS synthase to PS levels, PSS I cDNA was transfected into PSB-2 cells. As a result, PS synthesis from PC was restored, however, the synthesis of PS from PE (the other activity of PSS I) was still defective. Thus, this suggests that the majority of PSS I activity lies in the conversion of PS from PC and that PSS I alone cannot replace activity of PSS II in CHO cells [70].

Supplement	Strain	PS	PE
		% of total	% of total
None	CHO-K1	5.9	16.6
	PSA-3	3.7	11.7
	PSB-2	1.2	8.5
PS	CHO-K1	6.1	17.5
	PSA-3	6.2	18.3
	PSB-2	6.8	15.8
PE	CHO-K1	5.3	30.9
	PSA-3	4.7	29.9
	PSB-2	1.8	31.5

Table 3.1
A table showing the relative PS and PE levels of wildtype CHO-K1 cells, PSA-3, and PSB-2 cells with respect to total phospholipids. The changes in phospholipid levels upon PS and PE supplementation are also shown for the latter cell types.

In mice, PSS I and PSS II are expressed in a wide variety of tissues with some overlap between each other. PSS I mRNA is ubiquitously expressed, with the highest expression in the liver, brain, kidneys, and testis. PSS II, on the other hand, is most highly expressed in Sertoli cells of the testis and Purkinje cells of the brain [61, 64, 71]. To understand why a partial overlap in PSS I and PSS II expression exists, various combinations of PSS I and II genotype mice were studied.

The *in vivo* importance of PSS II was assessed through the generation of a strain of *Pss2*$^{-/-}$ mice by. [71]. Initially, *Pss2*$^{-/-}$ mice were found to be outwardly normal with healthy growth rates and development. However, later it was discovered that 10% of male *Pss2*$^{-/-}$ mice had smaller testes than *Pss2*$^{+/+}$ mice. Histological analyses of the abnormal mice revealed that their testes had contracted spermatic ducts with no spermatocytes. Moreover, phospholipid analyses on a variety of different organs in *Pss2*$^{-/-}$ mice showed that all of their

major phospholipid levels were normal, suggesting that there may be a particular of pool of PS which is deficient in the reproductive organs of these mice [25, 71]. This observation indicated that in the majority of mouse tissues, increased PSS I activity compensates for a lack of PSS II activity.

After finding that *Pss2*$^{-/-}$ mice are viable, a strain of *Pss1*$^{-/-}$ mice was subsequently generated by *Arikketh et al.* [72]. Since the elimination of PSS I in CHO cells led to decreased viability, the investigators were surprised to find that the *Pss1*$^{-/-}$ mice appeared perfectly normal. When characterized, *Pss1*$^{-/-}$ mice had normal fertility, growth rates, and lifespans. Furthermore, through crossing *Pss1*$^{+/-}$ and *Pss2*$^{+/-}$ mice, it was found that only *Pss1*$^{+/-}$/ *Pss2*$^{-/-}$ and *Pss1*$^{-/-}$ *Pss2*$^{+/-}$ mice were born but not *Pss1*$^{-/-}$/ *Pss2*$^{-/-}$ mice suggesting that mice can tolerate the elimination of either PSS I or PSS II, but not both, and indicating that PS is essential for life [72].

3.6 Intracellular Transport of Phosphatidylserine

In mammalian cells, the synthesis of PS and PS derived PE are spatially separated. For PS to be decarboxylated into PE in mitochondria, the PS must first be transported from the MAM where it is synthesized to the mitochondrion [73]. Although the exact mechanism of this transport is unclear, it is known that a number of mammalian cells (including CHO cells) utilize this pathway as the primary source of both mitochondrial and cellular PE [61, 74-76].

In 1989, researchers in the laboratory of Dr. Dennis Voelker demonstrated that the transport of PS to mitochondria in mammalian cells requires ATP and is independent of cytosolic proteins [77]. Through a series of radiolabeling

experiments in CHO cells, the researchers discovered that the permeabilization of cells in which 99% of cytosolic proteins were released did not affect PS transport to mitochondria. Interestingly, the intracellular concentration of ATP was directly related to PS transport in these permeabilized cells [78]. Furthermore, researchers from the same laboratory also showed that the latter PS transport process was the rate-limiting step in mitochondrial PE biosynthesis [77]. Although the exact mechanism by which PS is transported from MAM to mitochondria is still unclear, the current evidence strongly suggests the existence of contract-transfer-mechanism. Firstly, the co-isolation of intact MAM and mitochondria from rat liver via Percoll gradient centrifugation provides evidence that the two membranes do not fuse [51, 79]. Secondly, electron microscopy visualizations of yeast MAM and mitochondria show that the two membranes likely dock rather than fuse, with areas of close (40nM) contact [80]. Finally, experiments with dinitrophenol, which have been shown to reduce the contact sites between the two membranes, have demonstrated to inhibit mitochondrial PS transport [81].

The notion that MAM to mitochondrion PS transfer is transport-protein independent was further supported in 1991 when *Ardail et al.* demonstrated radiolabeled PS-containing micelles were capable of efficiently transferring PS to isolated mitochondria [75].

In 2002, *Schumacher et al*. published reports about a yeast mutant which was defective in MAM to mitochondrion PS-transport [82]. Genetic analyses of this mutant showed that there was a mutation in the MET30 gene. MET30 encodes a subunit of the SCF (suppressor of kinetochore protein 1, cullin,F-box)

ubiquitin ligase complex [82]. The Met30 subunit has been shown to be important for the substrate recognition of SCF ubiquitin ligases [83]. Yeast cells which lack Met30 were found to have decreased MAM to mitochondrion PS transport and subsequently reduced levels of mitochondrial PE. When the mitochondria of Met30 deficient cells were centrifuged on a sucrose gradient, it was observed that they had abnormally high sedimentation densities compared to wildtype mitochondria (Fig. 3.1). This increase in sedimentation density was attributed to the decrease of phospholipid to protein ratios in mitochondria, as most proteins are denser than phospholipids [82].

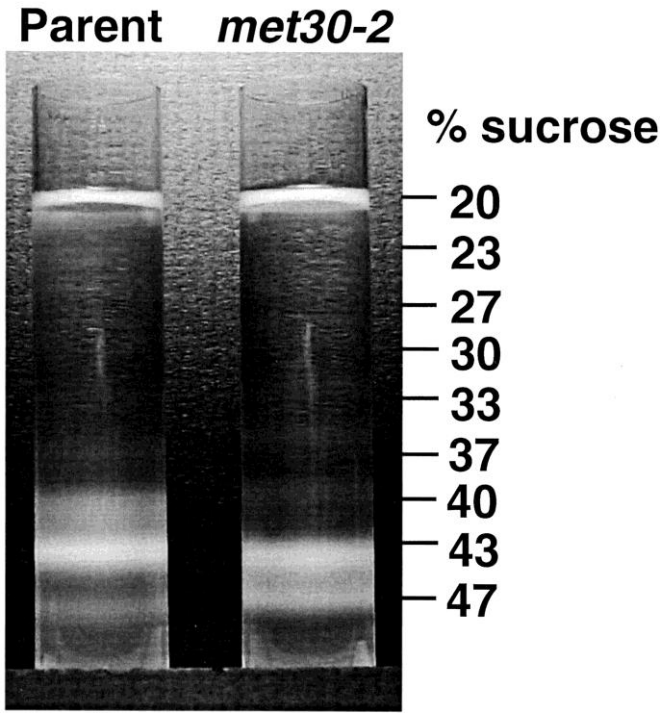

Fig. 3.1
The sedimentation densities of mitochondria from wildtype and Met30 mutant yeast. Note: Met30 mutant mitochondria show a higher sedimentation density compared to wildtype mitochondria. Figure adapted from *Schumacher et al.* [82].

A second PS transport step prior to its decarboxylation involves the transfer of PS from the outer mitochondrial membrane to the inner membrane.

This process was revealed when fluorescent PS analogs were used to show that PS molecules were readily partitioned to lipid-transfer domains between the mitochondrial outer and inner membranes [84]. Through chemical mutagenesis, a line of CHO cells which are presumed to have a defect in this transport step was cloned [21]. These cells, referred to as R-41 cells, will be one of the key foci of discussion in this thesis.

Although the regulation of PS transport to mitochondria in mammalian cells is not fully understood, an experiment with the yeast type I PSD enzyme (yeast have two PSD enzymes, reviewed in chapter 4) has provided insights into PSD regulation. In yeast, PS transport into mitochondria does not require ATP, and is regulated by an ubiquitin ligase like protein called Met30p. It has been shown that increased expression of Met30p can increase mitochondrial membrane affinity to PS and increase mitochondrial PE synthesis [82].

The specificity of PS to mitochondrion transport with respect to fatty acid substituents is still unclear. Experiments by *Heikinheimo et al*. in 1997 showed that PS molecules which had short-chained fatty acids as well as polyunsaturated fatty acids were preferentially transported into mitochondria [85]. However, a similar experiment performed by *Bleijerveld et al*. published in 2007 contradicts this finding [15].

3.7 Perspectives

Although the major mammalian metabolic pathways for PS synthesis have now been elucidated, much is still unknown about the regulation of PS biosynthesis and intracellular PS transport, both of which are crucial to

understanding the formation of cellular membranes. However, as new information regarding the transcriptional regulation of the PS synthases and computational simulations of PS transport are brought forth in the near future, new chapters in study of PS synthesis will be opened.

CHAPTER 4:

PHOSPHATIDYLSERINE DECARBOXYLASE

4.1 Phosphatidylserine decarboxylase

Phosphatidylserine decarboxylases (PSD) are enzymes which synthesize PE through the decarboxylation of PS (Fig. 1.1). In the following, a review of the current understanding of these enzymes with regards of their, classification, biosynthesis, and physiological importance will be offered. This discussion will primarily focus on the mammalian PSD enzyme, but because much of our understanding largely comes from lower organisms, the PSDs of bacteria and fungi will also be considered.

4.2 Classification

PSD activity was first documented by *Borkenhagen et al.* in 1961 when it was discovered that rat liver homogenates had the ability to decarboxylate the radiolabeled [^{14}C] L-3-serine moiety of PS into PE and CO_2 [86]. Later, when PSD activity was also discovered in bacteria, fungi and plants, a membrane topological classification was established to group the PSD enzymes into two types [87-89]. Generally speaking, type I PSDs encompass most mitochondrially associated and bacterial isoforms of the enzyme, and type II PSDs include enzymes which are localized to the endomembrane system (Golgi, ER, and vacuolar compartments) [90]. Since PSD enzymes are differently localized across species, with some species encoding several isoforms, the diversity of PSD enzymes shall be briefly discussed.

Type I PSDs

In mammalian cells, plant cells, and fungi, type I PSD enzymes reside in the intermembrane space of mitochondria where they associate with the inner

mitochondrial membrane [52, 90]. In bacteria, type I PSDs associate with the cytosolic face of plasma membranes [91].

Type II PSDs

Through subcellular fractionation of yeast (*Saccharomyces cerevisiae*), it was discovered that the Psd2p isoform of type II PSD enzymes is localized to the Golgi and vacuolar compartment of fungi [92, 93]. Furthermore, N-terminally tagged green fluorescent proteins (GFP) made from plant type II PSD enzymes, specifically Psd2p and Psd3p subtypes ,were found to be associated with vacuolar and ER compartments of plant (*Arabidopsis thaliana*) cells respectively [94].

The phylogenic analysis of PSD enzymes has not only demonstrated the diversity of PSDs but has also identified exceptions to the topological classification. For example, protists in the *Plasmodium falciparum* family contain a type I PSD enzyme which is localized in the ER [95]. Some species may utilize several subtypes of PSDs. For instance, fungi such as *Saccharomyces cerevisiae* have both type I and II PSD enzymes, and plants such as Arabidopsis thaliana contain three isoforms of PSD: Psd1p, Psd2p, Psd3p, of which the first is a type I enzyme and the latter two are type II enzymes [94].

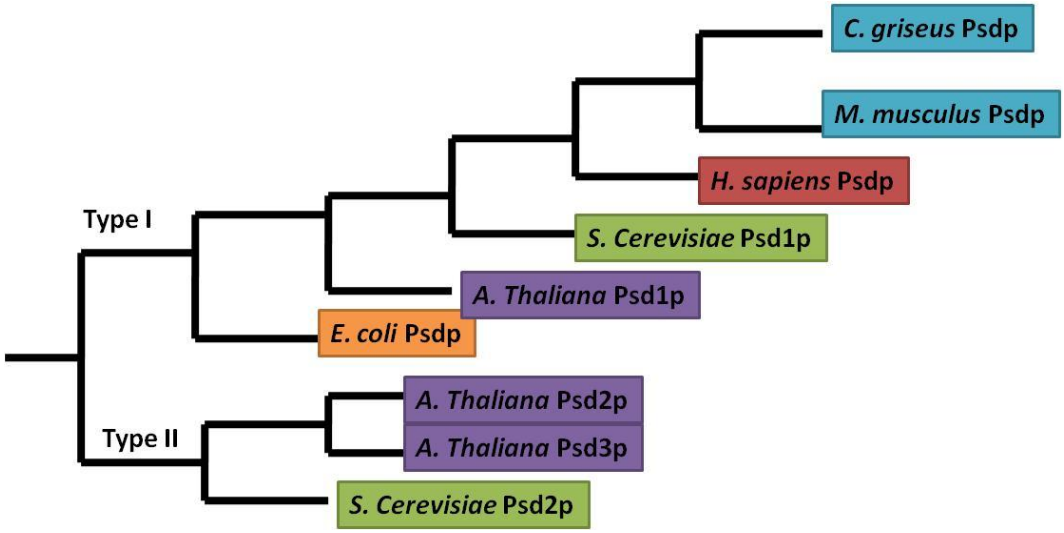

Fig. 4.1 A phylogenic tree of PSD depicting type I and II PSDs and their subclass classifications. (Adapted from Schuiki et al. 2009 [96])

Sequence alignment of PSD isoforms using the PHYLIP (phylogeny inference package) analysis has provided evidence that the diverse family of PSDs can all be traced back to a common ancestral peptide [97]. Alignment studies have also demonstrated that the amino acid sequences and sizes of PSD enzymes are also highly variable. The smallest PSD isoform, Psdp found in *Bacillus subtilis*, has a molecular weight of 29.7 kDa whereas the largest known to date is the 130kDa Psd2p from *Saccharomyces cerevisiae* [98].

The first eukaryotic PSD cDNA to be cloned and sequenced was the Psd1p of *S. cerevisiae*. When this type I PSD was compared to the type II Psd2p found in the Golgi, it was discovered that the two isoforms shared only 12.6% homology at the amino acid level [98]. Since the mitochondrial Psd1p of yeast is similar to the Psdp in mammalian mitochondria and in bacteria (with 44% and 35% amino acid sequence homology respectively), it has been speculated that the evolutionary divergence of PSD enzymes predates the endosymbotic events which led to eukaryotic life [98, 99].

Mammalian cells contain only one PSD isoform, and that is the mitochondrially associated PSD enzyme [58]. To date, only one mammalian PSD gene has been cloned, and that is the 409 amino acid, 409kDa CHO *C. griseus* PSD enzyme [100]. This enzyme is the primary focus of this investigation, and thus, I shall focus the majority of my discussion on its structure and physiological importance.

4.3 Structure

PSD enzymes belong to a small family of decarboxylases that are unusual in that they utilize a pyruvoyl prosthetic group for their catalytic activity[101]. Both type I and II PSD holoenzymes have α and β subunits which originate from a single proenzyme. This proenzyme is encoded in the nuclear genome and is translated on cytosolic ribosomes[102]. The maturation of the proenzyme involves several posttranslational modifications as well as the synthesis of a pyruvoyl prosthetic group which is required for catalytic activity [102]. One notable similarity between the two types of enzymes is that they both harbor their highly conserved pyruvoyl prosthetic groups within the α subunit [103].

Type I

From the N-terminus to the C-terminus, type I PSD enzymes begin with mitochondrial targeting sequences (MITs) followed by intermembrane space sorting sequences and sequences (IMs) for β and α subunits. It is believed that the maturation of type I PSD enzymes requires a series of three sequential N-terminal to C-terminal cleavages [99, 104]. Despite differences in amino acid sequences, all type I enzymes contain a conserved LGST motif which acts as a cleavage site

to generate the α and β subunits. The α subunit of type I PSD isoforms in mammals and yeast, but not prokaryotes, contain a FXFXLKXXXKXR motif. Preliminary structural evidence suggests that this motif, which is in close proximity to the catalytic carbonyl moiety, is responsible for substrate recognition [105].

Type II

Type II PSD enzymes are different from type I enzymes in that they contain endomembrane targeting sequences within their β subunits. The β subunit also harbors a putative C2 domain which is thought to facilitate the binding of calcium and PS. The α and β subunit cleavage sites also differ from type I enzymes in that they have a GGST residue motif instead of the LGST motif [92, 106].

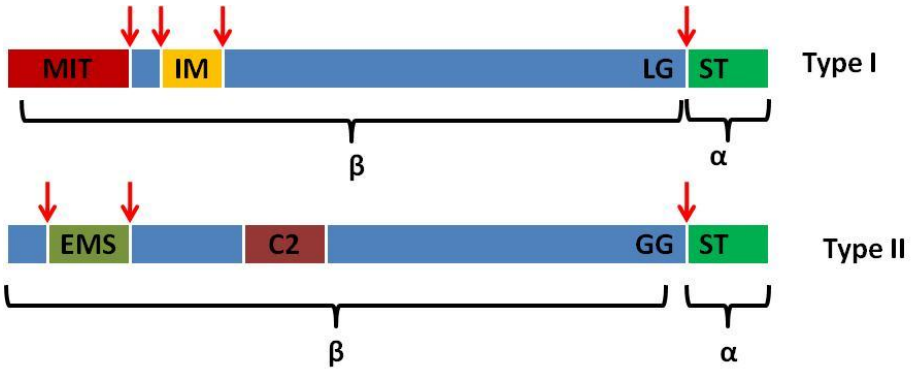

Fig 4.2
A comparison of type I and type II PSD amino acid sequences. The mitochondrial targeting sequences (MITs), intermembrane space sorting sequences (IMs), and endomembrane targeting sequences (EMS) are shown in red, yellow, and dark green respectively. Red arrows indicate sites of proteolytic cleavages.

Our understanding of mammalian PSDs comes almost exclusively from the study of PSD in CHO cells. In 1991, *Kuge et al*. cloned a cDNA encoding PSD and showed that the CHO PSD MIT is rich in positively charged amino acids

and low in acidic residues as with most mitochondrial targeting sequences [100]. In addition, the authors also showed the PSD proenzyme contained an evolutionarily conserved stretch of hydrophobic residues followed by basic residues which corresponded to amino acids 65-79 in the hamster PSD. Through homology studies, it was subsequently determined that this sequence was responsible for the mitochondrial intermembrane localization of PSD [104].

4.4 PSD Post-translational Processing and Activation

Posttranslational Processing

The post-translational processing of mammalian PSD was studied by *Kuge et al.* in 1996. Through using anti-PSD antibodies, it was demonstrated that the 46kDa primary PSD translation product is processed via 3 steps. In the first step, the proenzyme is transported to the inner mitochondrial membrane where its MIT is removed to yield a 42kDa product. In second step, the IM sequence is cleaved to give a 38 kDa product which is subsequently activated in the third step via an internal serinolysis reaction [104]. Mutagenesis experiments later confirmed that the 4kDa α subunit is responsible for PSD activity and the 34 kDa β subunit is necessary for association with the mitochondrial inner membrane MIM [21, 103].

Activation

All pyruvoyl-dependent decarboxylases are comprised of heterodimeric subunits. This heterodimeric structure is generated from the formation of the pyruvoyl moiety from a serine residue within the proenzyme [102]. Since pyruvoyl groups are not gene-encoded, pyruvoyl enzymes are created from post-translational modification of inactive proenzymes. The mechanism of this

activation was elucidated by *van Poelje et al.* in 1990 using reductive trapping of the enzyme with inhibitors at various stages of maturation[102]. In CHO cells, the activation of the PSD proenzyme has been proposed to involve four steps. The first step involves a serinolysis of the peptide bond between glycine-253 and serine-254, the second step takes place when an α,β-elimination of the β subunit occurs, the third and fourth steps subsequently occur with the hydration of dehydroalanine and elimination of ammonia to generate an amino terminal pyruvoyl prosthetic group on the α subunit [107]

4.5 Phosphatidylserine Decarboxylation Mechanism and Activity

The mechanism of type I PSD enzymes was revealed through the study of *E. coli* PSD in 1977 in the laboratory of Dr. Eugene Kennedy. Through a series of borohydride reductions and inactivations of radiolabeled PSD, it was determined that a Schiff base-requiring mechanism was necessary for the decarboxylation of PS [108]. The proposed four-step mechanism involves first the formation of a Schiff's base between PS and the α-carbonyl group of PSD enzyme. A second intermediate then forms when the unstable Schiff base undergoes electron rearrangements to expel CO_2 from the serine moiety of PS. The resulting azomethine intermediate is then protonated to give a PE linked to a Schiff's base. The final reaction occurs when water hydrolyses the latter linkage to produce PE and regenerate the pyruvoyl prosthetic group of PSD [107, 109].

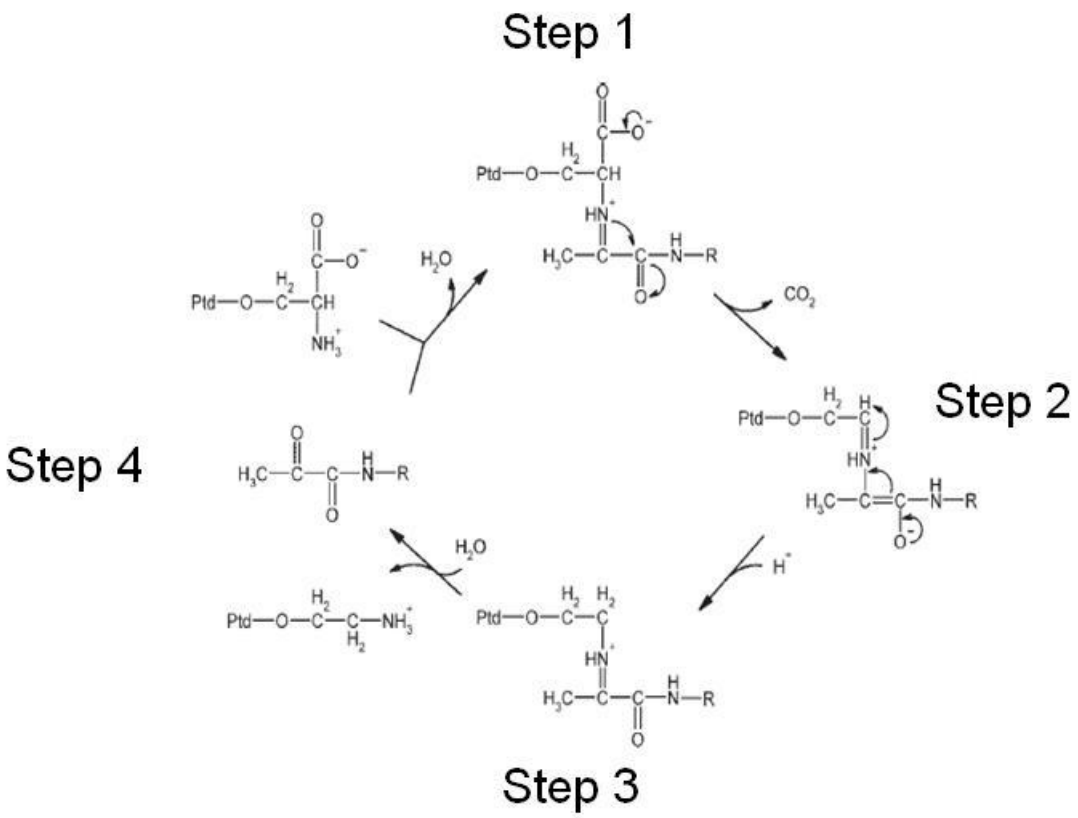

Fig. 4.3
A figure showing the four step reaction scheme of PS decarboxylation.
1) First, PS decarboxylation occurs via the formation of Schiff's between the a-carbonyl carbon of the covalently bound pyruvoyl prosthetic group and the primary amine of serine from PS.
2) Second, electron rearrangement favors decarboxylation and the formation of an azomethine intermediate. 3) This step is followed by a subsequent protonation which generates PE in a Schiff's base linkage with PSD. 4) The pyruvoyl prosthetic group is regenerated by addition of water across the Schiff's base, and thereby PE is released from the active site of the enzyme
Ptd refers to the phosphatidyl group of PS and R refers to the c-terminus of the PSD enzyme. Note: the pyruvoyl group is shown in amide linkage with the amino terminus of the catalytic subunit. (Adapted from Voelker, D. R. et al. 1997 [103])

In vitro, solubilized PSD from *E. coli* binds to a mixture of micelles composed of detergent and substrate. It was thus experimentally determined that PSD activity is dependent on the membrane environment as dictated by the critical micelle concentration and the availability of substrate [110].

Mammalian PSDs have also been shown to demonstrate substrate specificity. Through pulse labeling of both baby hamster kidney cells and CHO cells with [^{3}H] serine, it was determined that PSD enzymes preferred hydrophilic PS species to hydrophobic species. Furthermore, given the latter two cell types synthesize the majority of their PE via the PSD pathway, it was not surprising to that the amount of hydrophobic diacyl molecular species was much higher in PS than in PE [111].

Although most mammalian tissues contain polyunstaturated fatty acid PS constituents, the degree of preference between tissues appears to vary. Through liquid chromatography coupled to electron spray ionization mass spectrometry experiments *Kevala et al*. showed that rat brain cortex and liver have the highest specificity for hydrophilic PS molecules [112]. When mitochondrial PE levels were measured however, the specificity of PSD for acyl-substituents did not account for the small differences in PE acyl-chain-saturations across tissues [15]. Thus, this result suggests that the remodeling of PE by deacylation-reacylation may be more important to maintaining mitochondrial PE fatty acyl chain profiles than PS decarboxylation.

4.6 Regulation of PSD

Little is known about the regulation of PSD at the transcriptional and the post-translational levels. Studies by *Overmeyer et al*. however, have shown that the levels of Psd1p mRNA in yeast can be reduced by increases in intracellular inositol and choline [113]. Interestingly, however, Psd2p in the Golgi of yeast is unaffected by this repressive response, suggesting that different pools of PE may

exist within yeast membranes [114]. In addition, the amount of Psd1p in yeast is highest just prior to entrance into the growth phase, demonstrating that mitochondrial PE is important for yeast growth [114].

Despite the limited knowledge of PSD regulation, it is widely accepted that PSD is a physiologically important enzyme as it is ubiquitously expressed in all mammalian tissues.

4.7 Physiological Importance of the PSD Enzyme

The presence of PSD in all organisms and its ubiquitous expression across all mammalian tissues suggest that it is a critical enzyme for cellular survival [96]. Indeed, some organisms possess several PSDs, each unique to a specific subcellular location. However, PSD activity and its contribution to PE biosynthesis is variable across different cell types [68].

In most cultured cells, the majority of mitochondrial PE is synthesized by PSD. This was demonstrated by *Shaio et al*. in 1994 through measuring [^{3}H] serine incorporation into PE of mitochondrial membranes [18]. In the PSD pathway, serine is incorporated into PS and then decarboxylated on the MIM by PSD. After treating cells with hydroxylamine to inhibit PSD activity, it was found that there was a three-fold increase in MAM [^{3}H] PS and a ~50% reduction in mitochondrial PE synthesis [18]. Moreover, when [^{3}H] ethanolamine, a precursor to PE in the CDP-ethanolamine pathway was added, almost no [^{3}H] PE was detected on the MIM [18]. Together, these results demonstrated that the majority of mitochondrial PE is synthesized through the PSD pathway, and PE synthesized

from other pathways such as the CDP-ethanolamine pathway cannot be readily incorporated into mitochondrial membranes.

It is known that PE levels are tightly regulated in many organisms, as the over expression of both type I and II PSDs by several fold in bacteria, yeast, and plants does not alter PE levels or create physiological effects [98, 115, 116]. These results suggest that PSD is not the rate limiting enzyme in the biosynthesis of PE, and that cellular PE levels are most likely regulated by PSD substrate availability, which is dependent on PS import into mitochondria.

Reductions in PSD activity resulting in decreases in PE levels, however, can have dramatic effects on cellular physiology. Researchers in our laboratory have studied the effects of a complete elimination of PSD in mammalian cells through the use of knockout mice. From breeding *Pisd*$^{+/-}$ mice, it was discovered that a complete elimination of PSD results in embryonic lethality between days eight and ten after conception [19]. When MEF cells were generated from the *Pisd*$^{-/-}$ embryos and imaged via electron microscopy, it was observed that these cells contained large numbers aberrantly shaped and mislocalized mitochondria. In addition, these MEFs had poor viability and did not divide, which suggests that PSD is necessary for normal mitochondrial function [19].

Interestingly, heterozygous *Pisd* mice appear to be outwardly normal and do not have any defects with respect to vitality or fertility. Moreover, a 50% decrease in *Pisd* mRNA which corresponded to an approximately 40% decrease in PSD activity, did not change PE levels across the tissues in these mice [19]. Thus, these results suggest that there is a minimum level of PSD activity which is

required for life, and that the PSD pathway for PE synthesis cannot be substituted by another, such as the CDP-ethanolamine pathway.

At present, the minimum levels of PSD activity and PE synthesized required for mammals is not known. Thus, one aim of this thesis is to explore and understand the consequences of PE reductions in mammalian cells.

Since the elimination of mitochondrial PSD (Psd1p) in yeast results in decreased viability but not lethality because yeast have two PSDs, numerous yeast knockout experiments have been performed to ascertain other possible functions of PSD. In yeast, the type I PSD is the preferred enzyme for PS decarboxylation, as the mitochondrial Psd1p accounts for approximately 80%, and Psd2p for approximately 20% of the total PSD activity [92, 93]. The level of mitochondrial PE was decreased in a yeast model which had the Psd1p gene eliminated. Through culturing these cells in fermentable and non-fermentable carbon sources, it was observed that these cells were respiration deficient and highly dependent on fermentation. Supplementation of these cells with PE, however, completely rescued the phenotype [117]. These results suggest that in yeast there is a direct correlation between the PE that is synthesized via the type I PSD enzyme and mitochondrial function.

As a follow up to this experiment, a Psd1p and prohibitin (phb1/2D) double knockout yeast strain was generated [117]. Prohibitin is a protein complex associated with the inner mitochondrial membrane and it is thought to be a chaperone for the electron transport chain (ETC) proteins and a scaffold that regulates mitochondrial morphology. Furthermore, mutations in the *phb1/2* genes

in humans have been associated with breast cancer, implicating the proteins as tumor suppressors [118, 119].When lethality occurred in only the double knockout strains, but not in either the Psd1p or phb1/2D single knockout strains alone, an interaction between the mitochondrial prohibitin protein complex and Psd1p was proposed [117, 120]. Thus, it is likely that PE deficiencies might affect not only the membrane physiology of mitochondria alone, but also the function of mitochondrial proteins.

In addition to PS decarboxylation, the Psd1p enzyme in yeast has been demonstrated to contain a second activity. In yeast, the loss of mitochondrial genomes (a phenotype known as rho0) induces the transcription of multiple-drug-resistance genes [121]. The transcription factor Pdr3 activates the expression of an ATP-binding cassette transporter gene known as *PDR5 [122]*. Pdr5 is a known aminophospholipid translocase which catalyzes the net outward movement of PE. In Rho0 cells, overexpression of Psd1p induces *PDR5* transcription and confers multiple drug resistance in a Pdr3 dependent manner[123]. Moreover, loss of the PSD1 gene in rho0 cells prevents activation of PDR5 expression. To test whether decreased PE levels are responsible for loss of multiple drug resistance, a decarboxylation defective Psd1p enzyme was expressed in rho0 cells. Interestingly, the transcription of PDR5 was not decreased (Table 4.1) [121]. This surprising result indicates that the PSD enzyme, and not PE, is responsible for the induction of multiple drug resistance in yeast.

Rho 0	**↑ Pdr3**	**↑ Pdr5**	**↑ drug resistance**
Rho 0/PSD1 KO	**↓ Pdr3**	**↓ Pdr5**	**↓ drug resistance**
Rho 0/Defective PSD	**↑ Pdr3**	**↑ Pdr5**	**↑ drug resistance**

Table 4.1
A table summarizing the phenotypes of Rho0 yeast cells upon PSD1 elimination and defective PSD add back.

4.8 Insights into the Effects of Minimum PSD Activity

Despite the CDP-ethanolamine pathway's inability to substitute for the PSD pathway in mammalian cell survival, it has been demonstrated that certain cells lines depend more on one pathway than the other [96]. Indeed, work by *Fullerton et al.* shows that primary hepatocytes depend much more heavily on the CDP-ethanolamine pathway for PE synthesis than that of the PSD pathway [124]. This finding suggests that PE synthesized via the latter two pathways are spatially separated, and furthermore, the turnover and total requirement for these two pools must be different across tissues.

Currently, the effects of mitochondrial PE reductions to near critical threshold levels in mammalian cells are not fully understood, however, there has been considerable work in done in bacteria and fungi models.

Experiments with *E. coli* and *B. subtilis* as well as numerous other gram positive and negative bacteria show that PSDs are the only source of PE in prokaryotic organisms [125]. A conditionally lethal strain of *E. coli* has been generated in which the cells carry a temperature sensitive PSD enzyme. When these cells were grown at the non-permissive temperature of 40°C, large amounts of PS began to accumulate and then subsequently, the cells became filamentous and lost viability [89]. Interestingly however, it was discovered that *E. coli* with a

99% reduction in PE levels are viable when supplemented with divalent cations [126, 127]. These results strongly suggest that PE is a phospholipid which plays an important role in the electrostatic stability of biological membranes.

4.9 Perspectives

Fifty years after the initial discovery of the PSD enzyme, we now know that two types of PSD enzymes exist, and that they can be differentiated based on structure and intracellular localization. We have also gained insights into the enzyme's catalytic mechanism and physiological importance.

At present, much of our understanding of PSD enzymes comes from bacterial and fungal models and many important questions are still unanswered. Some of these questions include: How is the PSD enzyme regulated? What is the 3-dimensional structure of a eukaryotic PSD? Why do some eukaryotic organisms possess multiple isoforms of the enzyme in different subcellular locations? Why is there a differential contribution of PSD to the synthesis of PE in different mammalian tissues? What are the consequences of decreased PSD activity in mammalian cells? What is the minimum amount of PSD activity required for life in mammals? In the following thesis, I shall attempt to answer some of these questions with results from my experiments.

4.10 Other Minor Pathways for Mitochondrial PE Biosynthesis

As previously mentioned, the predominant pathway for CHO cell mitochondrial PE biosynthesis is the PSD pathway. However, three other quantitatively minor pathways also exist, and these are the: CDP-ethanolamine, lyso-PE acylation, and PS-ethanolamine base-exchange pathways.

The three reactions of the CDP-ethanolamine pathway parallel that of the CDP-choline pathway. First, ethanolamine is phosphorylated by ethanolamine kinase (ETNK1 or ETNK2), second, phosphoethanolamine is converted to CDP-ethanolamine by the enzyme CTP-phosphoethanolamine cytidylyltransferase (ET), and finally, CDP-ethanolamine is transferred to diacylglycerol to generate PE via CDP-ethanolamine:1,2-diacylglycerol ethanolaminephosphotransferase (EPT1) [12](Fig.4.4).

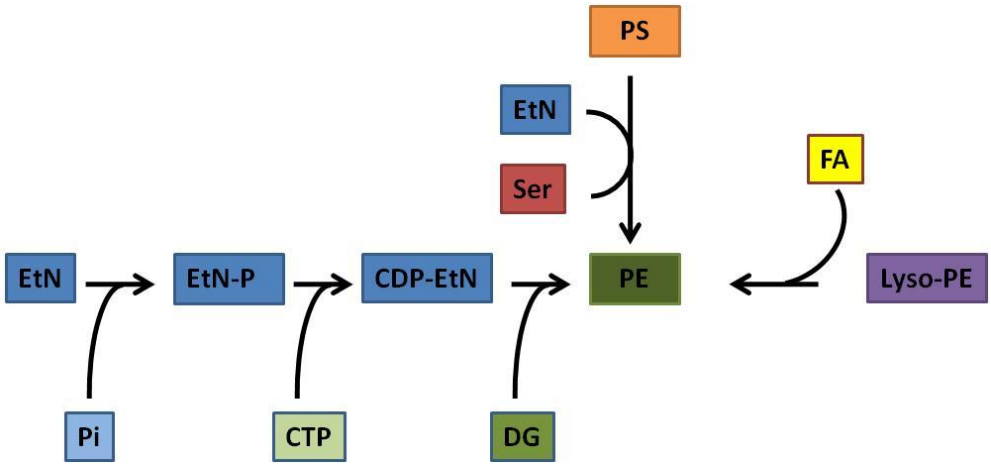

Fig. 4.4
A figure depicting the: CDP-ethanolamine, lyso-PE acylation, and PS-ethanolamine base-exchange pathways.

A quantitatively insignificant pathway by which the serine moiety of PS undergoes a base exchange with ethanolamine also occurs. Through using radiolabeled [2-^{3}H] ethanolamine, which can be distinguished from ethanolamine which is incorporated via the CDP-ethanolamine pathway, it was shown that ethanolamine can undergo a energy independent base exchange reaction with PS to generate PE [128].

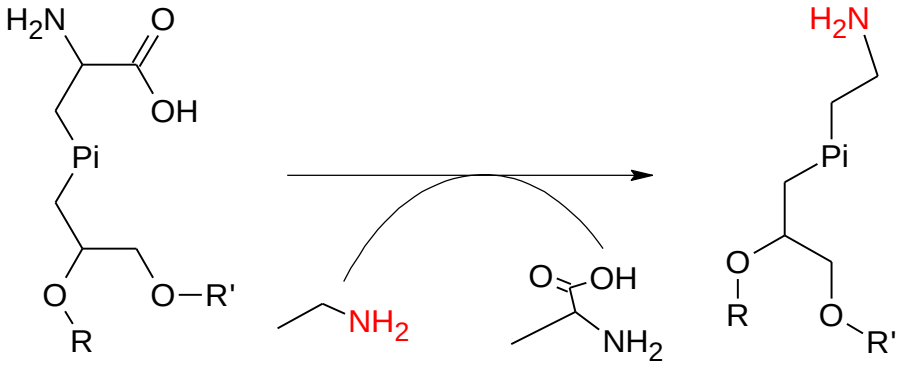

Fig. 4.5
A figure showing the base-exchange reaction by which PE is synthesized from PS. The amine moiety of ethanolamine is depicted in red.

Another quantitatively minor pathway by which PE may be synthesized is the acylation of lyso-PE. Although the uptake of exogenous lyso-PE and its subsequent conversion to PE in mammalian cells is not fully understood, a yeast model for this event has been studied by *Riekhof et al.* [129]. It is believed that lyso-PE is first imported across the plasma membrane by aminophospholipid translocases (Dnf1p and Dnf2p), and after uptake, an acyl-CoA-dependent acyltransferase then transfers a fatty acid molecule to the sn-2 position of lyso-PE to synthesize PE [129, 130].

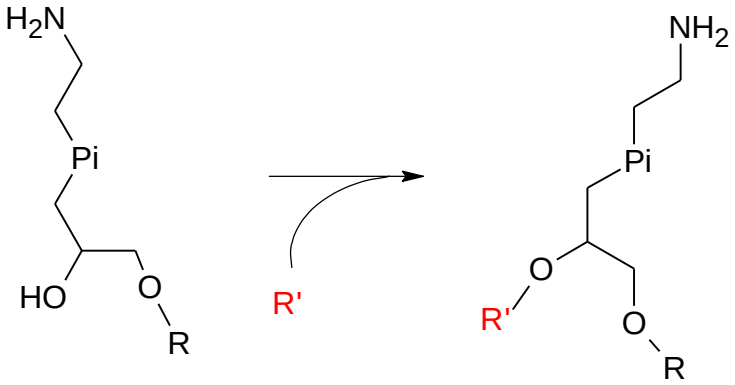

Fig. 4.8
A figure showing the acylation of lyso-PE at its sn-2 position to generate PE. R' in red represents a fatty acid molecule.

CHAPTER 5:

MITOCHONDRIAL PHYSIOLOGY

5.1 Introduction to Mitochondrial Function

Mitochondria are involved in a great number of cellular processes. In this chapter, I shall review some processes which pertain to this investigation, namely: mitochondrial electron transport and membrane potential maintenance, intracellular calcium regulation, mitochondrion-MAM interactions, and mitochondrial morphology.

5.2 Electron Transport and Membrane Potential

The average adult human being synthesizes roughly his or her own weight in ATP (100 to 150 moles or 50 to 75kgs) each day [131]. The majority of this massive amount of ATP comes from the process of oxidative phosphorylation. Eukaryotic oxidative phosphorylation occurs on the mitochondrial inner membrane (MIM) where a series of redox reactions sequentially release energy for ATP synthesis. The five enzymes in this pathway are multi-protein complexes called I, II, III, IV, and V, and together, they are called the respiratory chain. Complex I and II receive electrons from NADH and succinate, respectively, and pass them to a lipid soluble electron carrier called coenzyme Q which is mobile within the MIM. Complex III oxidizes the reduced coenzyme Q, and in turn reduces cytochrome c, which is also a lipid soluble electron carrier. Finally, complex IV couples the oxidation of cytochrome c to the reduction of molecular oxygen to create water (Fig. 5.1). The energy released by these exergonic reactions creates a proton gradient across the MIM where protons are pumped into the mitochondrial inter-membrane space. These protons then reenter the MIM through a specific channel in complex V. The energy released by this endergonic

process is thus, used by complex V to synthesize ATP [132]. In the following, I shall review proteins of the respiratory chain in greater detail.

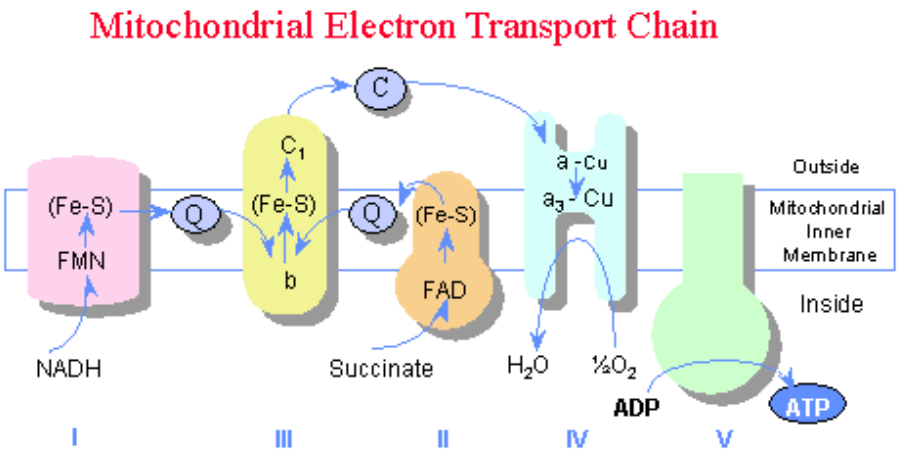

Fig. 5.1
A figure depicting the five respiratory chain complexes used for mitochondrial ATP synthesis.
(Adapted from http://aix-150.ion.ucl.ac.uk/neurochemistry/nmu/Mitochondrial-Disorders.htm, accessed July 2010)

Complex I

Complex I, also known as NADH-ubiquinone oxidoreductase, is a 45 subunit (900kDa) enzyme in mammals. The complex is composed of seven "core" polypeptides (designated ND1, 2, 3, 4, 4L, 5, and 6) which are encoded in the mitochondrial genome, and 38 nuclear encoded accessory peptides. Mutation studies using CHO cells have shown that at least 2 of the accessory subunits are required for life [133-135].

Complex I catalyzes the first reaction of the respiratory chain through reducing coenzyme Q (also called ubiquinone) with two electrons from NADH. The two electrons travel through complex I via a series of prosthetic groups which include flavin mononucleotide (FMN) and iron-sulfur clusters. During this

process 4 protons are pumped across the MIM. Finally, as the two electrons are transferred to ubiquinone, reducing it to ubiquinol, two more protons are pumped across the MIM [136].

A low-resolution structure of mammalian complex I has been solved via cryo-electron microscopy. In this structure, the enzyme is represented by an L-shape, with the long arm integrated into the MIM and the short arm reaching into the mitochondrial matrix. The short arm functions as NADH dehydrogenase and contains the FMN cofactors as well as seven iron-sulfur clusters. The long membrane bound arm, is believed to be involved in the translocation of protons [136-138].

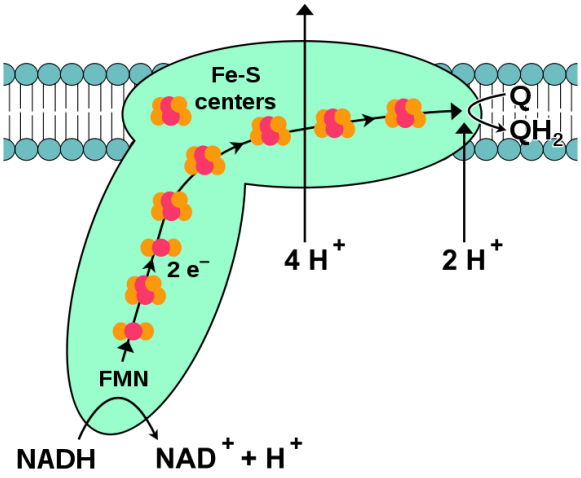

$$NADH + Q + 5\ H^{+}_{matrix} \rightarrow NAD^{+} + QH_2 + 4\ H^{+}_{intermembrane}$$

Fig 5.2
A figure showing complex I oxidizing NADH and then sequentially transferring two electrons to FMN, Fe-S, and ultimately to ubiquinone. The net equation of the reaction involving the translocation of four protons across the MIM is also depicted. (Adapted from: http://en.wikipedia.org/wiki/Oxidative_phosphorylation. Accessed July 2010)

Complex II

Complex II, also referred to as succinate: ubiquinone oxidoreductase, is the simplest enzyme in the respiratory chain, consisting of only four subunits. The two largest subunits, called SdhA and SdhB which contain flavoprotein (Fp) and iron-protein (Ip) groups respectively, protrude into the mitochondrial matrix and function as the enzyme succinate dehydrogenase in the citric acid cycle (Fig. 5.3). In mammals, the genes encoding SdhA and SdhB are both found in the nucleus and their corresponding peptide sizes are approximately 70 kDa and 27 kDa. These two subunits are anchored to the MIM by two other integral membrane proteins called SdhC and SdhD [139]. Interestingly, the x-ray crystallographic structure of SdhC and SdhD subunits together includes PE and cardiolipin within their hydrophobic core, which suggest that phospholipids may play an importance role in the structure complex II [140].

Electrons from the oxidation of succinate to fumarate in the citric acid cycle are channeled through complex II to ubiquinone. X-ray crystallographic analyses of *E. coli* complex II suggests that two electrons travel from succinate to ubiquinone via one flavin and three iron-sulfur prosthetic groups in a transfer that is reminiscent of complex I (Fig. 5.3). The transfer of electrons from succinate to ubiquinone, however, yields less energy than that of NADH from complex I, as no protons are being pumped across the MIM in complex II (Fig. 5.3). Thus, complex II is unique in that it directly links the citric acid cycle to the electron transport chain [141, 142].

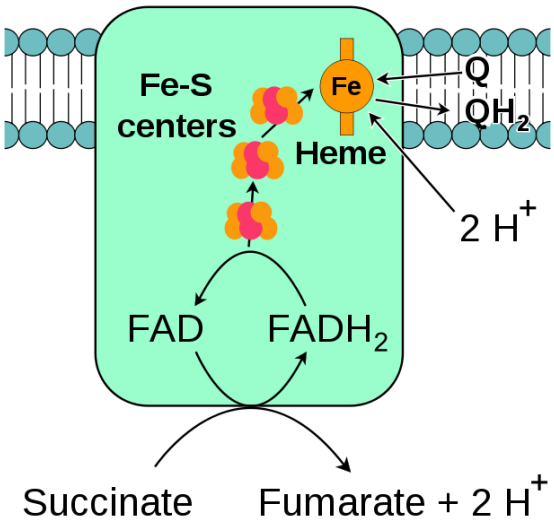

$$Succinate + Q \rightarrow Fumarate + QH_2$$

Fig. 5.3
A figure showing complex II within the MIM converting succinate to fumarate and transferring two electrons to ubiquinone in the process. (Adapted from: http://en.wikipedia.org/wiki/Oxidative_phosphorylation. Accessed July 2010)

A CHO cell mutant lacking complex II assembly and activity has been generated. The mutation has been established to be from a single nucleotide change in the tryptophan codon of SdhC [143]. As a result of this mutation, SdhA and SdhB subunits lack activity and are unable to associate and integrate into the MIM. Consequently, the cells were observed to be respiration-deficient and unable to grow in media with reduced glucose. Thus, these results suggest that SdhA and SdhB are assembled concomitantly with their attachment to the MIM, and the integral membrane proteins appear to participate in the folding and formation of succinate dehydrogenase [144].

Complex III

Complex III, also called ubiquinone-cytochrome c oxidoreductase or bc_1 complex after its two cytochromes, is a dimeric enzyme with each monomer

containing 11 subunits. Complex III catalyzes the oxidation of ubiquinol or QH_2 by sequentially transferring its two electrons to two molecules of cytochrome c. Since cytochrome c can only accept one electron, complex III uses a two step process to transfer electrons from QH_2 to cytochrome c (Fig. 5.4). In the first step, one electron from QH_2 is transferred to cytochrome c and another is transferred to a second Q molecule to generate a Q^- (ubisemiquinone radical). This step is complete when the oxidized QH_2 and reduced cytochrome c are released and two protons are pumped across the MIM. In the second step, a new QH_2 molecule arrives and donates one electron to cytochrome c and one electron to the previous Q^- radical. In this step, the Q^- radical is made into a QH_2 and two more protons are pumped across the MIM. Thus, the end result is that the equivalent of one QH_2 is oxidized, two cytochrome c molecules are reduced, and four protons are pumped (Fig. 5.4) [145-147].

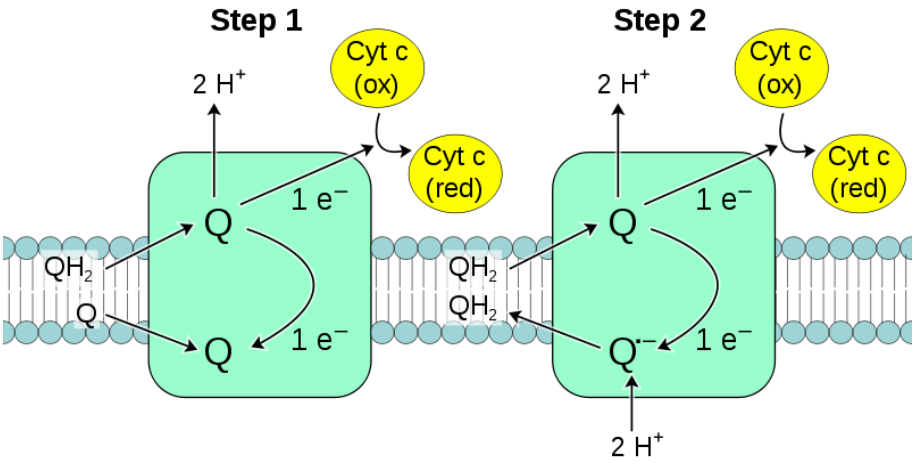

$$QH_2 + 2\ Cyt\ C_{oxid.} + 2H^+_{matrix} \rightarrow Q + 2\ Cyt\ C_{red.} + 4\ H^+_{intermembrane}$$

Fig. 5.4
A figure showing complex III dimers within the MIM catalyzing the transfer of two electrons from ubiquinol to two molecules of cytochrome c and pumping four protons in the process. (Adapted from: http://en.wikipedia.org/wiki/Oxidative_phosphorylation. Accessed July 2010)

In the mammalian complex III monomer, one peptide is encoded by the mitochondrial genome and is incorporated as cytochrome b. The other ten peptides are encoded by the nuclear genome and are imported and assembled within the MIM. Mutagenesis studies in yeast and *Neurospora* have shown that only the cytochrome b, c, and Rieske iron-sulfur protein are functionally important, as they are the only subunits participating in electron transfer and proton translocation. It is believed that the eight other subunits which have no prosthetic groups are involved in the processing and import of complex III proteins from the cytosol [147].

The phospholipid requirement of complex III for activity was first discovered through attempts to disassociate the complex using detergents and guanidine. When phospholipids were extracted from bovine heart mitochondria, it

was observed that complex III lost significant activity. However, the addition of PC and PE in Triton X-100 detergent was able to rescue the loss of activity, suggesting that complex III requires PC and PE for activity. Later quantitative measurements and structural modeling have provided evidence that the complex III dimers must are surrounded by a complete "annulus" of phospholipid[148]. Furthermore, in bovine complex III, it is believed that eight to nine tightly bound cardiolipin molecules surround each monomer. The removal of the cardiolipin by phospholipase digestion interestingly causes an irreversible loss of activity which cannot be rescued by phospholipid add-back, suggesting that cardiolipin is an integral part of complex III structure [149].

Complex IV

Complex IV, generally referred to as cytochrome c oxidase (COX), is the terminal enzyme of the mitochondrial electron transport chain. COX catalyzes the transfer of four electrons from four molecules of cytochrome c to O_2, resulting in two molecules of water (Fig 5.5). As the four electrons are transferred from the intermembrane space to the matrix, four protons are also transferred out of the matrix, resulting in a net transfer of four positive charges [150, 151].

In mammals, COX is 200kDa enzyme composed of 13 subunits, three of which are encoded in the mitochondrial genome (COX1, COX2, and COX3). The other ten subunits which are encoded in nucleus are named COX4, COX5a, COX5b, COX6a, COX6b, COX6c, COX7a, COX7b, COX7c and COX8 [150-152]. Structurally speaking, the core of COX is composed of the three large

mitochondrially encoded catalytic subunits surrounded by ten peripheral subunits [147].

COX was the first ETC complex to have its x-ray crystallographic structure determined at high resolution (~2.8Å) [152]. It is known that COX is active as a dimer, with each dimer requiring several prosthetic groups. These prosthetic groups include: a zinc complex, a magnesium complex, two hemes (a and a3), and two copper centers (CuA and CuB). In detail, the heme a and the a3-CuB center are both located within COX1, the CuA center is located in COX2, and the Zn^{2+} and Mg^{2+}ions are located COX5b. The mechanism of catalysis is believed to occur through the transfer of electrons from cytochrome c to the CuA site, to heme a, and then to oxygen in the heme a3-CuB center producing water (Fig. 5.5) [153].

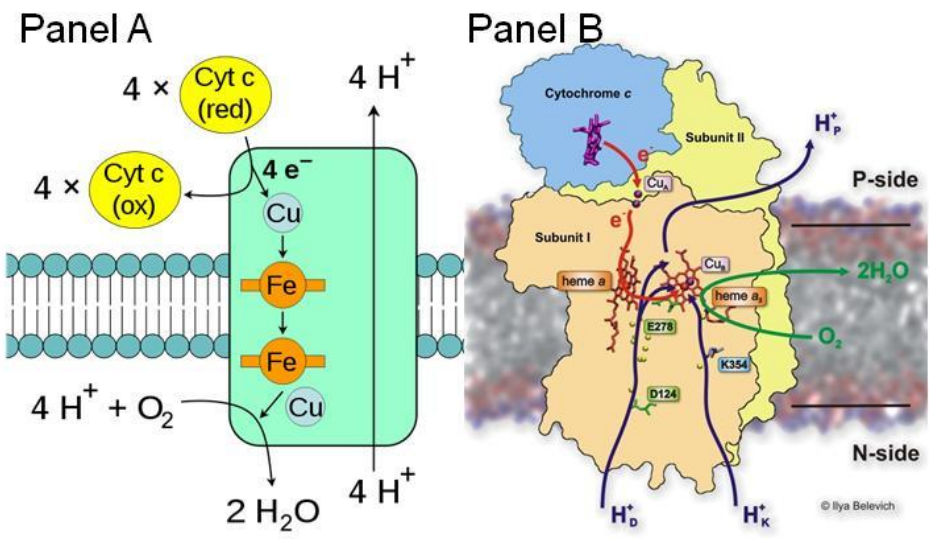

$$4\ Cyt\ C_{red.} + O_2 + 8H^+_{matrix} \rightarrow 4\ Cyt\ C_{oxid.} + 2\ H_2O + 4H^+_{intermembrane}$$

Fig. 5.5
(Panel A) A figure depicting the oxidation of four cytochrome c molecules and transfer of their electrons to molecular oxygen by complex IV. (Adapted from: http://en.wikipedia.org/wiki/Oxidative_phosphorylation. Accessed July 2010). (Panel B) The protein structure of complex IV with its heme and copper centers shown. (Adapted from Belevich et al. 2009) [154].

Since COX is the rate limiting enzyme in oxidative phosphorylation, its regulation has been extensively studied [153]. It is known that numerous hormones, kinases, secondary messengers, and membrane lipids are involved in the regulation of COX. For example, thyroid hormone can stimulate COX activity by binding to COX5a, ATP/ADP can inhibit/activate it by allosteric regulation, and kinases like c-SRC, PKCε, PKCδ, and cAMP dependent protein kinase can regulate its activity through the phosphorylation of different subunits[153].

The phospholipid requirement of COX for activity was first studied by *Paradies et al.* in 1997 through the addition of phospholipid liposomes to purified COX [155]. Through calculating the amount of cardiolipin required for electron

transport, it determined that COX has an *in vitro* Kd of <0.1μM. The binding of other phospholipids such as PC, PE, phosphatidylglycerol, and phosphatidic acid, however, were all much lower (Kd <20.0μM) [156]. Later, x-ray crystallographic studies showed that there are in fact 13 integral phospholipids involved in maintenance of COX protein structure. These 13 lipids, which were co-crystallized with COX include: two cardiolipins, one PC, three PEs, four phosphatidylglycerols, and three triacylglycerols [157]. The differential affinities of the lipids for binding COX was explained through studies using a combination of mass spectrometry and x-ray crystallography, which provided evidence that each lipid head group has a specific binding site within COX. Moreover, molecular simulations found that the fatty acid chain lengths and bond saturation positions were important to the dimerization of COX. To study the involvement of lipids in the electron transfer process, a synthetic amino acid label (dicyclohexylcarbodiimide) was incorporated into the O_2 transfer pathway of COX. When the two palmitate tails of phosphatidylglycerols interacted with dicyclohexylcarbodiimide and sterically blocked the transfer of electrons to O_2, it was proposed that the palmitates of phosphatidylglycerol are involved in the regulation of electron transfer [157]. Thus, these results strongly suggest that COX requires a particular group of lipids for structure and function.

COX deficiencies have been extensively studied in humans. The majority of human COX genetic defects are the result of mutations in nuclear encoded "accessory" subunits. The first identified COX deficiency with a nuclear origin was Leigh syndrome, which is a fatal neurodegenerative disorder that has an early

onset and affects the whole body [158]. LS patients who have 10 to 25% COX residual activity die between 6 months to 12 years of age[159, 160]. A less severe form of LS also exists and is known as the French–Canadian Leigh syndrome. The clinical presentation of this form includes mild regression of psychomotor skills and a fatal lactic acidosis with death occurring between 3 and 10 years of age. The measured COX activity in these patients was approximately 23 to 30% that of health individuals [161]. Thus, these results suggest COX activity is important for neuron function and that there is a minimum level of COX activity which is required for life.

ATP Synthase

ATP synthase also called, the F_oF_1 complex, is an enzyme which synthesizes ATP from ADP and inorganic phosphate. The name F_oF_1, comes from the two complexes which were initially isolated by *Hatefi et al*, with the F_1 complex being soluble and F_o portion being an insoluble membrane complex [162]. The F_o portion of the complex spans the MIM and contains a proton channel into the mitochondrial matrix, and the F_1 subunit utilizes the potential energy of protons passing through the F_o subunit to catalyze the synthesis of ATP. The F_1 complex has eight subunits which are named α, β, γ, δ, ε, F6, d, and OSCP. The most prominent feature of the F_1 complex is its α and β subunits which form three identical dimers which surround a γ subunit, resembling the structure of a rotary engine (Fig 5.9)[163].

The two step catalytic mechanism of ATP synthase was proposed by John Walker and Paul Boyer, for which they won the Nobel Prize in Chemistry. The

mechanism of ATP synthesis occurs through three conformational changes in the α-β dimer. These conformations are referred to as the loose (L), tight (T), and open (O) steps. In the first step, passage of a proton fuels a 120° turn of the F1 complex, which leads to the release of ATP from the T site and the binding of ADP and Pi bind to an (O) site. In the second step, an additional 120° rotation occurs which allows the ADP and Pi, now bound at a T site to undergo a spontaneous conversion to ATP, while the O site from which ATP was released binds another ADP and Pi to begin the process again (Fig. 5.6) [164].

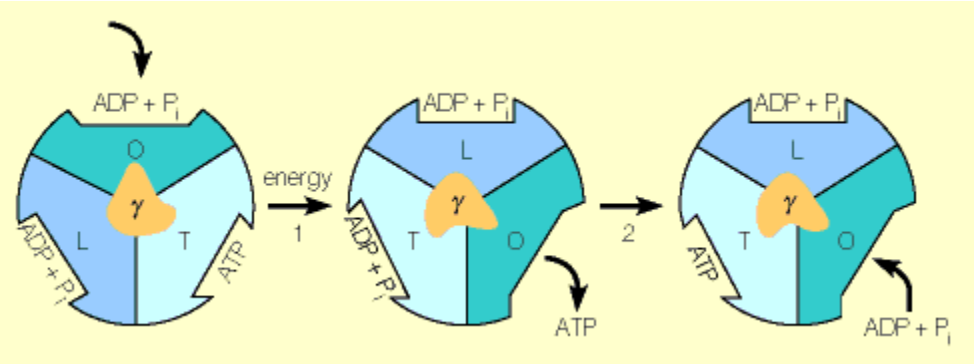

Fig. 5.6

A figure showing the loose (L), tight (T), and open (O) steps of ATP synthesis by ATP synthase. (Adapted from Zhou et al. 1997) [165].

The phospholipid requirements of ATP synthase for optimum activity have been studied in conjunction with MIM morphology in yeast. The MIM contains micro-compartments (cristae) which define the topology of the MIM [166]. It is know that these cristae are connected to the periphery of the MIM membrane by narrow tubular junctions (Fig. 5.7). The respiratory chain supercomplexes and ATP synthase are significantly enriched in the cristae near

the boundary membranes, as their high molecular weight prevents them from diffusing across the tubular junctions [167].

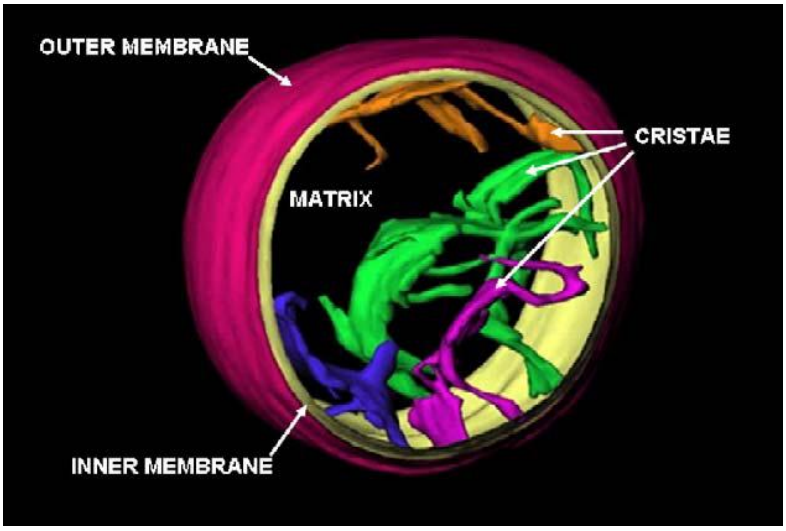

Fig. 5.7
A figure showing four spatially separated mitochondrial cristae invaginations and their contacts with the MIM (Adapted from Mannella et al 2006) [166].

Calculations of the electrostatic field strength at supercomplex rich regions of cristae show that there are significantly higher charge densities giving rise to local pH gradients. Thus, the mitochondrial cristae acts as proton trap for the optimum function of ATP synthase[168].

In vitro simulation experiments using large unilamellar vesicles containing PC, phosphatidylglycerol and cardiolipin have demonstrated that cardiolipin is essential to the formation of high charge density cristae-like membranes. Vesicles which lacked cardiolipin in particular, had reduced numbers of cristae-like membrane curvatures and lower charge density [169]. These results were further confirmed by electron microscopy studies of isolated yeast mitochondria lacking cardiolipin. These mitochondria were observed to have abnormal cristae

formation with decreased ATP synthase formation and activity [170]. Thus, these results show a strong connection between membrane phospholipid composition and cellular energetics as particular phospholipids such as cardiolipin are crucial to the formation and function of ATP synthase.

ATP Synthesis Calculation

In this section, I shall consider the major sources of cellular ATP. Glycolysis, pyruvate dehydrogenation, and the citric acid cycle are three processes which mostly contribute to ATP synthesis indirectly, as they only produce a net total of 4 ATPs directly (Fig. 5.9). However, six dehydrogenation steps, one in glycolysis, another in pyruvate dehydrogenation, and four more in the citric acid cycle together produce 10 molecules of NADH and 2 moles of FADH per molecule of glucose. Reoxidation of these two electron-rich molecules are what quantitatively yield the most ATP.

$$Glucose + 2\ ADP + 2Pi + 2NAD^+ \rightarrow 2\ Pyruvate + 2\ ATP + 2\ NADH + 2\ H2O + 2\ H^+$$
$$2\ Pyruvate + 2\ NAD^+ + 2\ CoA{\sim}SH \rightarrow 2\ acetyl{\sim}CoA + NADH + 2CO_2$$
$$\underline{2\ Acetyl{\sim}CoA + 4\ H_2O + 6\ NAD^+ + 2\ FAD^+ + 2\ ADP + 2Pi \rightarrow 4\ CO_2 + 6NADH + 2FADH_2 + 2CoA{\sim}SH + 2\ ATP + 4H^+}$$
$$Glucose + 10\ NAD^+ + 2FAD + 2H_2O + 4ADP + 4Pi \rightarrow 6CO_2 + 10NADH + 6H^+ + 2FADH_2 + 4ATP$$

Fig. 5.8
An equation showing the net products yielded after one molecule of glucose is oxidized through glycolysis, pyruvate dehydrogenation, and the citric acid cycle.

The quantity of ATP synthesized per mole of substrate oxidized is expressed as a P/O ratio. Thus, the P/O ratio expresses ATP synthesis with respect to the number of moles of phosphate incorporated into ATP relative to the number of moles of oxygen consumed. Experimental evidence from oxygen electrodes has demonstrated that mitochondrial oxidation of NADH and $FADH_2$ proceeds

with a P/O ratio of 3 and 2 respectively. Hence, for every mole of NADH and $FADH_2$ and oxidized, 3 and 2 moles of ATP are synthesized respectively. Thus, using the calculations from Fig. 5.8, 38 moles of ATP can be produced per mole of glucose (Fig. 5.9) [164].

$$4\ ATP + 10\ NADH\ \left(\frac{3\ ATP}{1\ NADH}\right) + 2\ FADH_2\left(\frac{2\ ATP}{1\ FADH_2}\right) = 38\ ATP$$

Fig. 5.9
Calculations for the number of ATP synthesized from the aerobic oxidation of one molecule of glucose.

Mitochondrial Membrane Potential

In respiring mitochondria, the process of pumping protons from the matrix to the intermembrane space generates a proton gradient. This proton gradient creates a pH differential and an electrical potential difference across the MIM. In fact, the pH inside an actively respiring mitochondrion is ~1.4 pH units higher than in the intermembrane space. This proton gradient also generates an electrical potential of approximately 0.14V across the membrane, because of the net outward movement of positively charges. The pH gradient (ΔpH) and the electrical potential ($\Delta\Psi$) together contribute to the proton motor force ($\Delta\mu_H$) (Fig. 5.10), which can also be expressed in terms of energy using the Nernst equation (Fig. 5.11) [132].

$$\Delta\mu_H = \Delta\Psi - 2.3(\frac{RT\Delta pH}{F})$$

Fig. 5.10
The definition of mitochondrial proton motor force ($\Delta\mu_H$) expressed as a sum of the mitochondrial membrane potential and pH gradient (note: the mitochondrial pH gradient is expressed as a negative value). Where $\Delta\Psi$ is the mitochondrial membrane potential, R is the ideal gas constant 8.314 J $K^{-1}mol^{-1}$, and F is the Faraday constant 96,485C mol^{-1}.

$$\Delta G^{\circ\prime} = -nF\Delta E^{\prime}$$

Fig. 5.11
The Nernst equation showing reduction potential is proportional to the number of moles of reactant multiplied by the reactant-half-cell potential. Where n is the number of moles of reactant, F is the Faraday constant 96,485C mol^{-1}, and $E^{\prime}$ is the net half cell potential of the reaction.

Given what we know about the proton and electrical gradients of the MIM, one can calculate the energy of proton motor force of at standard conditions as follows (Fig.5.12):

$$\Delta\mu_H = (0.14V) - 2.3\left(\frac{RT(-1.4)}{96.5\ kJ\ mol^{-1}V^{-1}}\right) = 0.224V$$

$$\Delta G^{\circ\prime} = -1\ mole\ H^{+}\left(96.5\ kJ\ mol^{-1}V^{-1}(0.224V)\right) = 21kJ$$

Fig. 5.12
A calculation of $\Delta\mu_H$ energy available for the synthesis of one molecule of ATP using formulas for proton motor force and the Nernst equation respectively.

Thus, the free energy available from the reentry of one mole of protons across the MIM is equivalent to 21kJ, which has been experimentally shown to be enough energy to synthesize one mole of ATP [132].

Regulation of Oxidative Phosphorylation

The regulation of oxidative phosphorylation is dictated by substrate availability and not by allosteric mechanisms. These regulatory substrates include ADP, Pi, O_2 and oxidizable metabolites such as NADH and $FADH_2$[171]. Early work by Lardy and Chance with isolated mitochondria demonstrated that oxidative phosphorylation is tightly coupled with ATP synthesis. Through

providing mitochondria with various substrates, it was observed that the rate of oxygen consumption is most tightly coupled to the supply of ADP and Pi. Not only is ATP synthesis absolutely dependent on continued electron flow from substrates to oxygen, but electron flow in normal mitochondria occurs only when ATP is being synthesized [172, 173]. This regulatory process called respiratory control makes metabolic sense because it ensures that substrates are not oxidized wastefully[171]. Thus, utilization of ADP and Pi is controlled by the physiological need for ATP. It is important to note that one of the main focuses of this thesis is on abnormal mitochondria which lack respiratory control. Later in this chapter, I shall consider established models for the effects of defective respiratory control.

In most aerobic mammalian cells, the level of ATP is approximately four- to ten-fold higher than that of ADP. If the energy demands on a cell cause ATP to be consumed at a high rate, the resultant accumulation of ADP will stimulate respiration and ATP synthesis [132]. Hence, one can calculate the theoretical mitochondrial membrane potential and proton gradient from the number of moles of ATP required for synthesis using the proton motor force formula (Fig. 5.10 and Fig. 5.11). The energy state of the cells has profound effects on the structure of their mitochondria. In actively respiring mitochondria, the MIM folds on itself, leaving a greatly enlarged intermembrane space (Fig. 5.13) [166].

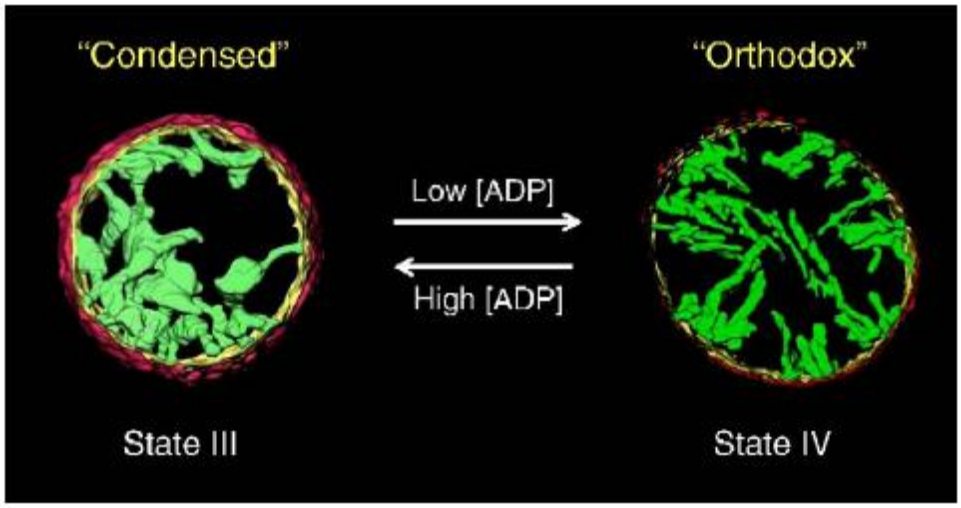

Fig. 5.13
A figure showing the changes in MIM structure with respect to cellular respiration activity. State III is a state of low oxidative phosphorylation and state IV is a state of high oxidative phosphorylation. (Figure adapted from *Mannella et al.* 2006) [166].

5.3 Mitochondrial Membrane Hyperpolarization

Although abnormalities in mitochondrial function leading to decreased membrane potential and cell death are commonly observed, there are few metabolic processes which lead to membrane hyperpolarization. The loss of respiration control resulting in mitochondrial membrane hyperpolarization is most prominently observed in cancer cells [174]. This effect was first proposed by *Warburg et al.* in 1930 when it was observed that cancer cells displayed an "aerobic glycolysis" phenotype [175-177]. Recent positron emission tomography (PET) imaging studies have confirmed this theory through showing that most malignant tumors have increased glucose uptake with reduced respiration [178]. It is believed that hyperpolarization occurs as a result of decreased ATP synthase activity. As ATP synthase activity is reduced, the mitochondrial proton gradient builds from the residual electron transport [179]. Thus, this abnormality in

respiratory regulation keeps cancer cell mitochondria in a meta-senescent stage [174]. At present, is unclear whether aerobic glycolysis is the cause or the result of oncogenesis, as there is no established link between mitochondrial damage and reduced membrane hyperpolarization [174].

Increased glycolysis and decreased cellular respiration leading to MIM hyperpolarization is favorable to cancer cell growth for several reasons. Firstly, early carcinogenesis typically occurs in hypoxic environments which require proliferating cells to rely on glycolysis for energy production [178, 180]. Secondly, glycolytic cancer cells have a proliferative advantage by excreting glycolytic metabolites such as lactic acid, which contribute to the breakdown of the extracellular matrix, providing the cells with increased metastatic potential [181]. Interestingly, as metastatic cancers proliferate into oxygen rich environments, they retain their phenotype, which gives rise to the paradox of aerobic glycolysis [181]. Thirdly, it is believed that cancer cells up-regulate glycolysis and inactivate mitochondrial metabolic processes to acquire resistance to apoptosis [182]. It is known that several oncoproteins can induce the activation of glycolytic enzymes. For example, the pro-survival signaling kinase, Akt, activates hexokinase, the enzyme which catalyzes the first committed step of glycolysis. Akt prevents apoptosis through mediating the translocation of hexokinase to the MIM where hexokinase binds to the voltage-dependent anion channel (VDAC) to prevent it from participating in the apoptosis cascade [183].

The understanding of how membrane hyperpolarization contributes to apoptosis resistance was elucidated through the normalization of membrane

potentials using anti-cancer drugs. Pyruvate dehydrogenase (PDH) is a key enzyme that determines whether glucose metabolism ends in glycolysis or continues on to the citric acid cycle to provide reducing substrates for cellular respiration [184]. In most metastatic cancer cells, PDH is down regulated. However, the reactivation of PDH by dichloroacetate restores reactions of the citric acid cycle [185]. The availability of reducing substrates allows ATP synthase to function, and thus, $\Delta\Psi$ becomes more positive as protons are utilized for ATP synthesis. Apoptosis is also restored through membrane depolarization. As $\Delta\Psi$ becomes more positive, the $\Delta\Psi$-sensitive mitochondrial transition pore (MTP) allows the efflux of cytochrome c and apoptosis inducing factor into the cytosol to initiate the apoptosis cascade [186]. Therefore, respiratory control, mitochondrial membrane potential, and apoptosis are tightly coupled processes which are key to oncogenesis.

5.4 Mitochondrial Calcium Storage

Calcium ions are powerful secondary messengers which participate in many important cellular signaling pathways, including cell death and proliferation, neurotransmitter release, and cellular excitability [187-189]. Under normal physiological conditions, cytosolic calcium levels are kept low (~$1x10^{-7}$M), such that they are 10,000 fold lower than extracellular levels. Cells achieve low cytosolic calcium concentrations through energy-dependent export and intracellular sequestration. Mitochondria are known to transiently import and export calcium through the use of their proton motor force. Mitochondrial calcium import mainly occurs through the $\Delta\Psi$-dependent inner membrane calcium

uniporter[190]. This import of calcium into the matrix is not only essential for the function of calcium sensitive mitochondrial ETC enzymes but also acts as a mechanism for the removal of calcium from local areas in the cytosol[191]. Mitochondrial calcium efflux occurs mainly through the permeability transition pore (PTP) [192]. Thus, mitochondria are essential for the maintenance of intracellular calcium homeostasis.

Pathological conditions which overload cytosolic calcium levels can cause a cascade of mitochondrial changes which eventually lead to cell death. Firstly, a high level of calcium induces the mitochondrial PTP to fully open in a high-conductance state which allows the diffusion of large molecules [193]. Next, the excessive entry of calcium into the mitochondria triggers the opening of the mitochondria permeability transition pore (MPTP), which in turn stimulates a vicious cycle of mitochondrial calcium-induced calcium release, leading to further MPTP opening [194]. The dramatic change in mitochondrial membrane permeability also collapses the $\Delta\Psi$. The decreased $\Delta\Psi$ leads to reduced oxidative phosphorylation and ATP synthesis which subsequently induces mitochondrial swelling [193]. The decreased $\Delta\Psi$ also stimulates the release of cytochrome c, activates caspases, and induces DNA fragmentation, all of which ultimately lead to cell death [195-197].

At present, abnormalities in mitochondrial calcium regulation have been associated with several neurodegenerative diseases, including glaucoma, diabetic retinopathy, Parkinson's disease, and Alzheimer's disease [198-200].

5.5 Interaction with MAM

The ER membrane contains a special domain called the mitochondrial associated membrane (MAM) which is transiently associated with the mitochondrion. The MAM is involved in a number of house-keeping cellular processes which include: lipid synthesis, non-vesicular lipid transport, and mitochondrion-ER calcium regulation and transmission [201-204]. In the following, I shall review the structure of MAM and its function in regulating cellular metabolism.

The discovery of MAM is credited to research from our laboratory which showed that there exists a special domain of the ER that co-isolates with mitochondria. Through labeling cells with [^{3}H] serine, it was found that MAM contained phospholipid synthetic activities not found on other membranes. These activities include: the PS synthases, phosphatidylethanolamine N-methyltransferase, and CDP-choline:diacylglycerol choline-phosphotransferase [51].

The visualization of MAM and its interaction with mitochondria emerged in the early 1990s through the use of high-voltage electron microscopes. It was discovered that only a small area of mitochondria, approximately 12% of the MOM associates with the MAM [205]. The distance between MAM and mitochondria, however, was estimated to be only approximately 10–25 nm [205]. This small distance is believed sufficient for the lipids and proteins of MAM and mitochondria to interact[205]. The disruption by homogenization of microtubules and intermediate filaments by which mitochondria and ER are anchored does not

separate MAM and mitochondria, suggesting that the two membranes are tethered together with filament proteins [206]. Although these proteins have not been identified, it is known that in living cells, ER membranes can migrate with highly mobile mitochondria. This co-localization can however, be disrupted both *in vivo* and *in vitro* through the alteration of calcium levels, suggesting that calcium sensitive filaments may be present [207].

The tethering of MAM and mitochondria at an appropriate distance has been shown to be important for mitochondrial function. For example, it is known that when the distance between the two membranes decreases below 5nm, mitochondrial calcium levels can rise to pro-apoptotic levels [205]. Moreover, increases in cytosolic calcium concentrations induced by the signal transduction molecule, inositol trisphosphate (IP3), have been shown to change this distance [205]. Indeed, receptors for IP3 have been found to be highly enriched in MAM [208]. Thus, the cellular homeostasis of MAM-mitochondrion interactions and calcium levels are two mutually dependant processes.

The MAM also regulates mitochondrial bioenergetics through changing mitochondrial calcium levels. It is known that mitochondrial calcium levels can regulate citric acid cycle and electron transport chain enzymes. For example, α-ketoglutarate and isocitrate dehydrogenase are directly activated by calcium, and pyruvate dehydrogenase is activated by calcium dependent dephosphorylation [209]. Hence, the presence of a wide range of hormones and neurotransmitter receptors which activate IP3 receptors on MAM can regulate the citric acid cycle by increasing mitochondrial matrix calcium concentrations.

PACS-2 is an ER protein which controls ER-mitochondrion communication, ER homeostasis, and apoptosis. In 2004, *Simmen et al*. showed that in Hela cells, ER-mitochondrion contact is dependent on PACS-2 [210]. Through silencing PACS-2 expression via siRNA transfection, it was shown that PACS-2 depletion results in decreased ER-mitochondrial contact and increased mitochondrial fragmentation. Interestingly, the $(\Delta\Psi)$ of PACS-2 depleted cells was normal compared to control cells, suggesting that PACS-2 regulates ER-mitochondria contact independently of pathways which compromise mitochondrial integrity [210].

The function of MAM in lipid synthesis and transport has been well documented since the early 1990s. After the initial reports of the PS synthases and phosphatidylethanolamine N-methyltransferase being enriched in MAM, other enzymes such as acyl-CoA: cholesterol acyltransferase (ACAT), and diacylglycerol acyltransferase (DGAT) were also identified to be highly enriched in MAM compared to the bulk of the ER [202, 211]. In addition, the transport of PS from MAM to mitochondria is the rate limiting step for mitochondrial PE synthesis via the PSD pathway [18, 103].

The cross-talk between MAM-calcium-signaling and lipid transport and biosynthesis was further investigated using a CHO cell model. Through altering the calcium levels in permeabilized cells with calcium chelation, it was found that both PS synthases depended on the ability of a calcium dependent ATPase at the MAM to uptake calcium into the ER [77]. As previously mentioned in chapter three, the transport of PS from MAM to mitochondria requires ATP. The addition

of 1mM calcium to permeabilized cells interestingly bypassed this ATP requirement and restored both PS synthesis and transport in calcium chelated cells [77]. Thus, if this process were to indeed occur *in vivo*, then the biosynthesis of PE would no doubt be regulated by MAM mediated calcium changes.

5.6 Mitochondrial Morphology

In vertebrates, mitochondrial size, shape, and number per cell greatly vary across cell types. For example, the human oocyte is estimated to contain greater than 100,000 mitochondria, while spermatozoa have only three to five exceptionally large mitochondria [212, 213]. The above mitochondrial diversity can be best understood through the dynamic process of mitochondrial fusion and fission, which together at equilibrium maintain mitochondrial numbers and morphology. In the following, I shall discuss the mechanisms of these two processes as well as the enzymes responsible.

Fission

Mitochondria grow through the insertion of new components into its membranes and matrix and divide into daughter organelles through the process of fission [132]. Although the regulation of mammalian mitochondrial fission is unknown at present, the process by which it occurs has been visualized via electron microscopy [214]. In yeast, mitochondrial fission begins with the association of three major proteins which reside on the mitochondrial outer membrane [215]. Fission is initiated by Fis1, which is an integral membrane protein with a single transmembrane domain. Its C-terminus is anchored to the outer membrane while its N-terminal domain contains a series of six helical tetra-

peptide fold pockets [215]. These pockets contact Mdv1p and Caf4p. Once, associated, this complex incorporates a dynamin-related GTPase called Dnm1p. Dnm1p and dynamin are known to assemble at the location of constriction where a daughter organelle buds [216, 217]. It has been proposed that Dnm1p and dynamin together, assemble in a spiral and constrict the inner and outer membranes in a GTP-dependent manner [218]. However, the exact mechanism of this constriction is unknown, as it is unclear whether contraction occurs through conformational changes in dynamin or through the loss of dynamin monomers [215]. In vitro evidence from experiments with unilamellar vesicles suggest that fission also requires lipid remodeling and lateral tension, which might be provided by microtubules pulling the organelle along intracellular tracks [219].

A pathway for calcium induced fission and mitochondrial fragmentation has recently been proposed. It is believed that, when cytosolic calcium rises as a result of mitochondrial dysfunction, Dnm1p is translocated to the mitochondrial outer membrane [220]. Dnm1p is further activated by dephosphorylation and is protected from ubiquitin-proteasome degradation by SUMOylation [221]. Thus, it is possible that mitochondrial fission, calcium dysregulation, and apoptosis may all be interrelated through mitochondrial health.

Fusion

Mitochondrial fusion is a unique process in that the mitochondrial inner and outer membranes must fuse sequentially without interaction [132].

Understanding of mitochondrial outer membrane fusion came about through the analysis a fruit fly mutation which results in sterility [222]. The

enzyme responsible for the latter sterility was identified as a mitochondrial outer membrane GTPase, named fuzzy onion (Fzo), after its large onion like structure [222]. This enzyme, named mitofusin (Mfn1 and Mfn2) in mammals, has two transmembrane domains linked to a cytoplasmic GTPase [223]. It is believed that fusion of the outer membranes occurs through the collisions of membrane-membrane contact sites. These collisions are thought to be brought about by interactions within cytoskeletal elements and ATP-dependent molecular motors. Once in contact, the mitofusins act as tethers, similar to the SNARE proteins in the secretary pathway to fuse the two outer membranes. This process is known to be dependent on mitochondrial inner membrane ΔpH but not the electrochemical gradient ΔΨ [224].

Mitochondrial inner membrane fusion requires an enzyme called OPA1, which when mutated, causes optic atrophy [225]. OPA1 is an integral membrane protein found on the inner membrane which has a GTPase localized in the intermembrane space. Although the exact mechanism of inner membrane fusion is unclear, it is known that OPA1 must interact with mitofusin and sufficient levels of GTP must be available [226, 227]. Inner membrane fusion interestingly is also different from outer membrane fusion in that both electrochemical and ΔpH gradients must exist [224, 228].

Mitochondrial fusion is a developmentally programmed process which has many genetic implications. For example, it is believed that fusion in heteroplasmic cells allows for particular mitochondria to have more than one genome at a time. Thus, this process may serve to homogenize mitochondrial

genomes in cells with many mitochondria and reduce the effects of mutagenesis [132].

5.7 Mitochondrial Motility

Mitochondrial motility has been examined in a variety of different cell types including: mammalian, plant, fungal, and algal cells [229]. Under confocal microscopy, mitochondria appear to slither and slide at rates ranging from 2 to 30μm/min in the direction of their long axes. This displacement is also accompanied by subtle shape changes, such as thickening and contracting along their long axes [230]. These small morphological changes have been proposed to be reflective of local changes in the internal arrangement of the cristae [231]. Interestingly, microinjections of ATP have been shown to immobilize mitochondria, suggesting that mitochondrial mobility is influenced by metabolic conditions [229].

Staining of mitochondria and cytoskeletal structures has clearly shown an association between the two. In insects, mitochondria have been observed to surround the mitotic and meiotic spindles suggesting that mitochondria are partially aligned or even possibly trapped within arrays of microtubules[231]. Studies using highly aligned microtubules of uniform polarity from the nutritive tubes of insect ovaria have shown that mitochondrial movement occurs in a salutatory fashion which is characteristic of motor-driven movements and is not compatible with simple Brownian motion [229, 231].

A series of experiments elucidating the connection between mitochondrial motility and cytoskeletal elements were performed by researcher at the

Hollenbeck laboratory. To determine whether motility is the result of microtubules (MT) or microfilaments (MF), chick sympathetic neurons were treated with vinblastine and cytochalasin E to remove the latter two cytoskeleton elements respectively [232-235]. In cells which were cultured with cytochalasin E, mitochondria retained bidirectional motility and appeared normal. However, in the cells which were cultured with vinblastine, the mitochondria had low motility and were trapped within the cell bodies, suggesting the MF alone was insufficient to support mitochondrial movement [235]. A second set of experiments was performed with mature neurons with axons already containing mitochondria. Now, when mature neurons were treated with cytochalasin E, mitochondrial motility increased, however, the net directional movement decreased, suggesting that MF may be important for directional motility [233]. When mature neurons were treated with vinblastine, motility was again significantly decreased, however, this time, it was observed that net retrograde transport was favored. Hence, these studies provide evidence that mitochondria use MF for slow short distance movements and MT for fast long distance movements [233].

Although the regulation of mitochondrial motility is still not fully understood, current evidence supports the idea that a number of GTPases, G proteins, and growth factors have the ability to affect mitochondrial motility in neurons [233, 236]. Furthermore, it has been observed that mitochondria with low membrane potentials are often transported towards the cell bodies of neurons, which may possibly reflect upon an aspect of quality control by turnover [237].

CHAPTER 6:

MATERIALS AND METHODS

Materials and Methods

6.1 Cell Lines

CHO-K1 cells

CHO-K1 cells were obtained from American Type Culture Collection. Cells were cultured in Ham's F-12 medium supplemented with 10% (by volume) fetal bovine serum (FBS) (Invitrogen), penicillin G (100 units/ml), streptomycin sulphate (100 lg/ml), and incubated at 5% CO_2 atmosphere with 100% humidity at 37 °C.

PSB-2 cells

PSB-2 cells were obtained from the laboratory of Dr. Osamu Kuge (National Institute of Infectious Disease, Tokyo, Japan) [20]. PSB-2 cells were cultured in Ham's F-12 medium supplemented with 10% (by volume) FBS (Invitrogen), penicillin G (100 units/ml), streptomycin sulphate (100 lg/ml), and incubated at 5% CO_2 atmosphere with 100% humidity at 37 °C.

Ethanolamine supplementation

A stock solution of 1.0M ethanolamine was prepared using phosphate buffered saline (final pH 7.4). The ethanolamine stock solution was added to the growth medium to achieve a final concentration of 20µM.

R-41 Cells

R-41 cells were obtained from the laboratory of Dr. Masato Umeda (Laboratory of Supramolecular Biology Institute for Chemical Research Kyoto University, Kyoto, Japan) [21]. R-41 cells were cultured in Ham's F-12 medium supplemented with 10% (by volume) FBS (Invitrogen), penicillin G (100

units/ml), streptomycin sulphate (100 lg/ml), and incubated at 5% CO_2 atmosphere with 100% humidity at 37 °C.

PSD KD Cells

PSD KD cells were cultured in Ham's F-12 medium supplemented with 10% (by volume) FBS (Invitrogen), penicillin G (100 units/ml), streptomycin sulphate (100 lg/ml), and incubated at 5% CO_2 atmosphere with 100% humidity at 37 °C.

The knockdown of PSD in CHO-K1 cells was achieved through the transfection of 10nM dicer substrate siRNA (dsiRNA) duplexes purchased from Integrated DNA Technologies (IDT). Three different dsiRNA duplexes, with each targeting a different region of the PSD gene (Accession number M62722) were used. A dsiRNA duplex which does not target any eukaryotic gene sequence was used as a negative control.

dsiRNA PSDKD1	
sense	5’ ACA UCC UUG GGA ACG ACA UAG AC dCdC 3’
antisense	5’ UGU AGG AAC CCU UGC UGU AUC UGG GAC 3’
dsiRNA PSDKD2	
sense	5’ CGG AGU UUC UAC UCG UGU UAU CA dUdC 3’
antisense	5’ GCC UCA AAG AUG AGC ACA AUA GUA GAG 3’
dsiRNA PSDKD3	
sense	5’ GAG CGA CUC CAA AGC CAU CAC CA dCdG 3’
antisense	5’ CUC GCU GAG GUU UCG GUA GUG GUG CAG 3’
dsiRNA negative control	
sense	5’CGU UAA UCG CGU AUA AUA CGC GU dAdT 3’
antisense	5’ AUA CGC GUA UUA UAC GCG AUU AAC GAC 3’

Transfection

Cells were plated 24 hours prior to transfection at approximately 60% confluency in antibiotic free media. Transfection complexes were made through mixing dsiRNA and Lipofectamine 2000 (Invitrogen) in diluted Opti-mem

Reduced Serum Media (Invitrogen) as described by *Amarzguioui et al.* [238]. The final concentrations of Lipofectamine 2000 and dsiRNA were 2.5µl/ml and 10nM respectively. Transfection was performed through the addition of dsiRNA-Lipofectamine 2000 complexes to cells incubated in Opti-mem Reduced Serum Media. After five hours of dsiRNA-Lipofectamine 2000 complex incubation, the transfection was terminated through diluting of Opti-mem Reduced Serum Media with Ham's F-12 media (Invitrogen) supplemented with 20% fetal bovine serum (FBS) at 1:1 (v:v).

6.2 Real-Time PCR

Isolation of CHO cell mRNA was performed through Trizol isopropanol 5:1 (v:v) extraction as described by *Rio et al.* [239]. The reverse transcription of CHO cell mRNA to coding DNA (cDNA) was performed using 5µg of total RNA in a 20µl reaction with an oligo(dT) primer (Invitrogen) and Superscript II reverse transcriptase enzyme (Invitrogen) at 48°C for 45 minutes.

Quantification of PSD mRNA was performed using a RotaGene RG-3000 thermocycler (Corbett

Research). The 20µl quantitative RT-PCR reaction contained 100ng of cDNA with 10µl of Platinum Sybr Green qPCR UDG Supermix (Invitrogen), and 200nM primers (IDT). PSD mRNA quantification was performed with respect to the housekeeper gene cyclophilin. PSD and cyclophilin amplicons had annealing temperatures of 57°C and 63°C respectively.

PSD PCR Primers

Forward	5’ CAC TCC CCT ACT GAC TGG AC 3’
Reverse	5’ CAC GCT CAT TGT GAC AGA AGA 3’

Cyclophilin
Forward 5'TCC AAA GAC AGC AGA AAA CTT TCG 3'
Reverse 5' TCT TCT TGC TGG TCT TGC CAT TCC 3'

6.3 Mitochondrial Isolation

Cells were harvested using isolation media which was comprised of 250mM mannitol, 5mM 4-2-hydroxyethyl-1-piperazineethanesulfonic acid (HEPES), 0.5mM ethylene glycol tetraacetic acid (EGTA), and 0.1% (weight to volume) bovine serum albumin. The homogenization of CHO cells was performed using a Balch Homogenizer (Isobiotec Precision Engineering, Heidelberg, Germany) as described by *German et al.* with approximately 30 homogenization strokes [240]. The subcellular fractionation of CHO cells to obtain pure mitochondria was performed using methods described by *Croze et al*. [241]. In brief, this fractionation contained three steps. First, plasma membrane, nuclei, and other cellular debris were pelleted at 500g for 5 minutes using a JA-20 rotor in a Beckman J2-21M centrifuge. Next, crude mitochondria were obtained from pelleting the latter supernatant at 10,300g for 10 minutes. Finally, pure mitochondria were enriched from crude mitochondria using a 20% Percoll gradient (GE Healthcare Corp., Quebec, Canada) centrifuged at 95,500g in a Ti.70.1 rotor with a Beckman L7-55 ultracentrifuge. The Percoll gradient was comprised of 225mM mannitol, 25mM HEPES, 1mM EGTA and 0.1% (weight to volume) bovine serum albumin. Purified mitochondria were isolated from the Percoll gradient and diluted in a buffer containing 10mM Tris and 250nM sucrose. Finally, purified mitochondria were centrifuged at 6300g for 10minutes in a JA20 rotor and resuspended in the latter buffer for subsequent analysis.

6.4 Cytochrome C Oxidase Assay

Cytochrome C oxidase activity from pure mitochondria and whole cell homogenates was quantified using methods described by *Smith et al.* [242]. In brief, 25µg of total protein from each sample was used to assay the oxidation of reduced cytochrome c (Sigma-Aldrich) in a 1.0ml solution of 0.5% Triton X-100 and 100mM potassium phosphate buffer (pH 7.4). In each assay, the absorbance change at 550nm was monitored for 5minutes in a Shimatsu UV-250 spectrophotometer.

6.5 Protein Concentration Determination

Protein concentrations were determined using the bicinchoninic acid assay described by *Smith et al* with bovine serum albumin (Pierce Scientific) as protein standard [243]. Colorimetric changes in absorbance were measured in a Shimatsu UV-250 spectrophotometer at 562 nm.

6.6 Lipid Extraction

Lipid samples containing 100mg of protein were extracted as described by *Folch et al.* with 2.5ml of chloroform and methanol 2:1 (v:v) [244]. After lipid extraction, the samples were centrifugated at 750g for 5 minutes to separate their aqueous phase (upper) from their organic phase (lower). After separation, the aqueous phases were removed and discarded and the organic phases were washed with methanol and water 1:1 (v:v). This process of separation and washing was performed three times to remove all protein contaminants and amphipathic molecules. The lipids were subsequently dried under a stream of nitrogen gas and resuspended in chloroform for later thin layer chromatography separation.

6.7 Thin Layer Chromatography (TLC)

Separation of PS, PE, and PC

PS, PE, and PC separation was performed through by thin-layer chromatography on silica gel TLC G60 plates (EMD Chemicals, Gibbstown, PA) in chloroform, methanol, acetic acid, formic acid, and water 70:30:12:4:2, (v/v). The separated phospholipids were visualized by exposure to iodine vapor and identified by comparison to five micromoles of phospholipid standards (Avanti).

Separation of Cardiolipin

The separation of cardiolipin from other lipids was performed using silica gel TLC G60 plates (EMD Chemicals, Gibbstown, PA) in chloroform hexane methanol acetic acid 50:30:10:5 (v:v). The separated cardiolipin was visualized by exposure to iodine vapor and identified by comparison to 1µmole of cardiolipin standard (Avanti).

6.8 Phosphorus Assay

Phospholipid quantification through phosphorus analysis was performed as described by *Rouser et al.* [245]. Phospholipids scraped from TLC plates were incubated in 0.5ml of perchloric acid and water 3:1 (v:v) for 90 minutes at 180°C alongside phosphate standards used for the standard curuve. Phosphate standards containing 5, 10, 20, 50, 100, 150 nmoles of potassium phosphate made up to 150µl with double distilled water were used. The samples were then diluted with 2.5 ml of double distilled water and then incubated in 0.5ml of 10% ascorbic acid (Fischer Chemical Corp.) and 0.5ml of 2.5% ammonium molybdate (Sigma-Aldrich) for 15 minutes at 95°C. Phospholipid phosphorus was then quantified

through measuring spectrometric absorbance at 820nm using a Shimatsu UV-250 spectrophotometer.

6.9 Measurement of PS Synthase and PSD Activities in CHO Cells

The rates of [^{3}H] serine incorporation into PS and its subsequent decarboxylation into PE were measured using [^{3}H] Serine (Amersham Corp., Illinois, USA) labeling. Cells were incubated in serum-free Ham's F-12 media containing 5µCi/ml of [^{3}H] Serine and subsequently harvested after 1, 3, 5, and 10 h. The [^{3}H] PS and [^{3}H] PE were extracted and separated as described in sections 6.7 and 6.8 respectively. The quantification of [^{3}H] PS and [^{3}H] PE was performed via liquid scintillation counting in a Beckman LS6500 instrument with EcoLit (MP Biomedical Corp, Ohio, USA) scintillation fluid. The data are subsequently expressed as dpms of radioactivity in PS and PE per milligram of sample protein.

6.10 Cell Doubling Time Measurements

Cell doubling times were quantified in 12 well plates marked with 1mm x 1mm grids. The total number of cells in each 1mm x 1mm grid was counted visually at 24 and 48 h after plating.

6.11 ATP Quantification

Cells were plated at approximately 25% confluency 24 h prior to ATP quantification. The cells were harvested in phosphate buffered saline (pH 7.4) and subsequently centrifuged at 600g for 5 minutes. ATP was extracted from the cells using 60µM trichloroacetic acid (TCA). The mixture was neutralized to pH 7.4 using 60µM sodium bicarbonate and 100mM Tris as described by *Stanley et al.* [246]. After extraction, cell lysates were centrifuged at 600g for 10 minutes. The

supernatants containing ATP were subsequently quantified using a luciferase assay kit (catalog# A22066, Invitrogen) per manufacturer's instructions in a Perkin Elmer DLR 96 microplate luminometer.

6.12 Mitochondrial Membrane Potential Quantification

Cells were stained with 10nM tetramethyl rhodamine methyl ester (TMRM) (Molecular Probes, Eugene, Oregon), 100nM Mitotracker Green (Molecular Probes, Eugene, Oregon), and 50nM Hoechst stains (Molecular Probes, Eugene, Oregon). The stains were added to cells growing in antibiotic free Ham's F-12 media supplemented with 10% FBS. A group of control cells were treated with 10µM carbonyl cyanide-p-trifluoromethoxyphenylhydrazone (FCCP) (Sigma-Aldrich) for 10 minutes, which uncouples $\Delta\Psi$ and blocks TMRM loading. Cells were subsequently imaged with the stains onboard on top of a 37°C heated stage at 250X magnification with a Zeiss 510 two-photon confocal microscope. TMRM and Mitotracker Green staining quantifications were performed on individual cellular cytoplasm via region-of-interest calculations on an LSM510 software package [185].

6.13 Visualization of Mitochondrial Motility

Cells were plated at approximately 50% confluency 24h prior to imaging. Mitochondrial morphology was visualized through staining cells with 150nM Mitotracker Red CMX-ROS (Molecular Probes, Eugene, Oregon). Cells were stained for 30 minutes in Ham's F-12 media supplemented with 10% by volume FBS at 37°C in a 5% CO_2 atmosphere incubator. After staining, cells were washed and imaged in Tris buffered Ham's F-12 media pH 7.4. Imaging was

performed for 5 minutes on a heated stage at 250X and 1000X magnifications on a Zeiss 510 two-photon confocal microscope.

6.14 Visualization of Mitochondrial Morphology

Cells were plated at approximately 50% confluency 24h prior to imaging. Mitochondrial morphology was visualized through the z-stack imaging of cells stained with 150nM Mitotracker Red CMX-ROS. Cells were imaged using a Zeiss 510 two-photon confocal microscope taking 25 z-stacks images at 0.2µm slices using a magnification of 1000X.

6.15Flow Cytometry

Cells were incubated in Ham's F-12 media supplemented with 10% FBS containing 100nM TMRM for 30 minutes. Cells were subsequently trypsinized with 0.25% trypsin containing 10mM ethylenediaminetetraacetic acid (EDTA) (Gibco, California, USA) and centrifuged at 600g for 3 minutes. After pelleting, cells were resuspended in pH 7.4 phosphate buffered saline containing 1% FBS and their fluorescence was quantified via flow cytometry on a FACSCan instrument (Becton Dickinson, BD Biosciences).

CHAPTER 7:

Results and Discussion

RESULTS AND DISCUSSION

7.1 PSB-2 Mitochondria Have Reduced PS and PE Levels

PS is a functionally important, albeit quantitatively minor, phospholipid comprising ~10% of cellular phospholipids and ~4% of mitochondrial phospholipids [12]. PS synthesis in mammalian cells occurs through the exchange of L-serine with the base moieties of either PC or PE by PSS I and PSS II respectively. PSB-2 cells are a mutant strain of CHO-K1 cells which have only 5% PS synthase activity compared to wildtype cells [20]. In this investigation, PS, PE, and PC levels in PSB-2 mitochondria were measured.

The mitochondrial PS levels in PSB-2 cells were 36.1% lower than in wildtype cells (Fig. 7.1). Considering that PS synthase activity is required for mammalian cell survival [72] and that PSB-2 cells were documented by *Saito et al.* to contain only 5% residual PS synthase activity, this latter decrease in activity represents a significant reduction in mitochondrial PS.

PS is a precursor of PE in the PSD pathway, and thus reductions in PS levels would be expected to decrease PE levels. It was found PSB-2 mitochondrial PE levels were reduced by 36.5% compared to wildtype levels. Interestingly, this ratio of PS to PE decrease is roughly 1:1 which suggests that mitochondrial PE synthesis is tightly coupled to cellular PS synthesis. Indeed, this ratio of PS and PE decreases was also documented by *Saito et al.* in whole cell homogenates when they initially isolated and characterized PSB-2 cells [20].

Although PC is required for the synthesis of PS by PSS I on the MAM, there were no measurable changes in mitochondrial PC levels. This observation suggests that PC synthesis and /or turn over likely changed to accommodate

decreased PS synthesis. Moreover, since PC mass in mitochondria is roughly ten times that of PS, it is likely that PC levels would not be significantly changed by decreases in PS levels.

Kuge et al. previously documented that the supplementation of PSB-2 cells with 20μM ethanolamine rescues them of their PS and PE deficiencies, presumably because PE can be synthesized from the CDP-ethanolamine pathway [59]. To study the effects of ethanolamine supplementation on mitochondria, PSB-2 cells were cultured with 20μM ethanolamine in this investigation. PS and PE levels in PSB-2 mitochondria were normalized to wildtype levels with long-term ethanolamine supplementation (Fig. 7.1 and Fig. 7.2). Hence, it is likely that a long-term up-regulation of PE biosynthesis in the ER via the CDP-ethanolamine pathway can rescue mitochondrial PE deficiencies.

When *Saito et al.* initially isolated PSB-2 cells, they had observed 80% and 49% decreases in cellular PS and PE levels respectively through culturing cells in media supplemented with 10% dialyzed FBS lacking phospholipids. Furthermore, it was reported that PSB-2 cells cultured without phospholipid supplementation were incapable of growth and exhibited low viability [20]. Thus, for the purposes of this investigation, PSB-2 cell were cultured in non-dialyzed 10% FBS. This difference in medium phospholipid concentrations is therefore likely the cause of differences in PS and PE measurements between this investigation and previous reports [20].

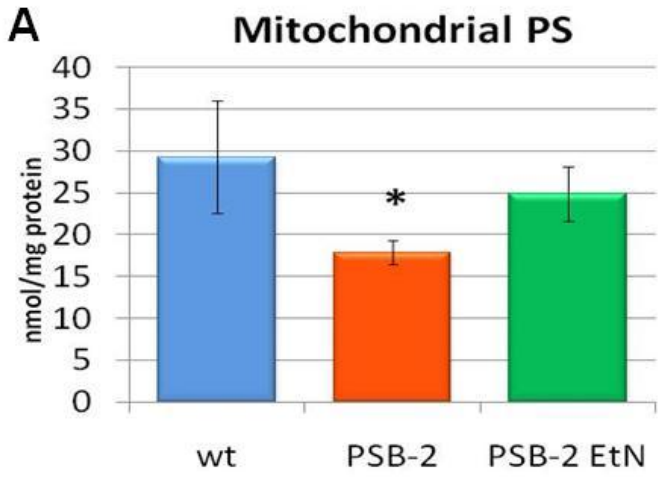
A
Mitochondrial PS
nmol/mg protein
40
35
30
25
20
15
10
5
0
*
wt
PSB-2
PSB-2 EtN

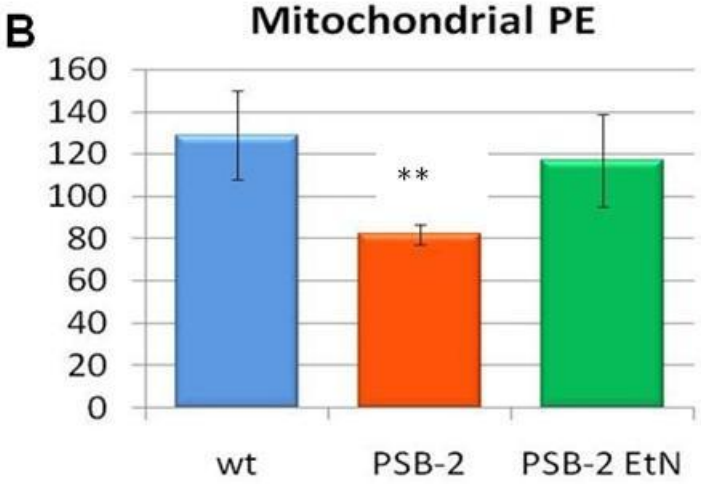
B
Mitochondrial PE
160
140
120
100
80
60
40
20
0
**
wt
PSB-2
PSB-2 EtN

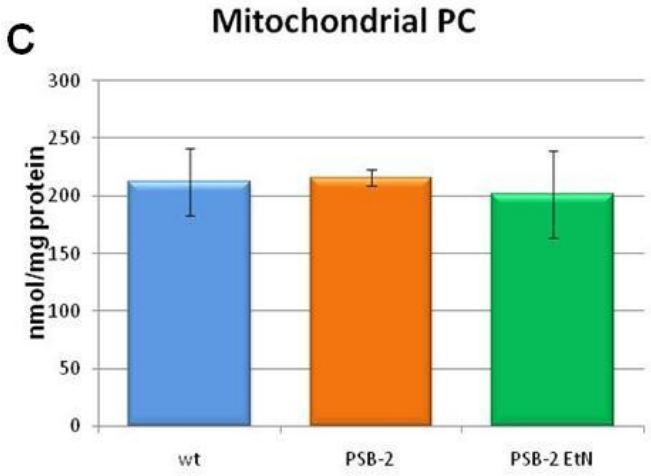
C
Mitochondrial PC
nmol/mg protein
300
250
200
150
100
50
0
wt
PSB-2
PSB-2 EtN

Fig. 7.1
The molar masses of mitochondrial PS (Panel A), PE (Panel B), and PC (Panel C) per milligrams of mitochondrial protein were quantified for wildtype CHO-K1 cells (wt), PSB-2 cells, and PSB-2 cells cultured in 20μMethanolamine (EtN). The above data represent four independent preparations of mitochondria for each cell line (six for wildtype). The p-values were * $9.7x10^{-3}$ (Panel A) and ** $1.9x10^{-3}$ (Panel B) using the student's t-test.

PSB-2 Cell Homogenate Phospholipids

The whole-cell molar masses of PS, PE, and PC in wildtype cells, PSB-2 cells, and PSB-2 cells supplemented with 20μM ethanolamine were compared via phosphorus analysis. There were no statistically significant differences in PS, PE, or PC levels among the three cell types as their calculated p-values were all greater than 0.05. This result is different from the original report made by *Saito et al*., who had documented 49.8% reductions in PSB-2 PE levels compared to wildtype levels. This difference might be explained by the availability of PS and PE in the culture media of PSB-2 cells. Since the FBS used in this investigation was not dialyzed to remove PS, PE and ethanolamine, it is likely that the PSB-2 cells documented here contained higher levels of cellular PE.

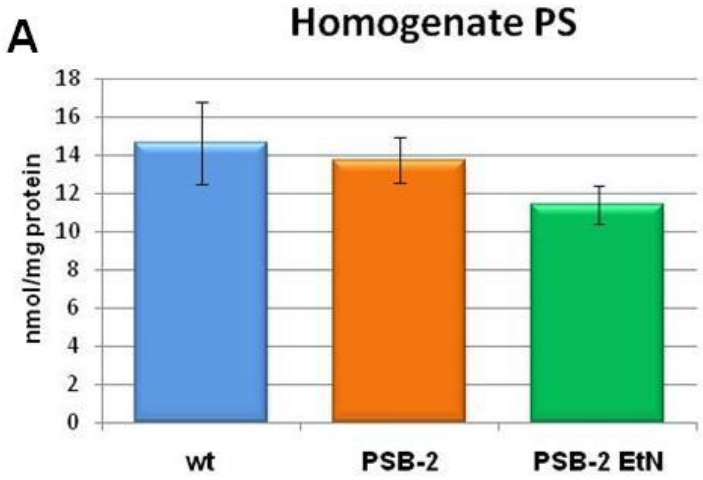
A
Homogenate PS
nmol/mg protein
18
16
14
12
10
8
6
4
2
0
wt
PSB-2
PSB-2 EtN

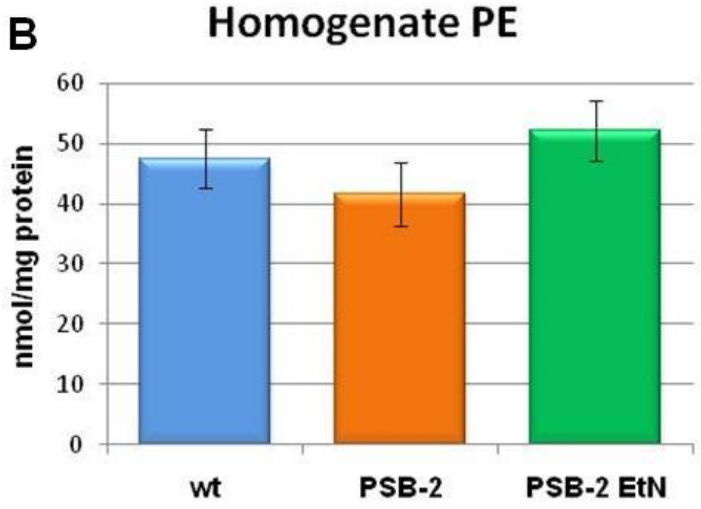
B
Homogenate PE
nmol/mg protein
60
50
40
30
20
10
0
wt
PSB-2
PSB-2 EtN

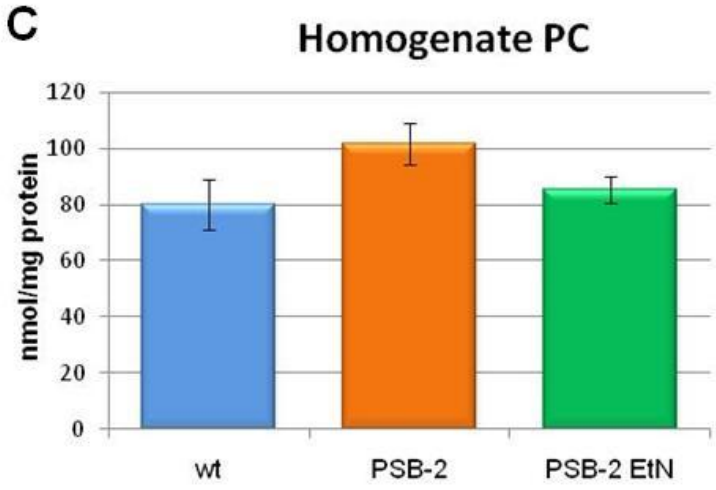
C
Homogenate PC
nmol/mg protein
120
100
80
60
40
20
0
wt
PSB-2
PSB-2 EtN

Fig. 7.2
The molar masses of whole-cell PS (Panel A), PE (Panel B), and PC (Panel C) per milligrams of protein were quantified for wildtype CHO-K1 cells (wt), PSB-2 cells, and PSB-2 cells cultured in 20μM ethanolamine (EtN). All calculated p-values were >0.05.

PSB-2 Mitochondrial Cardiolipin Analysis

Cardiolipin is an important mitochondria phospholipid which comprises ~15% of mitochondrial membranes [12]. Cardiolipin not only functions in the maintenance mitochondrial membrane integrity but is also required for the function of mitochondrial ETC enzymes. Here, PSB-2 cardiolipin levels quantified via phosphorus analysis were unchanged compared to wildtype levels. This result is reasonable given that cardiolipin and PS syntheses are not coupled.

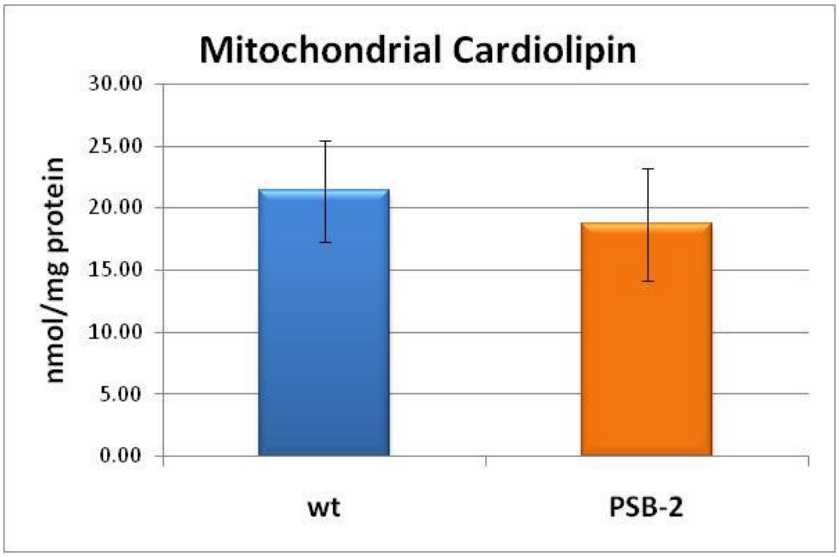

Fig. 7.3 A figure showing wildtype (wt) and PSB-2 mitochondrial cardiolipin levels in nmol/mg of mitochondrial protein. Cardiolipin molar mass per milligram of protein was measured using three preparations of pure mitochondria from wildtype and PSB-2 cells each. The p-value was >0.05.

[^{3}H] Serine incorporation Into PS in PSB-2 Cells

After the molar masses of PS and PE in PSB-2 cells were measured, their rates of synthesis were investigated in intact cells. The incorporation of serine into PS and PE was measured in wildtype and PSB-2 cells through radiolabeling with 5µCi/ml [3-^{3}H] serine. At 1, 3, 5, and 10h time points, PSB-2 cells had 86.3%, 86.7%, 82.8%, and 77.8% less serine incorporation than wildtype cells (Fig. 7.4 Panel A). Decarboxylation of the [^{3}H] serine moiety on PS by PSD was also reduced by 86.0%, 87.8%, 86.8%, and 82.1% in PSB-2 cells at 1, 3, 5, and 10h time points (Fig. 7.4 Panel B). The sum of [^{3}H] PS and [^{3}H] PE radioactivity represents the total cellular incorporation of [^{3}H] serine into PS because all [^{3}H] in PE was derived from [^{3}H] PS. The combined radioactivity of [^{3}H] PS and [^{3}H] PE in PSB-2 cells was calculated to be 86.3%, 86.7%, 82.8%, and 77.8% lower than wildtype levels at 1, 3, 5, and 10 h time points respectively (Fig. 7.4 Panel C). This decrease in [^{3}H] serine incorporation is likely due the reduced PS synthesis in PSB-2 cells. Therefore, results are similar to previous reports by *Saito et al.*, whereby they documented 95% reductions in PS synthesis.

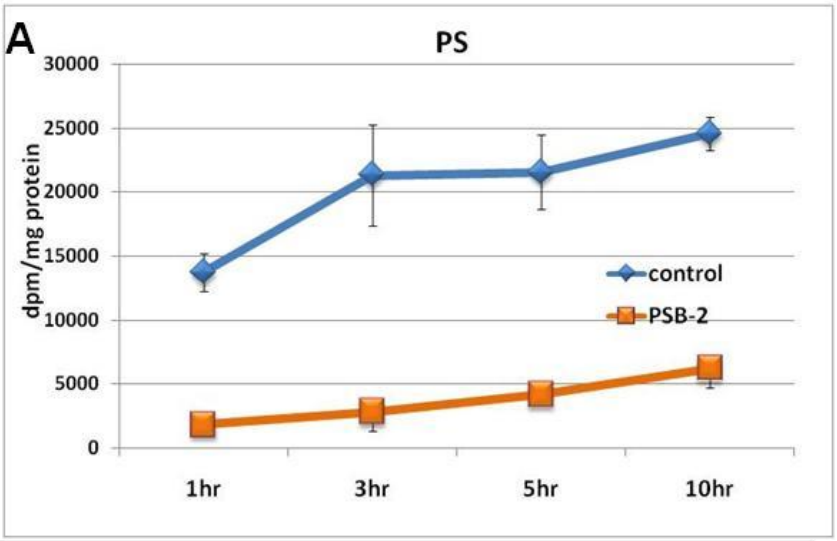
A
PS
dpm/mg protein
30000
25000
20000
15000
10000
5000
0
control
PSB-2
1hr
3hr
5hr
10hr

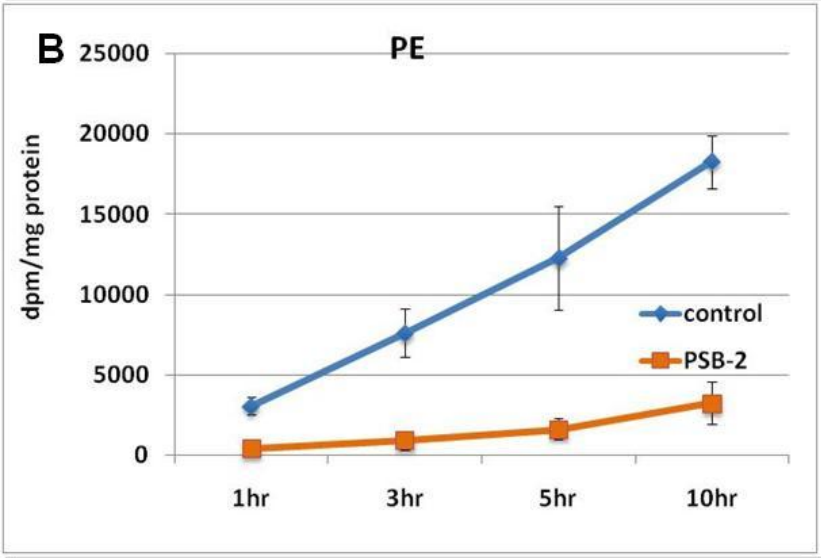
B
PE
dpm/mg protein
25000
20000
15000
10000
5000
0
control
PSB-2
1hr
3hr
5hr
10hr

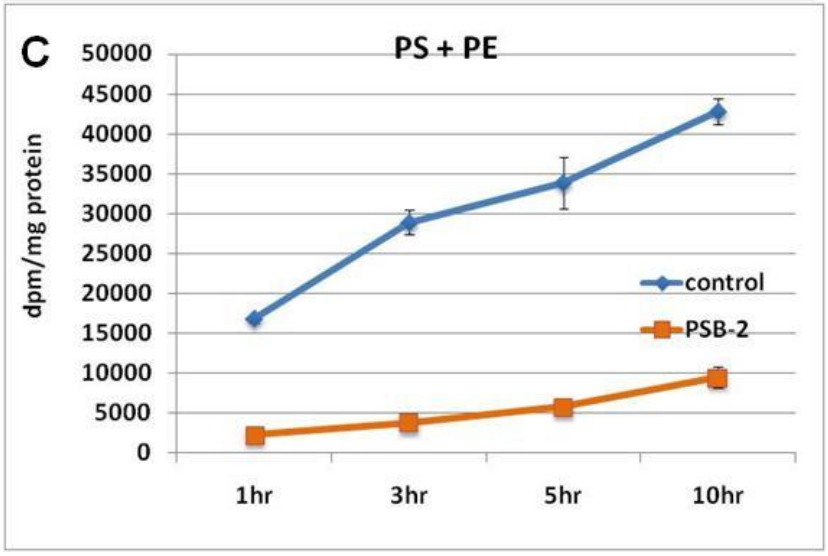
C
PS + PE
dpm/mg protein
50000
45000
40000
35000
30000
25000
20000
15000
10000
5000
0
control
PSB-2
1hr
3hr
5hr
10hr

Fig. 7.4
The radioactivity of [^{3}H] PS and [^{3}H] PE at 1, 3, 5, and 10 hour time points were quantified in dpms per milligram of cellular protein for wildtype and PSB-2 cells (Panel A and Panel B). The sum of [^{3}H] PS and [^{3}H] PE radioactivity per milligram protein, which represents total [^{3}H] serine incorporation with respect to time, was calculated for wildtype and PSB-2 cells (Panel C). The incorporation of [^{3}H] serine into wildtype and PSB-2 cells was quantified using three independent experiments with biological triplicates each time. A representative experiment is shown in Fig. 7.4. All of the above data points had p-values < 0.05.

7.2 PSB-2 Cells Have Reduced Doubling Time

PSB-2 cell growth was measured through counting changes in the number of cells in an area of $1mm^2$ 24 hours after plating. It was observed that PSB-2 cell have slower growth rates than wildtype cells with 39.5% longer doubling times (Fig 7.5). Given that cell division requires sufficient amounts of subcellular membranes, and PSB-2 cells have 36.1% and 36.5% reductions in mitochondrial PS and PE levels, the decreased growth rate is not a surprising result.

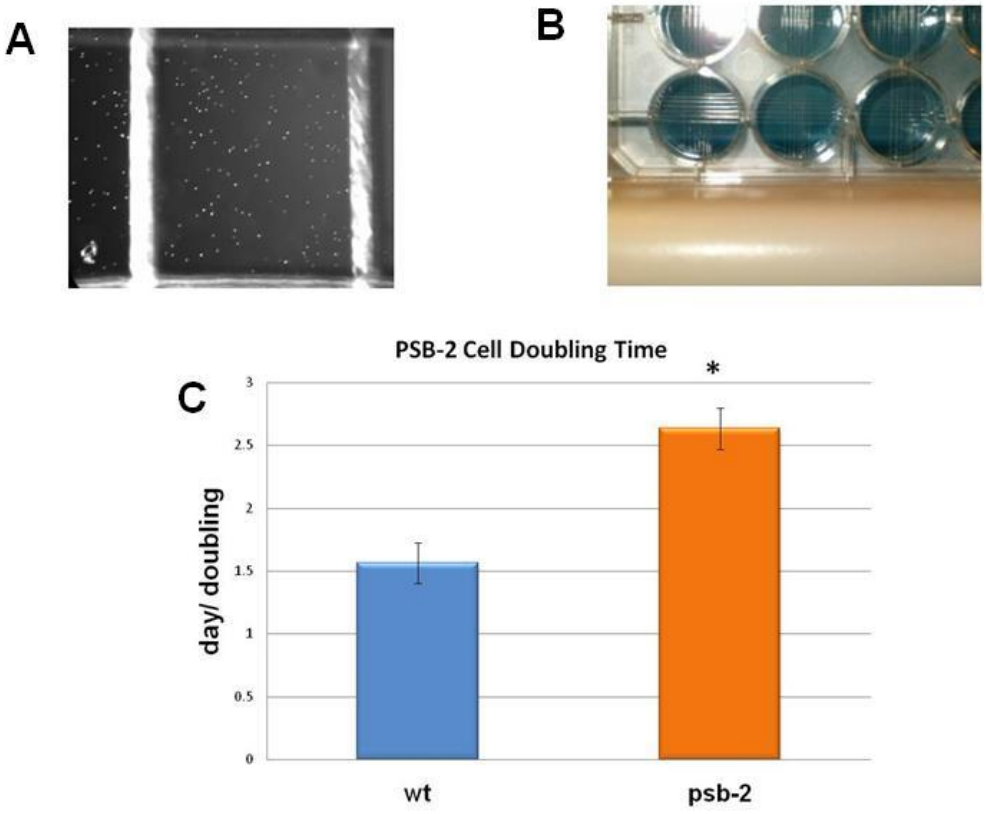

Fig. 7.5
Images depicting 1mm x 1mm grids marked on a 24 well plate which were used to quantify cell doubling times (Panel A and B). The above data (Panel C) show the average of three independent experiments. In each experiment, the change in number of cells in three 1mm x 1mm grids was counted between 24 and 48 hours after plating. It was found that PSB-2 cells have 39.5% longer doubling times compared to wildtype cells (wt). The above difference has a p-value of $1.7x10^{-2}$.

7.3 PSB-2 Mitochondria Have Increased Sedimentation Density

Increases in mitochondrial density resulting from decreases in phospholipid levels in *Saccharomyces cerevisiae* were previously reported by *Schumacher et al* [82]. Through centrifuging PE deficient yeast mitochondria on a sucrose gradient, they showed that mitochondria with decreased phospholipid to protein ratio can have abnormally high sedimentation densities. The centrifugation of PSB-2 mitochondria on Percoll gradients showed that PSB-2 mitochondria have higher sedimentation densities compared to wildtype mitochondria (Fig. 7.6). This increase in sedimentation density is likely due to the decrease in phospholipid to protein ratio, as proteins are denser than most phospholipids. Interestingly, the MAM of PSB-2 cells retain a sedimentation density similar to wildtype MAM. This is most likely because MAM phospholipid content was unchanged, as whole-cell phospholipid levels in PSB-2 cell were similar to wildtype levels.

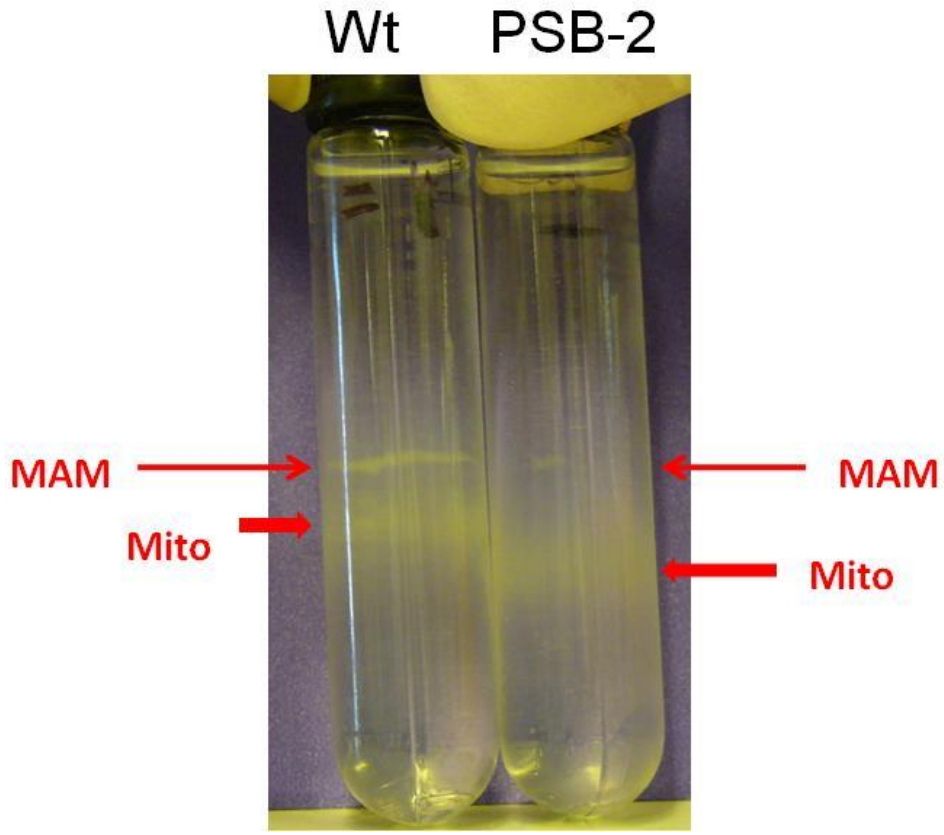

Fig. 7.6
Mitochondria and MAM from wildtype and PSB-2 cells on a 20% Percoll gradient after centrifugation. Pure mitochondria were isolated from wildtype and PSB-2 cells in four independent experiments.

7.4 PSB-2 Mitochondrial Physiology

Cytochrome c Oxidase Activity

As previously discussed in chapter five, cytochrome c oxidase, or COX, is the terminal component of the mitochondrial ETC and catalyzes the transfer of electrons from cytochrome c to molecular oxygen. COX is a complex multisubunit membrane-bound enzyme which requires phospholipids for structure and function. The crystal structure of mammalian COX includes 13 molecules of membrane lipids which include: two cardiolipins, three triacylglycerols, four phosphatidylglycerols, one PC, and three PEs [157]. In this investigation, the *in vitro* activity of COX from PSB-2 mitochondria was determined. PSB-2 mitochondria showed a 21.9% reduction in cytochrome c oxidase activity compared to wildtype mitochondria (Fig. 7.8). This modest decrease in COX activity was interestingly rescued through ethanolamine supplementation, which normalized PSB-2 mitochondrial PS and PE levels (Fig. 7.1). Hence, it is likely that optimum COX activity requires PE and possibly PS. This rescue-effect of ethanolamine supplementation is congruent with previous findings by *Paradies et al*. with long-term cardiolipin supplementation in cardiolipin deficient cells [155].

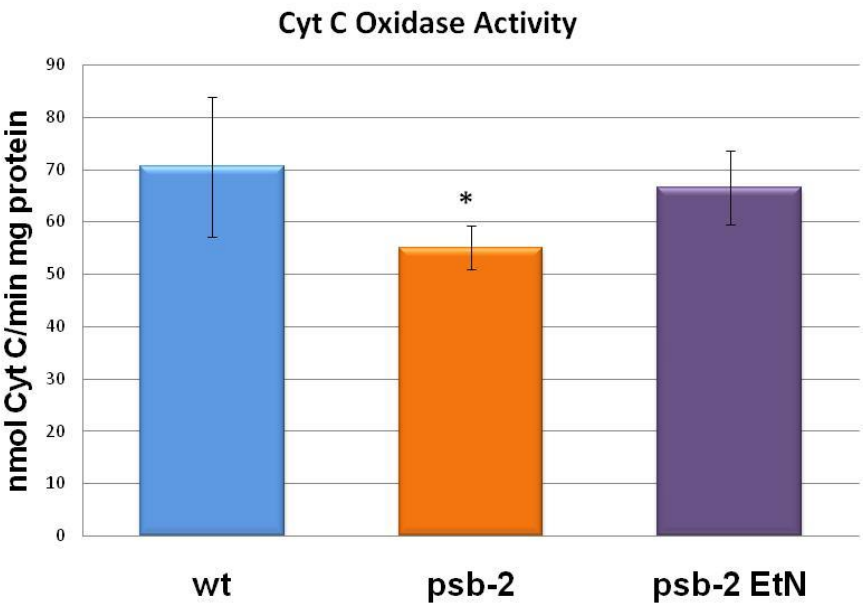

Fig. 7.8
Cytochrome c oxidase activity was measured in mitochondria of wildtype cells, PSB-2 cells, and PSB-2 cells supplemented with 20µM ethanolamine. Cytochrome c oxidase activity was assayed using four independent preparations of mitochondria in reaction triplicates from wildtype (wt), PSB-2, and PSB-2 cells supplemented with 20µM ethanolamine. The above difference between PSB-2 and wt mitochondria has a p-value of 2.7×10^{-2}.

PSB-2 Cells have Increased ATP Levels

ATP is an important multifunctional nucleotide which transports chemical energy within cells for metabolism. As previously reviewed in chapter 5, the majority of cellular ATP is synthesized through the process of oxidative phosphorylation, which in eukaryotes, occurs on the MIM. Oxidative phosphorylation utilizes a series of mitochondrial ETC enzymes which are known to have strict phospholipid requirements for structure and function. Since PSB-2 mitochondria have reduced PS and PE levels and decreased COX activity, the steady state ATP levels of PSB-2 cells were thus measured and compared against wildtype levels. Through quantifying ATP in cellular lysates via luciferase lumination analysis, it was found that PSB-2 cells had a ~40% higher cellular ATP level (Fig. 7.9). This finding is remarkable given that COX, the terminal component of the ETC has a 21.9% decreased activity.

This decrease in mitochondrial functionality combined with increased ATP production suggests several possible phenomena may be occurring. Firstly, the ER is very metabolically active organelle which utilizes ATP synthesized by mitochondria [4]. The author of this thesis speculates that ATP travelling from the mitochondrion to the ER is likely transported through the MAM. Given that PSB-2 cells were observed to have reduced levels of MAM, it may be possible that ATP was trapped in mitochondria and unable to be transported to the ER. This scenario is also supported by the decrease in growth rates observed in PSB-2 cells suggesting that not enough energy was available for enzyme function on the ER.

Thus, to confirm this proposal, the ATP levels of intact mitochondria and ER must measured and compared between PSB-2 cells and wildtype cells.

Secondly, it may be possible that PS and PE deficiencies in PSB-2 cell are limiting cellular growth and trapping cells in energetically intensive phases prior to cell division. This would mean that there is a buildup of ATP in anticipation of cell division.

Thirdly, calcium is a powerful intracellular signaling molecule which regulates many cellular processes and mitochondria are known to be storage sites for intracellular calcium. The flux of mitochondrial calcium is known to be $\Delta\Psi$ dependent [190]. In this investigation, PSB-2 cells were also observed to have abnormally high $\Delta\Psi$ (Fig. 7.9). These pieces of evidence suggest PSB-2 cells may be demanding excessive amounts of ATP through abnormal calcium signaling without the means to utilize it due deficiencies in particular phospholipid pools. For example, PE is necessary for membrane fusion [11], contractile ring disassembly during cytokinesis [11], and the formation of autophagosomes for autophagy[46]. A lack of PE may mean that the latter processes would function inefficiently and require more ATP than normally necessary.

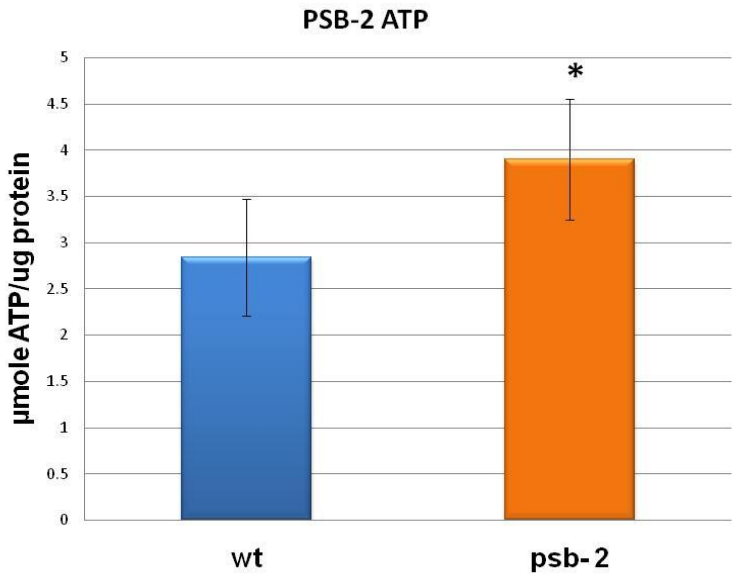

Fig. 7.9
ATP levels in lysates of wildtype (wt) and PSB-2 cells. ATP was isolated through trichloroacetic acid (TCA) extraction and quantified through luciferase lumination analysis. ATP was quantified from three independent experiments. In each experiment, ATP was quantified triplicate reactions. P-value = 4.7×10^{-3}.

PSB-2 Cells Have Increased Mitochondrial Membrane Potential

In metabolically active mitochondria, protons are pumped from the mitochondrial matrix to the intermembrane space by ETC enzymes. This process generates the mitochondrial membrane potential, or $\Delta\Psi$, which is a key component of cellular respiration. $\Delta\Psi$ is not only important for the process of ATP synthesis but also necessary for the maintenance of cellular calcium homeostasis [247]. In addition, $\Delta\Psi$ can also be an indicator of energy metabolism, as significant increases in $\Delta\Psi$ have been linked to cancer phenotypes and reduced oxidative phosphorylation.

In this investigation, the $\Delta\Psi$ of PSB-2 mitochondria was measured via tetramethyl rhodamine methyl ester (TMRM) fluorescence using confocal microscopy. Fig. 7.10A shows that the TMRM fluorescence intensity in PSB-2 mitochondria was ~112% greater than that of wildtype mitochondria. This increase in fluorescence indicates a dramatic increase in $\Delta\Psi$. Since PSB-2 mitochondria have altered sedimentation densities and presumably altered membrane surface areas, it was necessary for their TMRM fluorescence to be normalized to mitochondrial surface area, as TMRM fluorescence may be greater in mitochondria with greater ratios of ETC enzymes to membranes. Thus, TMRM fluorescence measurements were normalized to mitochondrial surface area using Mitotracker Green, a non-membrane potential dependent mitochondrial stain which has been shown to evenly adhere to the MIM surface. When PSB-2 cells were stained with both TMRM and Mitotracker Green, PSB-2 mitochondria had a ~186% higher TMRM:Mitotracker Green fluorescence than wildtype cells (Fig.

7.10B). Since PSB-2 cells have a decrease in mitochondrial membrane phospholipids, a decrease in mitochondrial membrane to ETC protein ratio could account for this observed hyperpolarization. Thus, this result supports the theory that TMRM fluorescence is greater in mitochondria which have greater ratios of ETC enzymes to MIM surface.

Although the mechanism of PSB-2 $\Delta\Psi$ increase is not understood, it is likely that PSB-2 cells may share similar phenotypes as cancers cells which are hyperpolarized. Hyperpolarization in cancer cells is a result decreased respiration and increased glycolysis, which leaves a residual hyperpolarized $\Delta\Psi$ on the MIM after ATP synthase activity is reduced. At present, there is no evidence for PSB-2 cell dependence on glycolysis. Thus, to fully understand the mechanism of PSB-2 mitochondrial hyperpolarization, future experiments which study glucose oxidation and all five mitochondrial respiration complexes will be necessary.

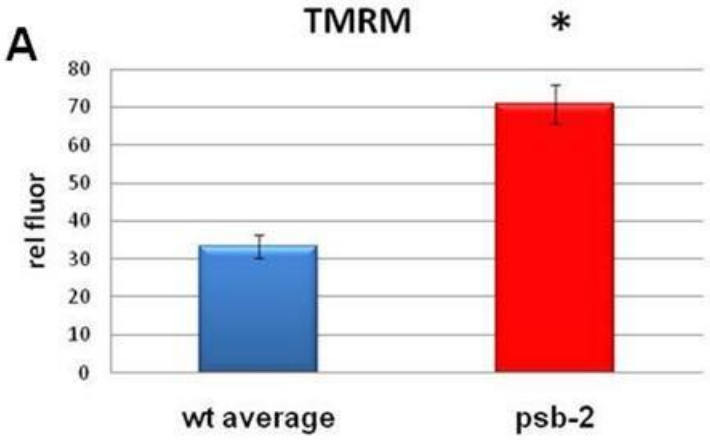
A
TMRM
*
rel fluor
80
70
60
50
40
30
20
10
0
wt average
psb-2

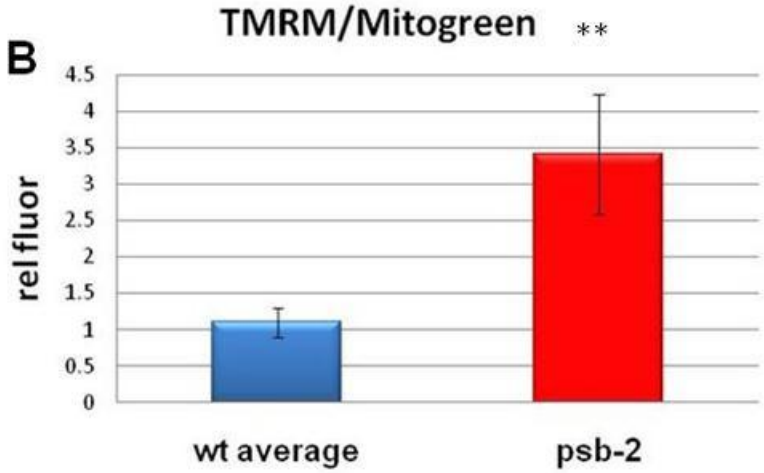
B
TMRM/Mitogreen
**
rel fluor
4.5
4
3.5
3
2.5
2
1.5
1
0.5
0
wt average
psb-2

Fig. 7.10
The $\Delta\Psi$ of wildtype (wt) and PSB-2 cells was measured using relative TMRM fluorescence quantification (Panel A). $\Delta\Psi$ was also quantified with respect to mitochondrial surface area using the ratio of TMRM fluorescence to Mitotracker Green fluorescence (Panel B). Wildtype and PSB-2 $\Delta\Psi$ were quantified using confocal microscopy for three independent experiments using triplicate dishes each time. In each dish, three images were taken, and fluorescence of 20 cells was measured per image. P-values of * = 1.19×10^{-11} and ** = 2.45×10^{-5}.

TMRM Response to Changes in ΔΨ

TMRM is a known indicator of ΔΨ. To confirm that TMRM does indeed specifically stain CHO-K1 cell mitochondria in a ΔΨ dependent manner, ΔΨ was increased and decreased using oligomycin and FCCP. Oligomycin is an inhibitor of ATP synthase which transiently increases ΔΨ through the buildup of protons across MIM, and FCCP is an uncoupler which permeabilizes the MIM for protons to freely defuse across it. Oligomycin and FCCP were sequentially added to CHO-K1 cells stained with TMRM in 10 minute increments and ΔΨ was monitored through confocal microscopy. Thus, incubation of wildtype cells in 10μM oligomycin for 10 minutes increased TMRM fluorescence by of ~160%, and the subsequent incubation of the same cells in 10μM FCCP for 10 minutes decreased TMRM fluorescence by ~42% (Fig. 7.11). These results indicate that TMRM can effectively respond to changes in ΔΨ in a timely manner, and that the TMRM quantification method of this investigation is valid.

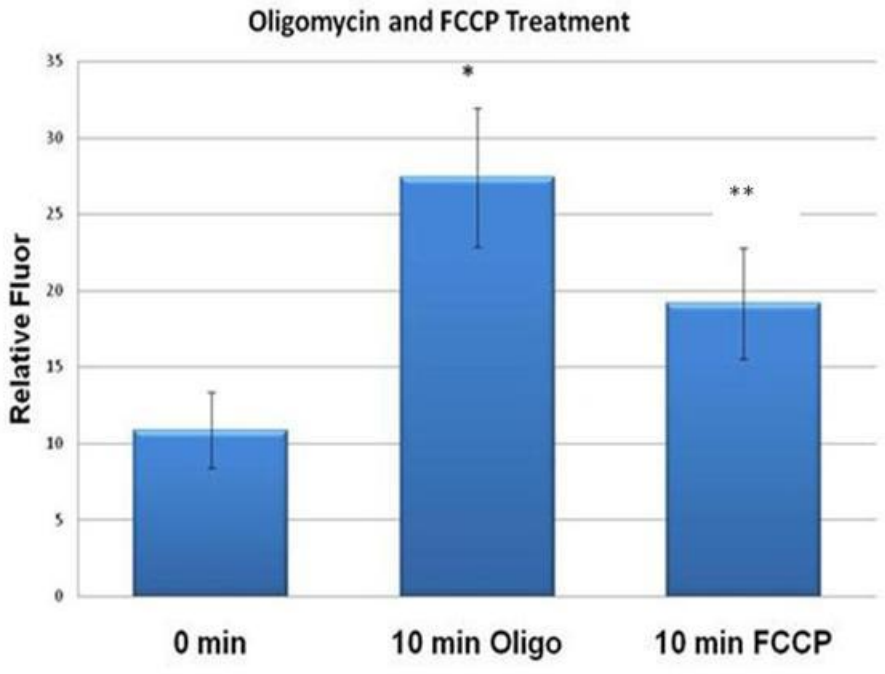

Fig. 7.11

Fluorescence of TMRM responds to changes in $\Delta\Psi$. $\Delta\Psi$ is increased from ATP synthase inhibition by oligomycin and decreased by FCCP uncoupling. Wildtype cells were incubated for 30 minutes with 10nM TMRM to quantify$\Delta\Psi$. The above experiment was performed using triplicate dishes and the TMRM fluorescence of 20 cells was quantified per dish at the respective time points. Time "0 min" represents TMRM fluorescence after the initial 30 minutes of incubation, time "10 min Oligo" represents TMRM fluorescence subsequently after 10 minutes of olygomycin treatment, and time "10 min FCCP" represents TMRM fluorescence after 10 minutes of FCCP treatment. P-values of * = $2.6\text{x}10^{-7}$ and ** = $8.8\text{x}10^{-4}$.

PSB-2 TMRM Quantification via Flow Cytometry

Flow cytometry is an efficient technique for quantifying cellular fluorescence in large populations of cells. In this investigation, PSB-2 cell TMRM fluorescence was quantified using flow cytometry in addition to confocal microscopy. The TMRM fluorescence of wildtype cells, PSB-2 cells, and PSB-2 cells supplemented with 20μM ethanolamine, was compared (Fig. 7.12). It was observed that PSB-2 cells showed ~304% higher TMRM fluorescence than wildtype cells, moreover, PSB-2 cell supplementation with ethanolamine resulted in a 56.4% decrease in this increased fluorescence. These results were consistent with the previous microscopy quantifications of PSB-2 cell mitochondrial hyperpolarization and also demonstrated the ethanolamine supplementation can reduce PSB-2 mitochondrial hyperpolarization. Most importantly, this latter finding provides strong evidence for the correlation between mitochondrial hyperpolarization and abnormalities in mitochondrial PS and PE levels.

Confocal microscopy and flow cytometry quantifications of TMRM fluorescence were calculated to yield different amounts of relative hyperpolarization. Through confocal microscopy, PSB-2 cells were observed to show ~152% more TMRM fluorescence than wildtype cells. However, flow cytometry results yielded a larger difference of ~304% between the two cell types. This difference in relative TMRM fluorescence can be attributed to fact that cells imaged via confocal microscopy were adhered to dishes whereas cell quantified via flow cytometry were measured in suspension, representing two different environments for measurement. Furthermore, cell imaged via confocal

microscopy were stained with 10nM TMRM whereas cells quantified via flow cytometry were stained with 100nM TMRM. This difference in relative fluorescence suggests that TMRM florescence may not linearly correlate with stain concentration.

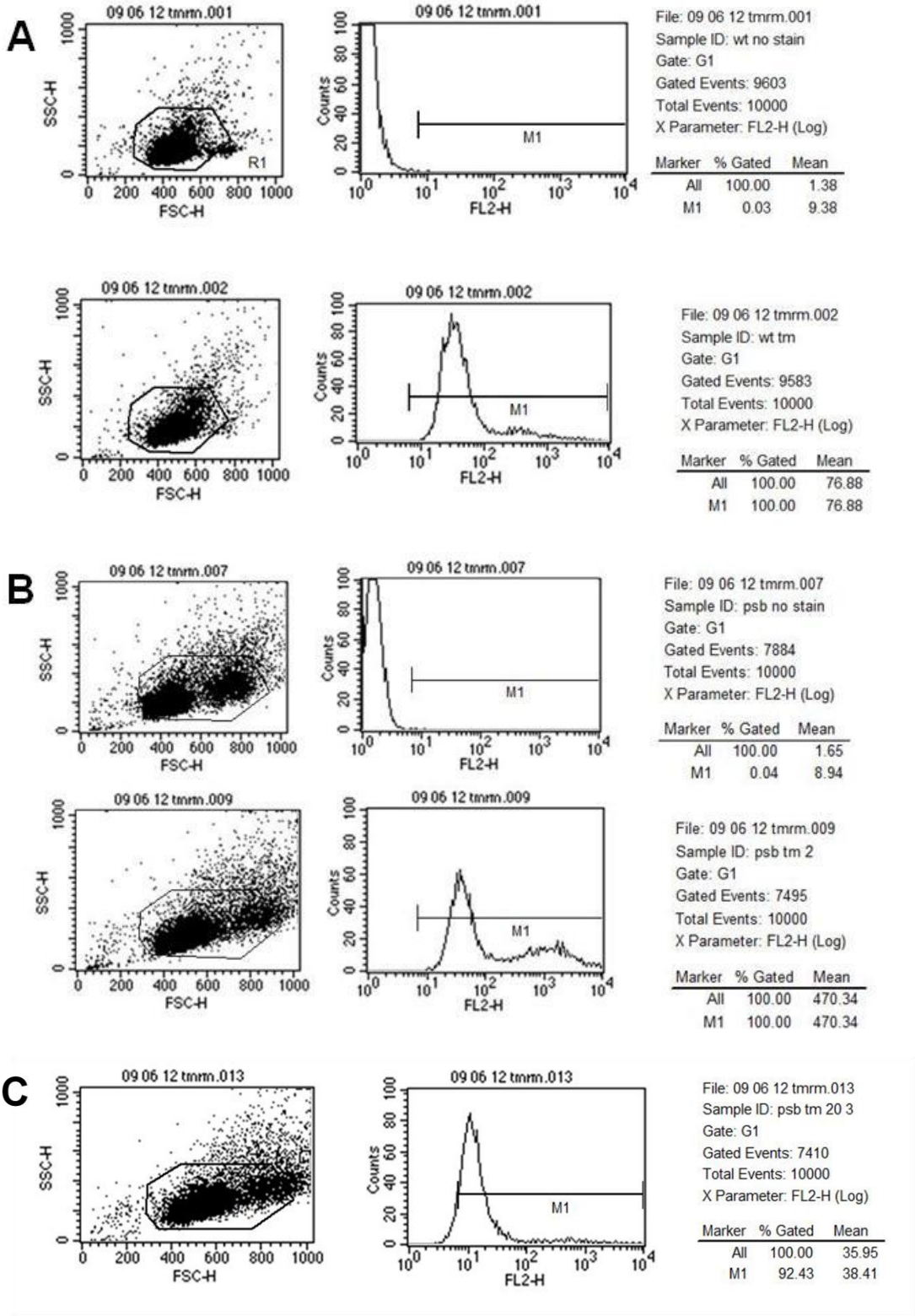
A
09 06 12 tmrm.001
SSC-H
FSC-H
R1
09 06 12 tmrm.001
Counts
FL2-H
M1
File: 09 06 12 tmrm.001
Sample ID: wt no stain
Gate: G1
Gated Events: 9603
Total Events: 10000
X Parameter: FL2-H (Log)
Marker % Gated Mean
All 100.00 1.38
M1 0.03 9.38
09 06 12 tmrm.002
SSC-H
FSC-H
09 06 12 tmrm.002
Counts
FL2-H
M1
File: 09 06 12 tmrm.002
Sample ID: wt tm
Gate: G1
Gated Events: 9583
Total Events: 10000
X Parameter: FL2-H (Log)
Marker % Gated Mean
All 100.00 76.88
M1 100.00 76.88
B
09 06 12 tmrm.007
SSC-H
FSC-H
09 06 12 tmrm.007
Counts
FL2-H
M1
File: 09 06 12 tmrm.007
Sample ID: psb no stain
Gate: G1
Gated Events: 7884
Total Events: 10000
X Parameter: FL2-H (Log)
Marker % Gated Mean
All 100.00 1.65
M1 0.04 8.94
09 06 12 tmrm.009
SSC-H
FSC-H
09 06 12 tmrm.009
Counts
FL2-H
M1
File: 09 06 12 tmrm.009
Sample ID: psb tm 2
Gate: G1
Gated Events: 7495
Total Events: 10000
X Parameter: FL2-H (Log)
Marker % Gated Mean
All 100.00 470.34
M1 100.00 470.34
C
09 06 12 tmrm.013
SSC-H
FSC-H
09 06 12 tmrm.013
Counts
FL2-H
M1
File: 09 06 12 tmrm.013
Sample ID: psb tm 20 3
Gate: G1
Gated Events: 7410
Total Events: 10000
X Parameter: FL2-H (Log)
Marker % Gated Mean
All 100.00 35.95
M1 92.43 38.41

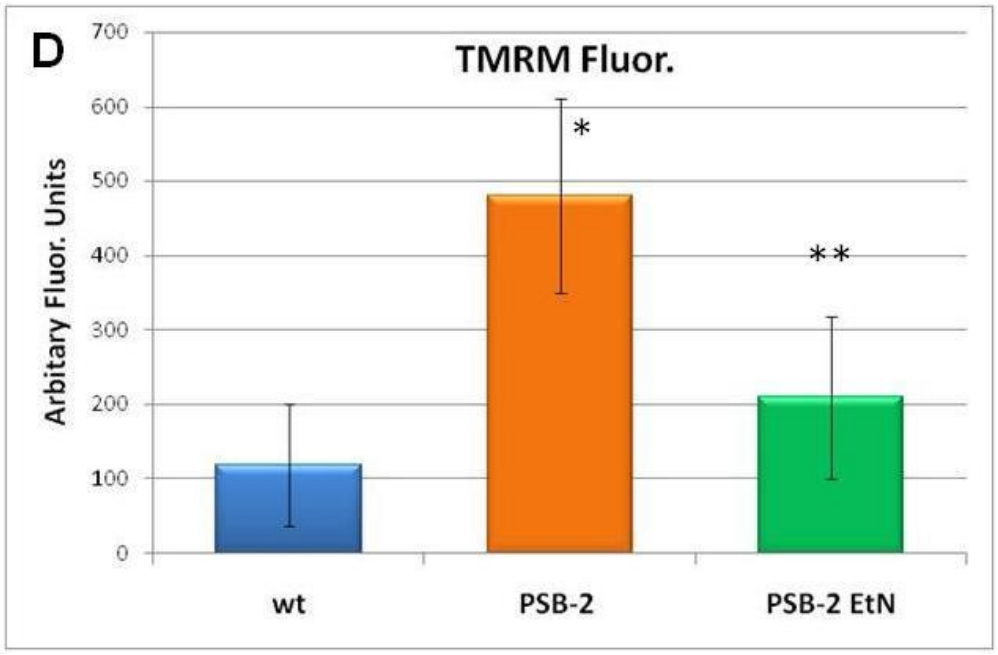

Fig. 7.12
The TMRM fluorescence of wildtype (Panel A), PSB-2 (Panel B), and PSB-2 cells grown in the presence of 20µM ethanolamine (EtN) (Panel C) was analyzed via flow cytometry. Wildtype (wt) and PSB-2 cells were treated with and without 100nM TMRM and subsequently assayed. The relative TMRM fluorescence for the three cell types are shown above (Panel D). Three independent experiments were performed, in each experiment three dishes were used per cell type, and 10,000 cells were assayed per dish. The statistical significance between: wildtype and PSB-2 cells, and wildtype and PSB-2 cells supplemented with ethanolamine had p-values of * 2.16×10^{-6}, ** 3.9×10^{-2} respectively.

7.5 PSB-2 Mitochondrial Morphology and Motility

PSB-2 Mitochondrial Morphology

As previously discussed in Chapter 5, mitochondria can exist in a wide variety of different morphologies across cell types. These differences in morphologies across cell types often represent differences metabolic demands and physiological requirements. However, mitochondrial morphology variations in same cell type often suggest metabolic abnormalities. Since PSB-2 cells exhibit increases in mitochondrial sedimentation density, decreases in COX activity, increases in steady-state ATP levels, and increases mitochondrial $\Delta\Psi$, there was a preponderance of evidence to believe that PSB-2 mitochondria may have an abnormal morphology. Thus, the morphology of wildtype and PSB-2 mitochondria was compared at 5000X magnification using confocal microscopy. Through Mitotracker Red CMX-ROS staining, it was observed that PSB-2 mitochondria showed a much more punctate morphology compared to wildtype mitochondria (Fig. 7.13). Mitochondrial morphology was also visually assessed through z-stack imaging where 25, 0.2μm transverse image slices were reconstructed to provide a 3-D image. From examining PSB-2 mitochondria at different focal planes, it was found that PSB-2 cells only contained punctate mitochondria (Fig. 7.13).

Although the exact mechanism for this punctate morphology is unknown, two possible defects may be occurring. Firstly, it may be possible that PSB-2 mitochondria are exhibiting a defect in fusion, as PE is necessary for membrane fusion [22]. If this were the case, then PSB-2 mitochondria would have relatively

less mitochondrial DNA per mitochondrion suggesting that mitochondrial protein synthesis may be decreased. Secondly, it may be possible that PSB-2 mitochondria are exhibiting an increase in fission. This possible scenario is supported by the evidence that PSB-2 cells contain increased levels of ATP, which can signal for mitochondria to divide in anticipation of cell division.

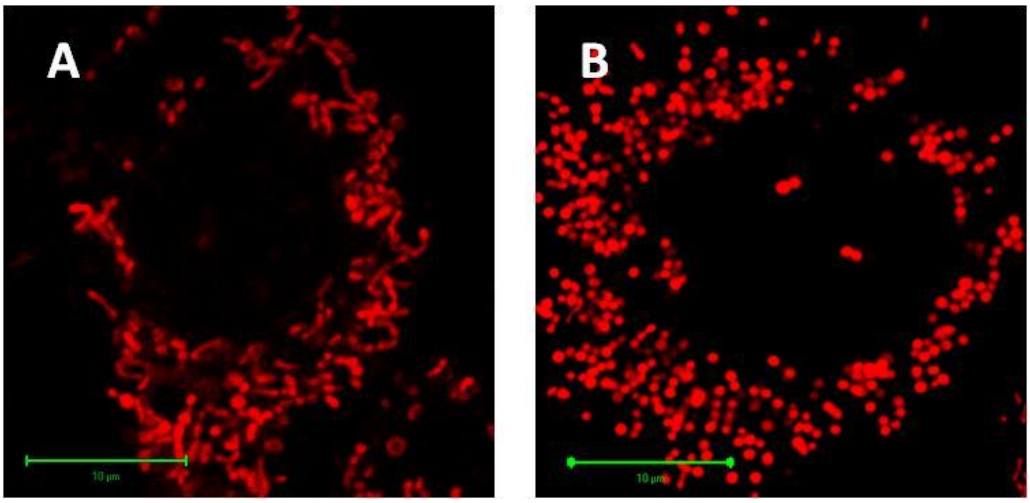

Fig. 7.13
Wildtype (Panel A) and PSB-2 (Panel B) cells were stained with 150nM Mitotracker Red CMX-ROS and imaged at 5000X. Green size bars represent 10µm. Three independent experiments were performed using two 2 dishes each. In each dish, three representative cells were chosen for imaging.

PSB-2 Mitochondrial Motility Analysis

Mitochondrial movement is an intrinsic process displayed by almost all mitochondria. Typical mitochondrial velocities along the long axes of mitochondria can range from 2 to 30μm/min [230]. This process of slithering and sliding has been demonstrated to be influenced by cellular ATP levels, as it is believed that mitochondria are more likely to move to cellular locations where energy is needed [232-235]. Moreover, damaged mitochondria may move in a retrograde fashion from distal portions of the cell back to proximal regions to be recycled through autophagy.

As previously discussed in chapter 5, long-distance mitochondrial movements along MTs are known to require ATP and short-distance movements along MFs have been shown to be ATP independent. Since PSB-2 mitochondria have increased ATP levels and a punctate cellular morphology, their motility was investigated through time-lapse confocal microscopy. From imaging wildtype and PSB-2 mitochondria stained with Mitotracker Red CMX-ROS for approximately 7.5 minutes, it was observed that PSB-2 mitochondria in comparison with wildtype mitochondria, lacked long-distance movement (Fig. 7.14). Moreover, the PSB-2 mitochondria also lack mitochondrial fusion as they were not observed to interact with one another. These observations suggest that several possible events may be occurring. Firstly, the increased cellular ATP along with the decreased cellular growth rates in PSB-2 cells may mean that their mitochondria are no longer needed at sites of high energy demand. Thus, PSB-2 mitochondria do not need to be constantly sent to distal regions of the cell and then brought back to

proximal regions for recycling. This finding is consistent with previous reports by *Bereiter-Hahn et al.* which showed that ATP microinjections into cells can inhibit mitochondrial motility [229]. Secondly, PE is a metastable hexagonal phase non-membrane forming phospholipid which is known to be involved in membrane fusion events. Hence, a lack of PE may decrease membrane fusion through increasing the activation energy of membrane topology changes for fusion, thus, the observed decrease in mitochondria fusion, which is likely responsible for the punctate morphology of PSB-2 mitochondria, may be due to a lack of PE.

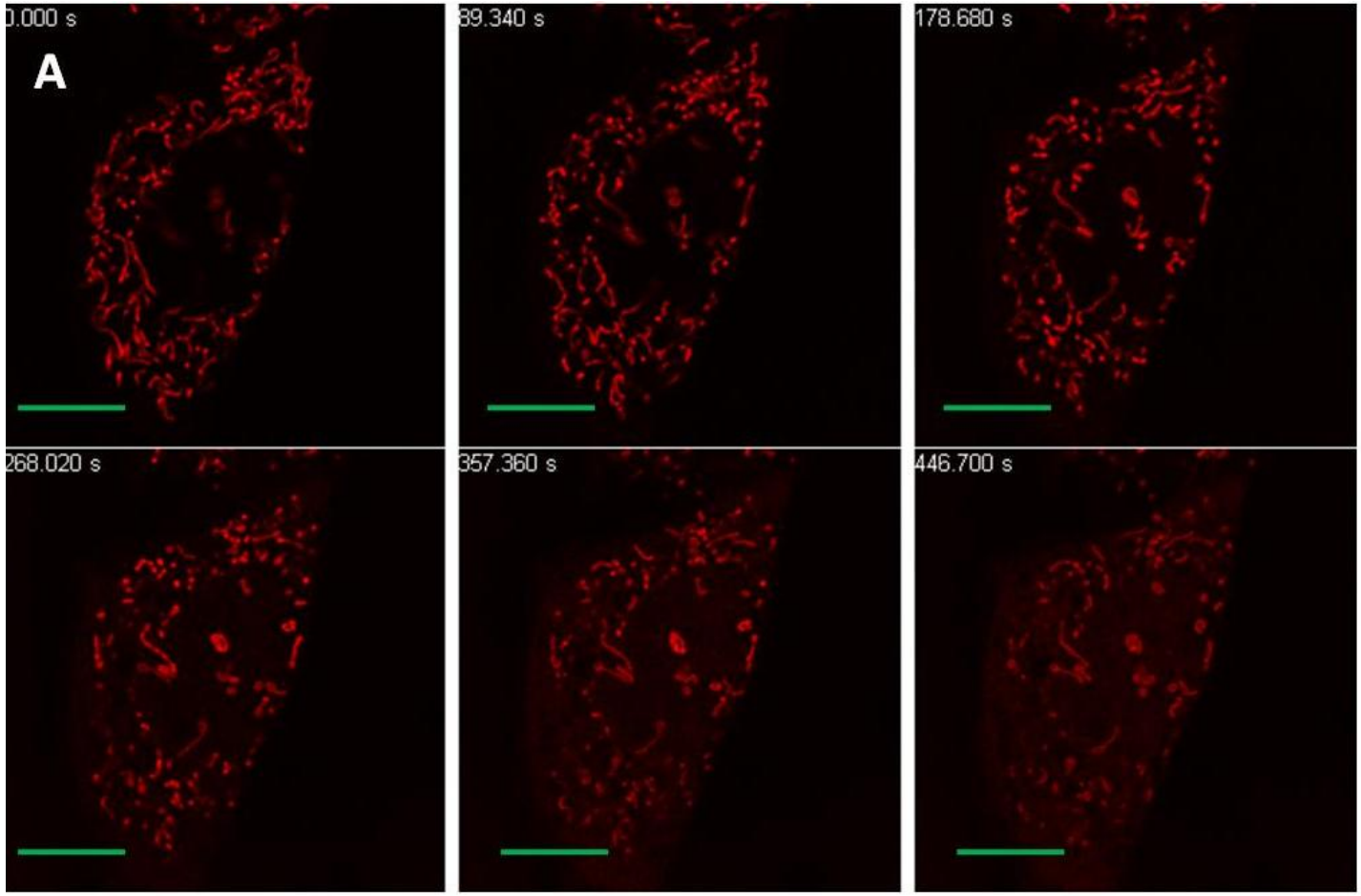
0.000 s
A
89.340 s
178.680 s
268.020 s
357.360 s
446.700 s

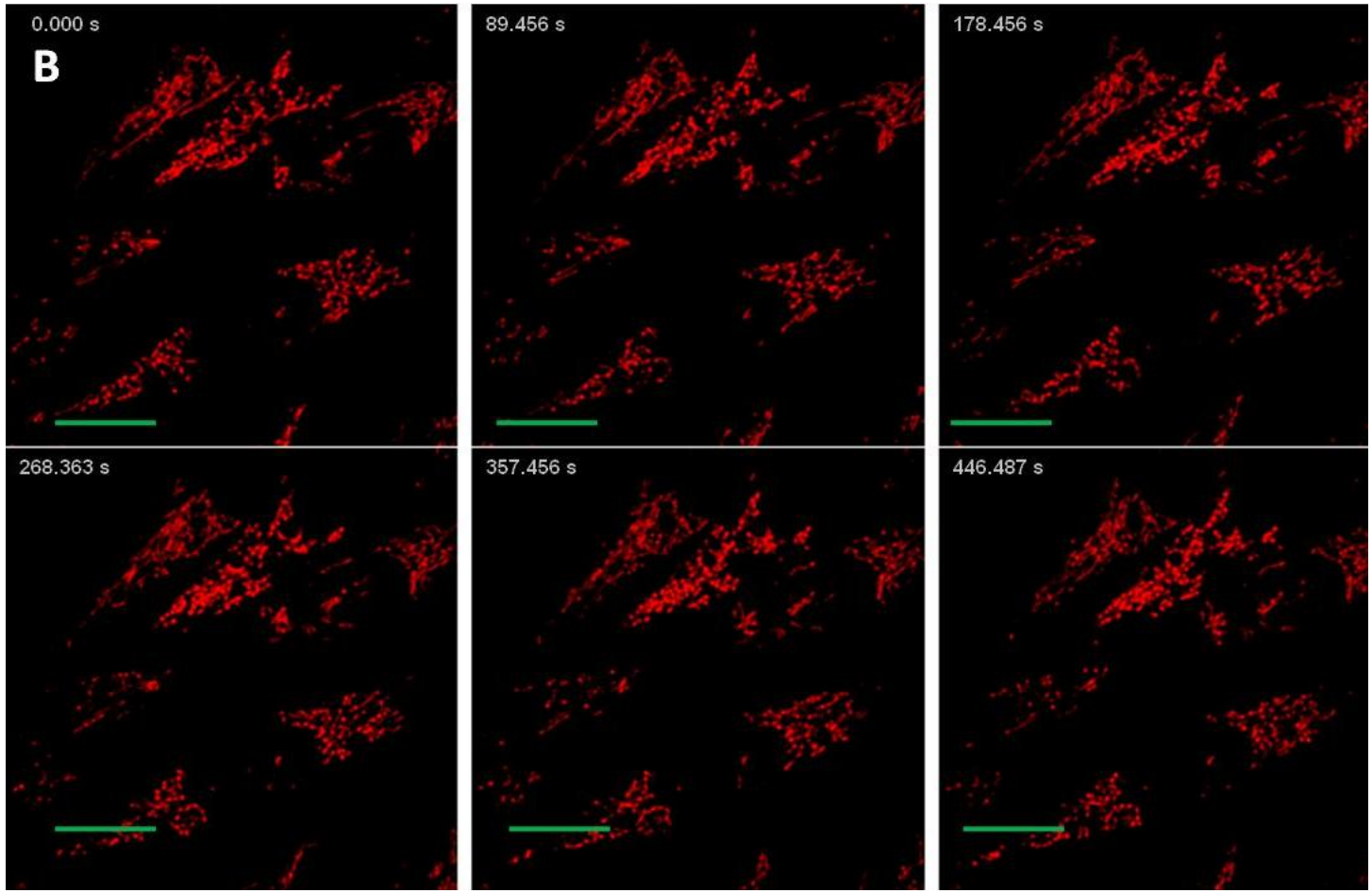
0.000 s
B
89.456 s
178.456 s
268.363 s
357.456 s
446.487 s

Fig. 7.14
Mitochondria from wildtype (wt) (Panel A) and PSB-2 (Panel B) cells were stained with Mitotracker Red CMX-ROS and imaged using timelapse video capture for approximately 7.5 minutes. Six images representing 90 second increments are shown above for each cell type respectively. Green size bars represent 10µm. Three independent experiments were performed using duplicate dishes of cells and three representative cells were imaged per dish for approximately 7.5 minutes.

7.6 R-41 Phospholipid Analyses

R-41 Mitochondria Have Reduced PE Levels

The transport of PS from its site of synthesis on the MAM to the mitochondrion is the rate limiting step of PE synthesis in the PSD pathway [12]. At present, the mechanism underlying this transport process is still relatively unknown, as the genes, proteins, and exact mechanism involved are still unidentified. In 1999, *Emoto et al.* isolated a strain of MAM to mitochondrion PS transport defective CHO-K1 cells named R-41 cells [21]. In this investigation, the mitochondrial PS, PE, and PC levels of the latter R-41 cells were measured via phosphorus analysis. It was found that the mitochondrial PE levels of R-41 cells were 36.0% lower than that of wildtype cells, and the PS and PC levels were unchanged (Fig. 7.15B). This result is not surprising given that the majority of mitochondrial PE in CHO cells is synthesized via the PSD pathway. Moreover, this finding is consistent with previous reports by *Emoto et al.* in which they have reported ~40% lower whole cell PE levels [21], suggesting that mitochondrial PE synthesized via the PSD pathway is also exported and utilized outside of the mitochondrion.

The decrease in R-41 mitochondrial PE is mass is reminiscent of the decrease previously seen in PSB-2 mitochondria, as PSB-2 mitochondria were measured to have a 36.5% reduction in PE mass. The PS levels of R-41 mitochondria are unlike that of PSB-2 mitochondria in that they are unchanged (Fig. 7.15A). PSB-2 mitochondria have decreased PS levels due to defects in cellular PS synthesis. However, despite having a defect in PS transport, R-41 cells

do not accumulate PS and their mitochondria do not show reduced levels of PS (Fig. 7.15). This result suggests that PS levels are tightly regulated in CHO cells in that they are never in excess. Furthermore, in conditions of reduced PS availability, R-41 mitochondria were observed to reduce their PE levels at the expense of PS, suggesting that PS regulation may be tighter than that of PE.

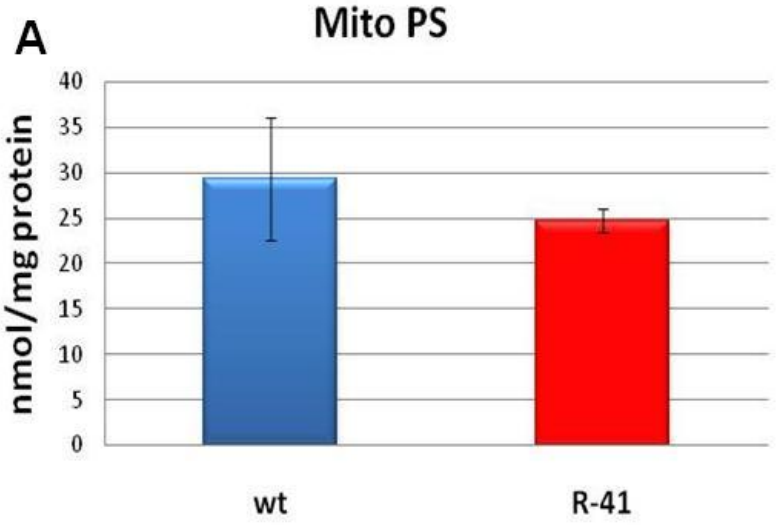
A
Mito PS
nmol/mg protein
40
35
30
25
20
15
10
5
0
wt
R-41

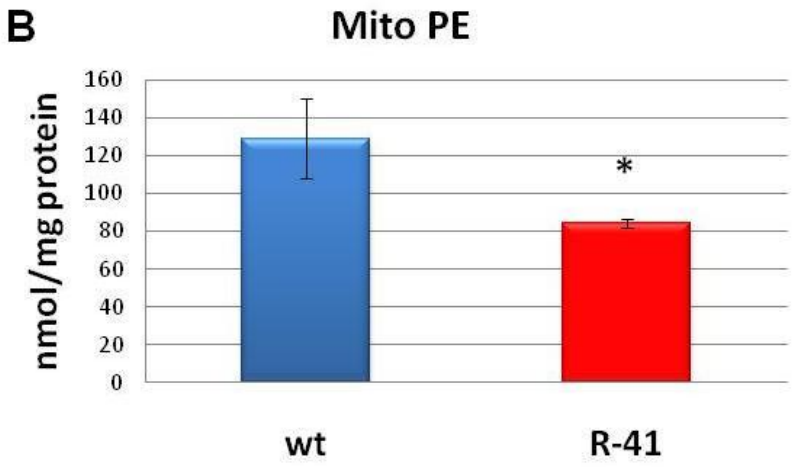
B
Mito PE
nmol/mg protein
160
140
120
100
80
60
40
20
0
*
wt
R-41

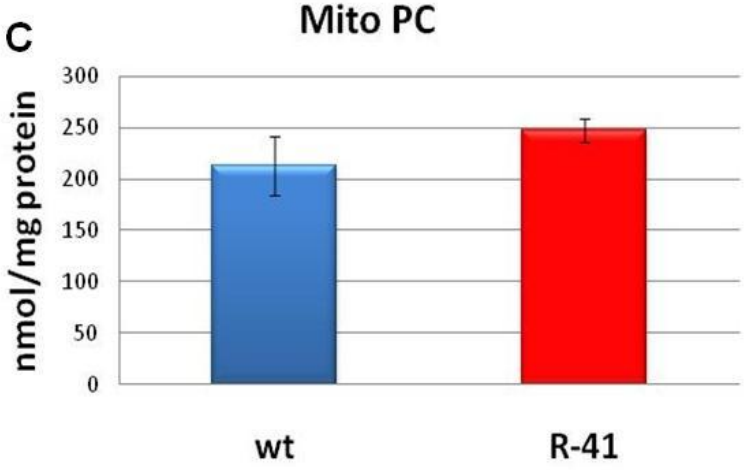
C
Mito PC
nmol/mg protein
300
250
200
150
100
50
0
wt
R-41

Fig. 7.15
The molar masses of mitochondrial (mito) PS (Panel A), PE (Panel B), and PC (Panel C) per milligrams of mitochondrial protein were quantified for wildtype (wt) and R-41 cells using phosphorus analysis. The above data represent the average of three independent experiments. P-value of * = 3.05×10^{-3}.

Phospholipid Content of R-41 Cell Homogenates

The whole-cell PS, PE, and PC levels of wildtype and R-41 cells were compared via phosphorus analysis. It was determined that R-41 cells had a 35.4% reduction in PE levels and a 28.7% increase in PC levels when compared to wildtype cells. The reduction in cellular PE and increase in cellular PC is consistent with previous reports by *Emoto et al.,* who have found ~40% decreases in cellular PE and ~14% increases in cellular PC [21]. Although the homogenate of PSB-2 and PSD KD cells in this investigation also show similar trends in decreased cellular PE and increased cellular PC, their changes were not statistically significant (Fig. 7.2 and 7.29).

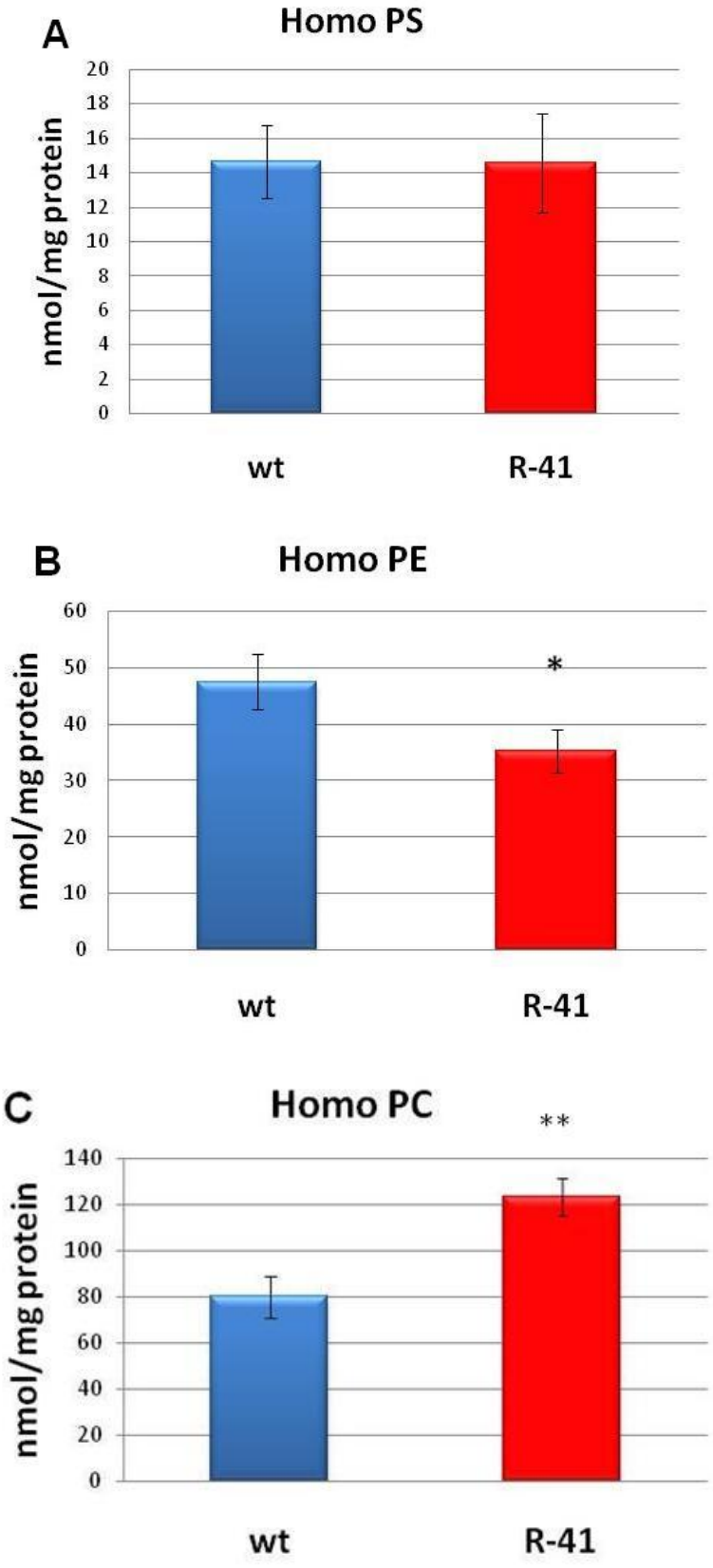
A
Homo PS
nmol/mg protein
20
18
16
14
12
10
8
6
4
2
0
wt
R-41
B
Homo PE
nmol/mg protein
60
50
40
30
20
10
0
*
wt
R-41
C
Homo PC
nmol/mg protein
140
120
100
80
60
40
20
0
**
wt
R-41

Fig. 7.16
The molar mass of whole cell homogenate PS (Panel A), PE (Panel B), and PC (Panel C) per milligrams of cellular homogenate protein was quantified for wildtype (wt) and R-41 cells using phosphorus analysis. The above data represent the average of three independent experiments. P-values of * = 0.0194 and ** = 0.00477.

R-41 Mitochondria Have Normal Levels of Cardiolipin

Cardiolipin is an essential mitochondrial phospholipid which is required for the proper structure and function of MIM enzymes. The cardiolipin levels of R-41 mitochondria were examined to investigate if reductions in PE could affect mitochondrial cardiolipin levels. Given that PE biosynthesis is not metabolically coupled to cardiolipin, it was not surprising to find that the cardiolipin levels of R-41 mitochondria were unchanged compared to that of wildtype levels (Fig. 7.18).

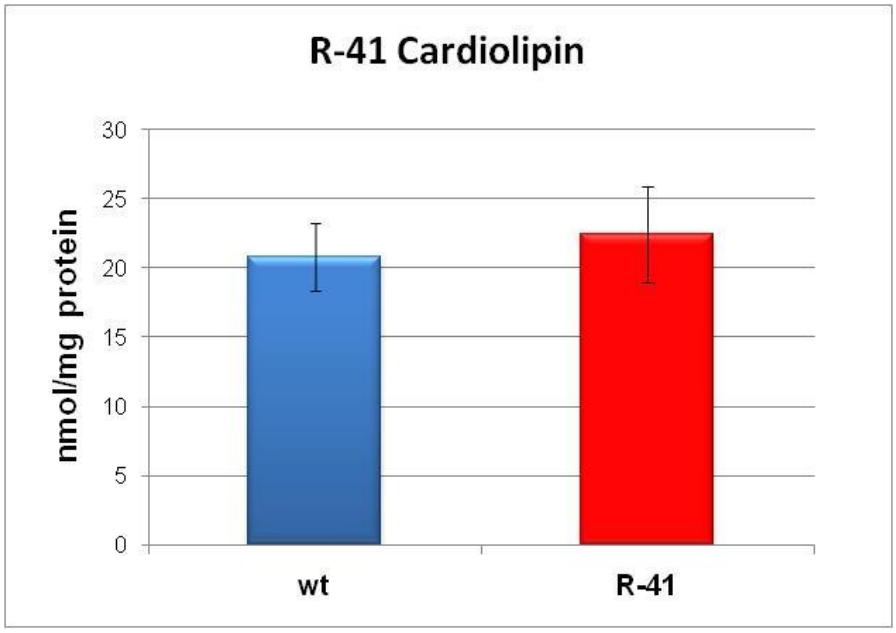

Fig. 7.18 Cardiolipin levels of wildtype (wt) and R-41 mitochondria. Mitochondrial cardiolipin was quantified using three independent preparations of pure mitochondria from wildtype and R-41 cells. Cardiolipin molar mass was measured through phosphorus analysis. P-value >0.05.

[^{3}H] Serine Incorporation into PS and PE in R-41 Cells

The incorporation of serine into PS and its subsequent decarboxylation to form PE were measured in R-41 cells using [^{3}H] serine radiolabeling. When cells were harvested after 1, 3, 5, and 10h of [^{3}H] serine incubation, R-41 cells showed 20.5% and 23.5% less [^{3}H] PS than wildtype cells at 3 and 10 h respectively (Fig. 7.19A). This result suggests that R-41cells have a modest decrease in the pool of [^{3}H] PS. When [^{3}H] PE levels were measured at 1, 3, 5, and 10h, it was found that R-41 cells had 47.8%, 49.5%, 35.8%, and 67.9% less [^{3}H] PE than wildtype cells. This result demonstrates that PE synthesis from PS is indeed reduced in R-41 cells as confirmed by PE mass quantifications earlier.

The sum of [^{3}H] PS and [^{3}H] PE radioactivity represents the total cellular incorporation of [^{3}H] serine. The combined radioactivity of [^{3}H] PS and [^{3}H] PE in R-41 cells was 22.4%, 19.6%, 20.5%, and 39.3% lower than wildtype levels at 1, 3, 5, and 10 h time points respectively. This decrease implies that R-41 cells incorporated less serine into PS due to reduced PE synthesis. In comparison to PSB-2 cells which have ~85% less incorporation of radiolabeled serine, this result is reasonable because R-41 cells only have a defect in mitochondrial PS transport. Thus, PS synthesis and mass are relatively unchanged in R-41 cells.

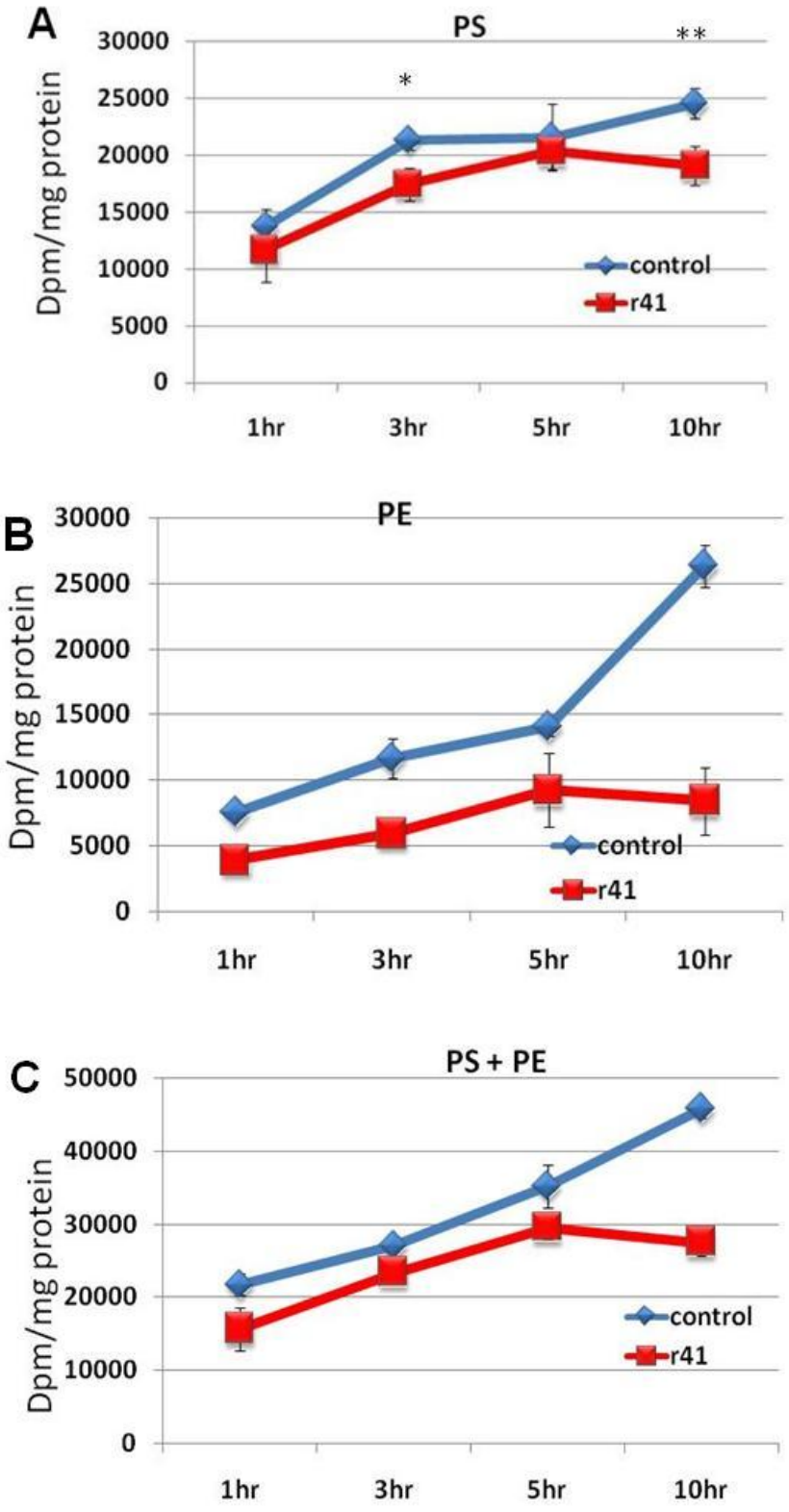
A
PS
**
*
30000
25000
20000
15000
10000
5000
0
Dpm/mg protein
control
r41
1hr
3hr
5hr
10hr
B
PE
30000
25000
20000
15000
10000
5000
0
Dpm/mg protein
control
r41
1hr
3hr
5hr
10hr
C
PS + PE
50000
40000
30000
20000
10000
0
Dpm/mg protein
control
r41
1hr
3hr
5hr
10hr

Fig. 7.19
R-41 and wildtype cells (wt) were incubated with 5μCi/ml [3-^{3}H] serine for 1, 3, 5, and 10 h after which PS and PE were isolated. The radioactivity of [^{3}H] PS and [^{3}H] PE at the above times was quantified in dpms per milligram of cellular protein for wildtype and R-41 cells (Panel A and Panel B). The sum of [^{3}H] PS and [^{3}H] PE radioactivity per milligram protein, which represents total [^{3}H] serine incorporation with respect to time, was calculated for wildtype and R-41 cells (Panel C). [^{3}H] serine incorporation into wildtype and R-41 cells was quantified using three independent experiments with triplicate dishes each time. Data from one of the three experiments is shown above. P-values for panel A were *0.0112 and **0.00674 at 5 and 10h time points, and all p-values for panel B and C were <0.05.

7.7 R-41 Cell Doubling Time

Since PSB-2 cells had reduced mitochondrial PS and PE levels and reduced cell growth, R-41 cell growth was examined to determine a possible correlation between mitochondrial PE and cell growth. Through measuring cell growth in pre-determined $1mm^2$ areas, it was found that R-41 cells do not have reduced cell growth (Fig. 7.20). Compared with the previous findings of PSB-2 cells (Fig. 7.5C), these results suggest that threshold levels of PS and PE together are important for cell growth. Studies of mammalian plasma membranes have shown that PS and PE make up the bulk of the inner leaflet phospholipids [12]. If the same were true of PS and PE in mitochondrial membranes, then the above decrease in cell growth would make good biophysical sense, as PS and PE are both cone shaped molecules which can accommodate the inward curvature of cellular membranes [22]. Thus, it is conceivable that a reduction in both phospholipids can limit cell growth whereas a decrease in one can be tolerated.

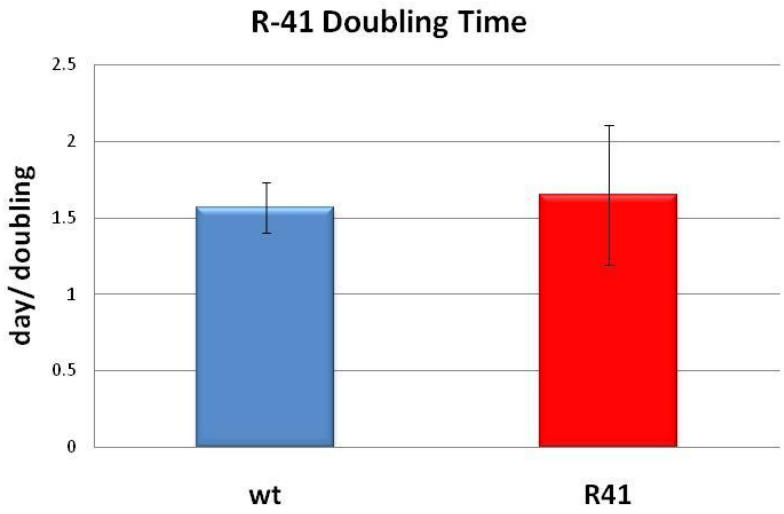

Fig. 7.20
Doubling times of wildtype and R-41 cells. The above figure shows the average of three independent experiments. In each experiment, the change in number of cells in three 1mm x 1mm grids was counted between 24 and 48 hours after plating. The statistical significance of the difference between wildtype and R-41 cells had p-value >0.05.

7.8 Increased Mitochondrial Density in R-41 Cells

The sedimentation of densities of wildtype and R-41 mitochondria were compared using Percoll gradient centrifugation. R-41 mitochondria showed an abnormally high sedimentation density compared to wildtype mitochondria. The MAM of R-41 cells, however, retained a normal sedimentation density compared to wildtype MAM (Fig. 7.21). As *Schumacher et al* have previously proposed, this phenomenon is likely due to a decrease in mitochondrial phospholipid to protein ratio, since proteins are denser than phospholipids.

This increased density of mitochondria is similar to the density previously observed in PSB-2 mitochondria which have decreased PS and PE. Since mitochondrial membranes are comprised of approximately ~30% PE and ~4% PS, it is likely that mitochondrial PS decreases are inconsequential to changes in sedimentation density and PE levels are a larger contributing factor [12].

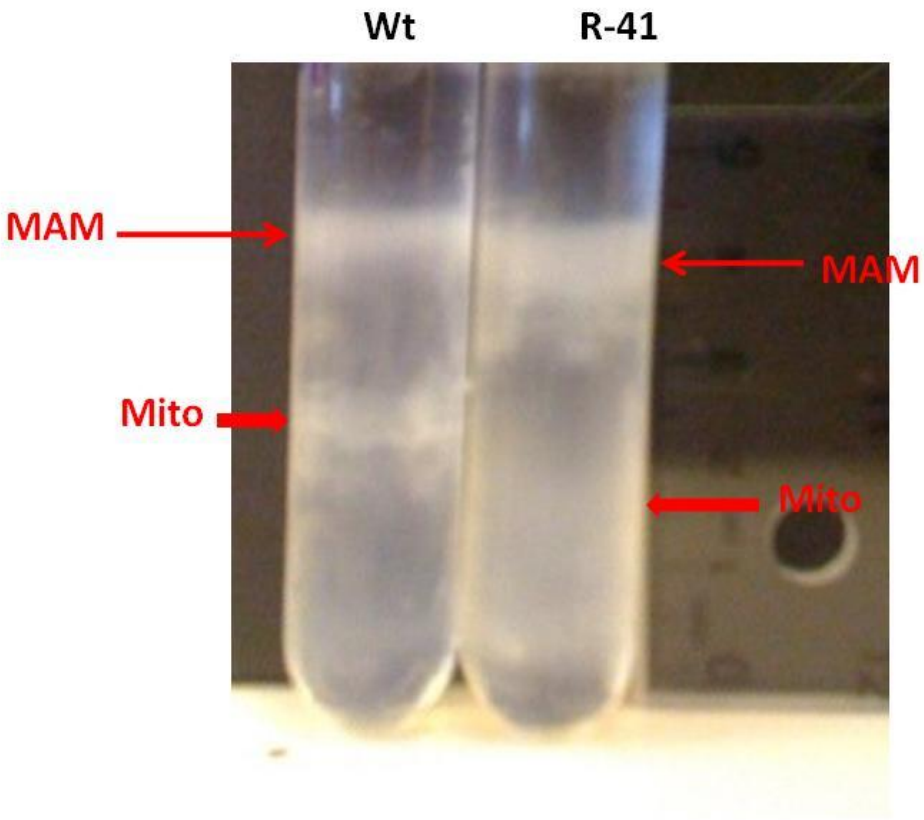

Fig. 7.21
Density gradient centrifugation of mitochondria and MAM from wildtype (wt) and R-41 cells on a 20% Percoll gradient. Pure mitochondria were isolated from wildtype and R-41 cells in three independent experiments with similar results.

7.9 R-41 Mitochondrial Physiology

COX is a MIM enzyme which requires phospholipids for function. At present, 13 molecules of membrane lipids have been reported to be part of the COX structure. These lipids include: two cardiolipins, three triacylglycerols, four phosphatidylglycerols, one PC, and three PEs [157].

In this investigation, COX activity was measured from pure preparations of R-41 mitochondria which were deficient in PE but not PS, PC, or cardiolipin (Fig 16. and Fig. 7.18). R-41 mitochondria contained the same COX activity as wildtype mitochondria. This result, in combination with what was previously learned from PSB-2 mitochondria, suggests that a ~35% reduction PE alone is not enough to change COX activity (Fig. 7.22). However, a decrease in both PS and PE by~35%, as observed in PSB-2 cells, is sufficient to moderately decrease COX activity. Thus, it is likely COX may have a relatively minor requirement for PS to maintain normal activity.

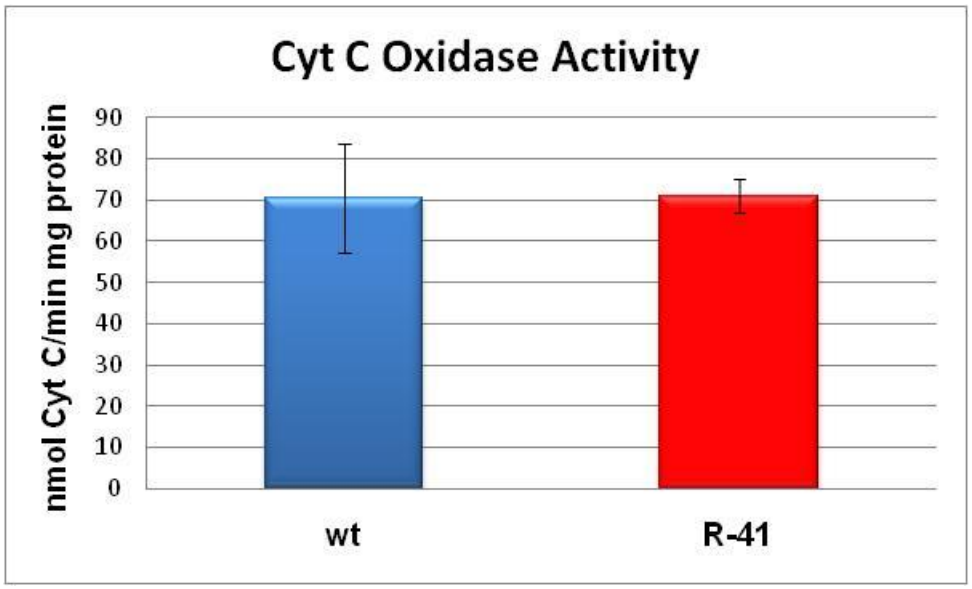

Fig. 7.22
Cytochrome c oxidase activity in mitochondria of wildtype cells (wt) and R-41 cells. Cytochrome c oxidase activity was measured from three independent preparations of pure mitochondria. Each sample was assayed in triplicate reactions. The difference in activity between the wildtype and R-41 cells had a calculated p-value of 0.413 using the student's t-test.

Reduced ATP Levels in R-41 Cells

As previously reviewed in chapter 5, ATP is the molecular currency of intracellular energy transfer. ATP is used by numerous enzymes and structural proteins in many cellular processes, some of which include metabolism, organelle motility, and cell division.

In light of the increased ATP levels previously observed in PSB-2 cells, the ATP levels of R-41 cells were examined. Through quantifying ATP in cellular lysates via luciferase lumination analysis, it was found that R-41 cells have 43.2% less ATP compared to wildtype cells (Fig. 7.23). This decrease in ATP is surprising given that both PSB-2 and R-41 cells have defects in the PSD pathway resulting in decreased PE levels. However, upon closer examination, PSB-2 and R-41 cells have rather different phenotypes. For example, PSB-2 cells have significantly reduced growth rates whereas R-41 cells have normal growth rates in comparison to wildtype cells.

Since many integral membrane proteins involved in the synthesis of ATP are known to require specific phospholipids, it is likely that both PSB-2 and R-41 cells suffer from metabolic inefficiencies in ATP production. For example, it is known that ATP synthase requires PC, phosphatidylglycerol, and cardiolipin for optimal function [169]. It is likely that the decreased ATP production in PSB-2 cells is masked by decreased cell growth and the R-41 cells also have a defect in ATP synthesis, however, they are able to fully utilize their synthesized ATP. Thus, in simplified terms, the above observations suggest that a decrease in

mitochondrial PE decreases cellular ATP, and a concomitant decrease in mitochondrial PE and PS increases cellular ATP.

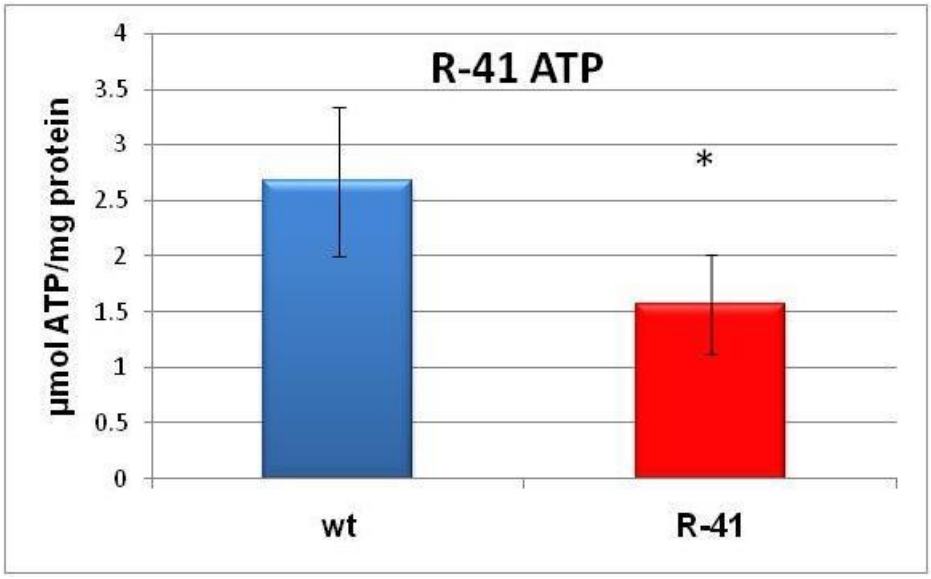

Fig. 7.23
ATP from wildtype (wt) and R-41 cell lysates was extracted using trichloroacetic acid (TCA) in three independent experiments with triplicate dishes of cells. Each dish was quantified in reaction triplicates through luciferase lumination analysis. P-value of * = 2.5×10^{-2}.

Increased Membrane Potential in R-41 Mitochondria

Previous observations of mitochondrial hyperpolarization in PSB-2 cells have provided evidence for a correlation between mitochondrial hyperpolarization and defects in the PSD pathway. This relationship is further examined here with R-41 cells which have a defect in MAM to mitochondrion PS transport (Fig. 1.2). When $\Delta\Psi$ was quantified using TMRM fluorescence via confocal microscopy, it was found that R-41 mitochondria have ~138% more TMRM fluorescence than wildtype mitochondria (Fig. 7.24A). This result demonstrates that R-41 mitochondria, like PSB-2 mitochondria are hyperpolarized. However, this difference in R-41 mitochondria was decreased to ~84% when TMRM fluorescence was normalized to mitochondrial surface area using Mitotracker Green (Fig. 7.24). This decrease can be contrasted to previous data with PSB-2 mitochondria, which were more hyperpolarized than wildtype cells after normalization to mitochondrial surface area. This result suggests that although R-41 mitochondria are hyperpolarized, their ratio of $\Delta\Psi$ to MIM surface area is not as great as that of PSB-2 mitochondria. This observation can be understood through the analysis of PSB-2 and R-41 mitochondrial morphology (Fig. 7.13 and Fig. 7.25). When compared to wildtype mitochondria, PSB-2 mitochondria are abnormally punctate and R-41 mitochondria were abnormally tubular. Thus, the punctate morphology of PSB-2 mitochondria gives rise to a greater membrane surface area to which TMRM fluorescence is normalized.

Since mitochondrial enzymes involved in ATP synthesis require phospholipids for optimal activity [166], it is likely that R-41 mitochondria are

hyperpolarized due to a defect in ATP synthesis. For example, it is possible that the mitochondrial ETC may built up a $\Delta\Psi$ which ATP synthase cannot effectively use due to an alterations in membrane phospholipid composition. This scenario is plausible because there were no significant changes in the activity of COX, the last enzyme of the ETC (Fig. 7.8), suggesting that electron transport is normal and is fully capable of generating a hyperpolarized $\Delta\Psi$. Since COX activity is only moderately reduced in PSB-2 cells (Fig.7.8) , the latter mechanism can be also be reasonably applied to PSB-2 cells. Therefore, an examination of all five components of the respiratory chain complexes is necessary to fully understand mitochondrial hyperpolarization in cells with defects in the PSD pathway.

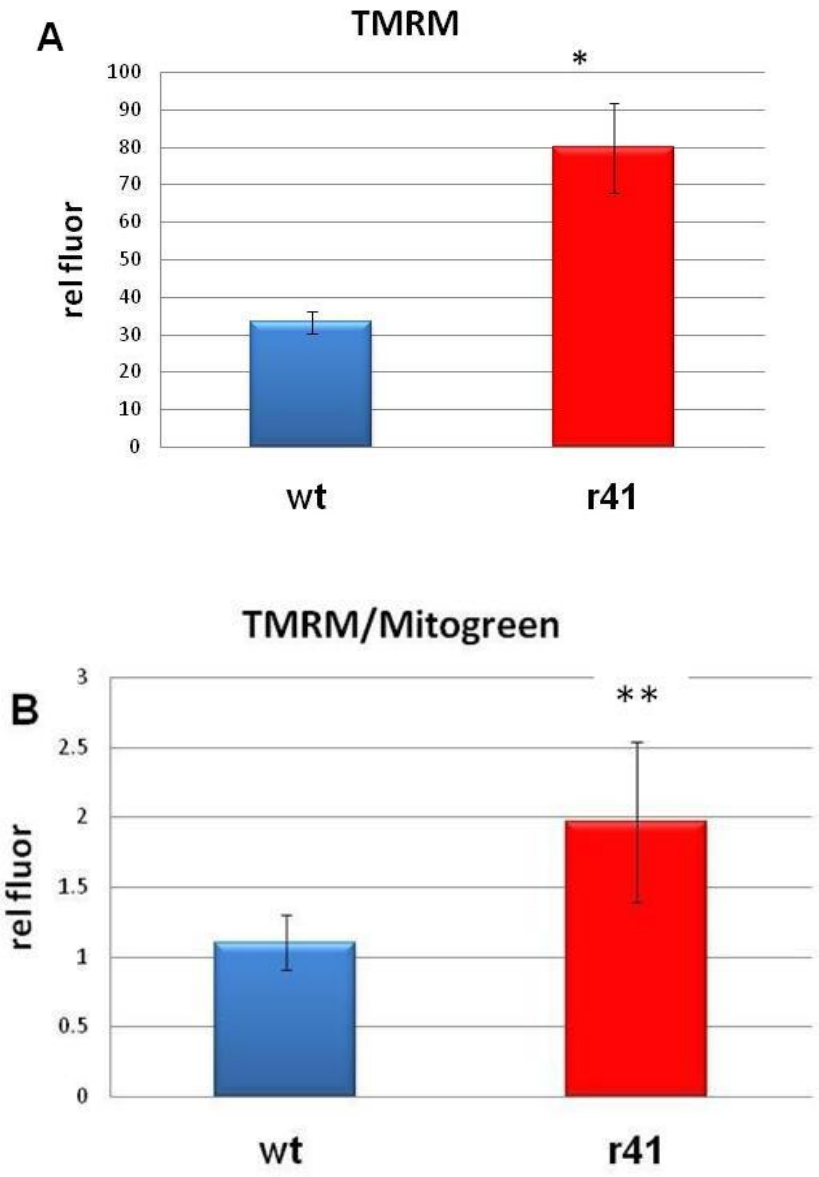

Fig. 7.24

The $\Delta\Psi$ of wildtype (wt) and R-41 mitochondria was quantified from three independent experiments using triplicate dishes. From each dish, three images were taken, and fluorescence of 20 cells was measured per image. The TMRM fluorescence of wildtype and R-41 mitochondria were compared (Panel A). The TMRM fluorescence of wildtype and R-41 mitochondria were normalized to Mitotracker Green fluorescence and subsequently compared (Panel B). P-values of *= 4.8×10^{-4} and **9.8×10^{-3}.

7.10 The Mitochondrial Morphology and Motility of R-41 Cells

R-41 Mitochondrial Morphology

Since PSB-2 cells contain abnormally punctate mitochondria, it was hypothesized that R-41 cells would also show defects in mitochondrial morphology. Surprisingly, when R-41 cells were visualized via confocal microscopy, it was found that they contained more tubular mitochondria than wildtype cells (Fig. 7.25). This was an unexpected result because the phospholipid defects in PSB-2 cells and R-41 are similar in that they both have defects in the PSD pathway. Thus, the differences in their defects must be responsible for their opposite phenotypes.

Unlike PSB-2 cells, R-41 cells have a defect in the MAM to mitochondrion transport of PS. It has been proposed that this latter transport process occurs through transient MAM and mitochondrion physical contact [51]. If PS transport is indeed reduced by defects in MAM to mitochondrion contact, then it is reasonable to believe that the transport of other molecules such as calcium ions and ATP may be impaired as well.

The mitochondrion and the ER are two organelles which are highly interdependent. It is known that the ER requires vast amounts of energy from mitochondria for protein and lipid synthesis. Conversely, mitochondria depend on the ER for the synthesis of many integral membrane proteins, nutrients, and metabolites. If the transport of molecules between MAM and mitochondria is impaired then it is likely that more contact sites would be made available. This

increase in contact sites might explain why R-41 mitochondria are tubular and pressed up against cell centers (Fig. 7.25).

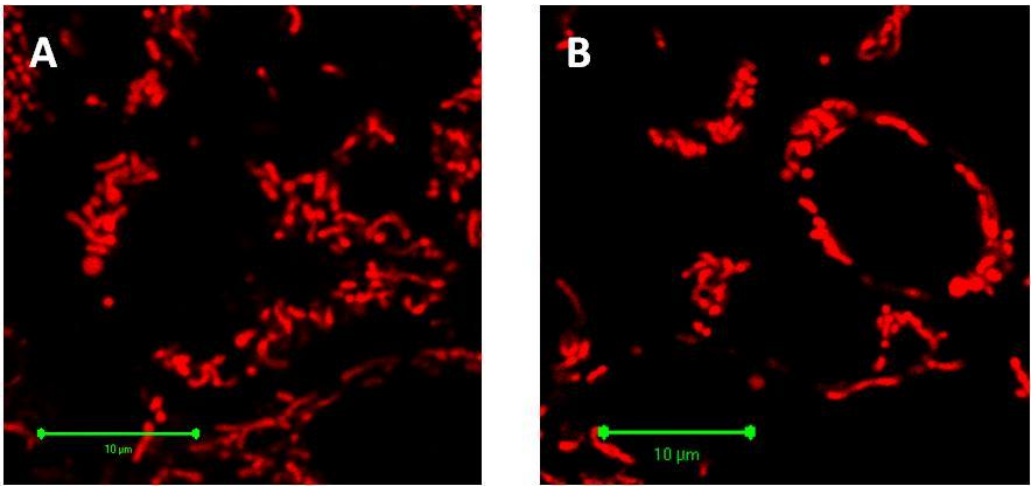

Fig. 7.25
Wildtype (Panel A) and R-41 (Panel B) mitochondrial morphologies were visualized via confocal microscopy at 5000X magnification. The cells were stained with 150nM Mitotracker Red CMX-ROS. Green size bars represent 10µm. Three independent experiments were performed using two 2 dishes each. In each dish, three representative fields of view were chosen for imaging.

R-41 Mitochondrial Motility

Since PSB-2 mitochondria showed decreased motility compared to wildtype cells, the movement of R-41 mitochondria was also compared to wildtype mitochondria via time-lapse confocal microscopy. Through imaging cells over ~7.5 min time courses, it was found that R-41 mitochondria showed dramatically less movement along their long-axes compared to wildtype mitochondria. In addition, the medial portions of R-41 mitochondrial chains were largely immobile while the distal ends of R-41 mitochondrial chains swung from side to side. This observation supports earlier assertions for why R-41 mitochondria are tubular and closely attached to the centers of cells, as it is very likely that R-41 mitochondria are immobile because they need to maintain contact with MAM. Therefore, it is more likely that the abnormal motility of the R-41 mitochondria is the cause, rather than the effect, of PE deficiency in R-41 cells.

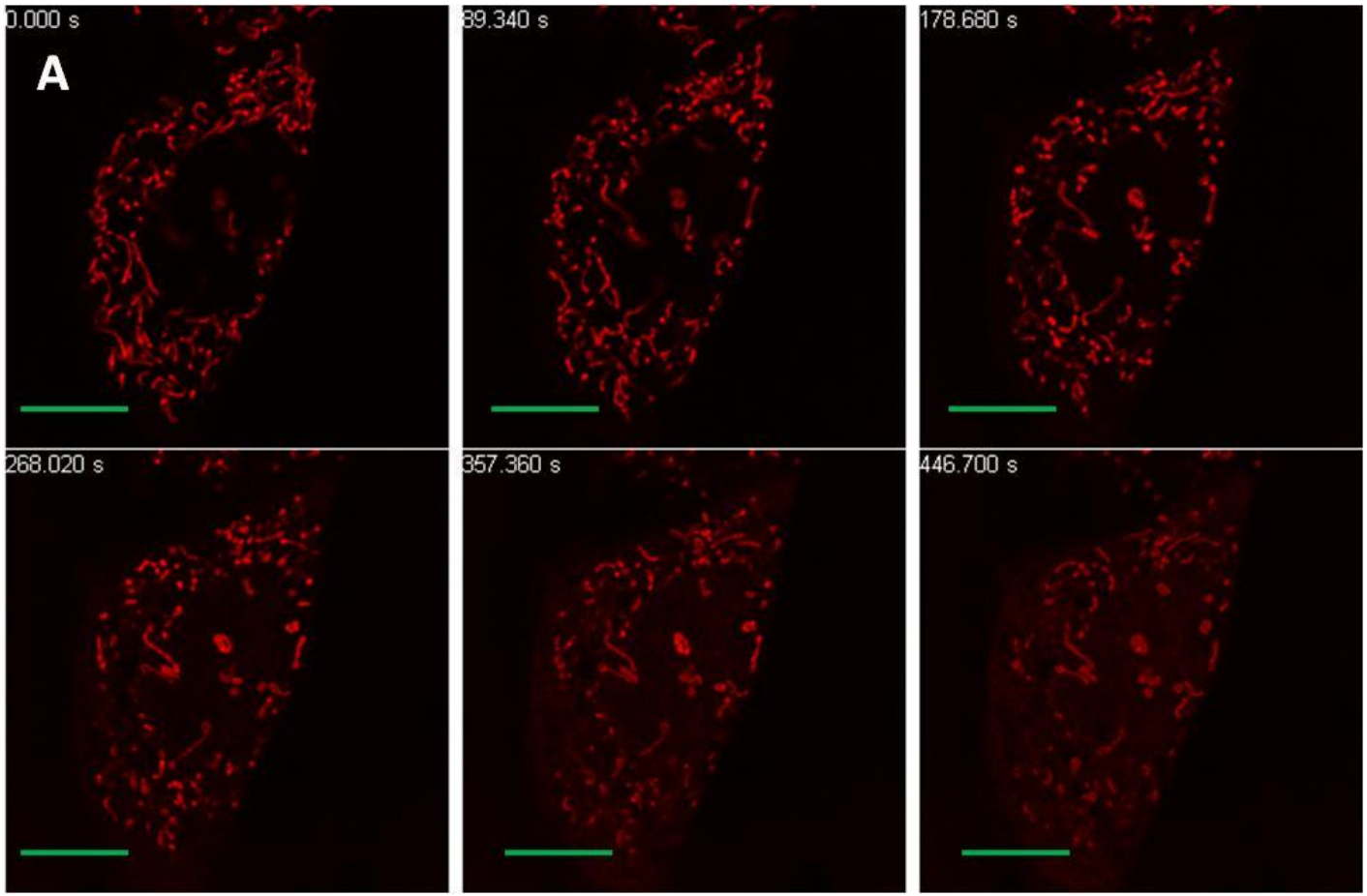
0.000 s
A
89.340 s
178.680 s
268.020 s
357.360 s
446.700 s

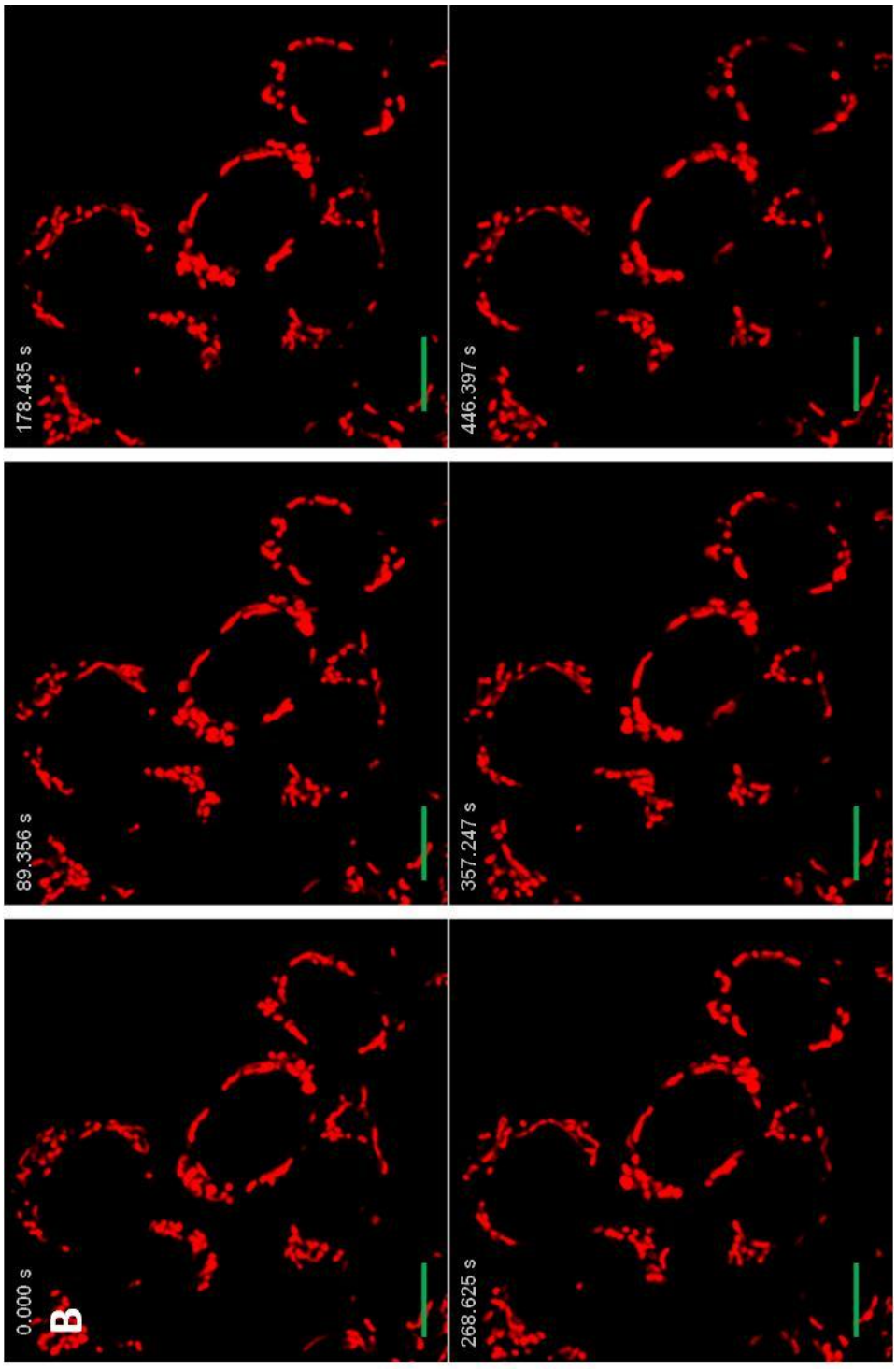
B
0.000 s
89.356 s
178.435 s
268.625 s
357.247 s
446.397 s

Fig. 7.26
Mitochondria from wildtype (Panel A) and R-41 (Panel B) cells were stained with Mitotracker Red CMX-ROS and imaged using timelapse video capture for approximately 7.5 minutes. Six images of wildtype and R-41 cells representing 90 second increments are shown above. The green size bars represent 10µm. Three independent experiments were performed using duplicate dishes of cells and three representative cells were imaged per dish.

7.11 The Knock-down of PSD in CHO-K1 Cells

The impetus of this investigation for examining mitochondrial PE deficiencies in PSB-2, R-41, and especially PSD KD cells is largely based on previous research from our laboratory by *Steenbergen et al* [19]. In 2005, *Steenbergen et al* showed that the elimination of PSD in mice causes embryonic lethality and defects in mitochondrial morphology, and thus, established that PSD is a necessary enzyme for mouse survival. When mouse embryonic fibroblasts were isolated from the *Pisd*$^{-/-}$ embryos, it was found that cells lacking PSD contained large numbers of aberrantly shaped and mislocalized mitochondria [19]. Hence, the hypothesis that PE synthesized from the PSD pathway is necessary for normal mitochondrial function was formulated. Since *Pisd*$^{-/-}$ mouse embryonic fibroblasts have reduced viability, PSD KD CHO cells were used to test this hypothesis.

The KD of PSD in CHO cells was achieved through dsiRNA transfection. Three different dsiRNA duplexes which targeted different regions of the hamster *Pisd* gene were used to eliminate the possibility of non-specific KD. Through the transfection of these three dsiRNAs, *Pisd* mRNA in CHO cells was reduced by 94.4%, 77.2%, and 92.5% compared to cells transfected with negative control dsiRNAs (Fig. 7.27).

After using numerous lipid transfection reagents and different siRNA and dsiRNA duplexes, it was found that the maximum obtainable knockdown of *Pisd* in CHO cells was ~95%. There are two possible reasons for why higher KD was not obtained. Firstly, it is possible that there are limitations to the lipid

transfection and dsiRNA knockdown efficiencies. Secondly, it is also possible that cells which received a KD of greater the 95% simply did not survive. Data presented in the following investigation supports this second possibility as PSD KD cells have a number of defects. Thus, if this second scenario is indeed true, then it would suggest that mammalian cells must have a minimum of 5% residual *Pisd* mRNA to survive. Therefore, to conclusively determine the levels of *Pisd* mRNA required for mammalian survival, one must perform experiments to add back PSD to cells lacking *Pisd*.

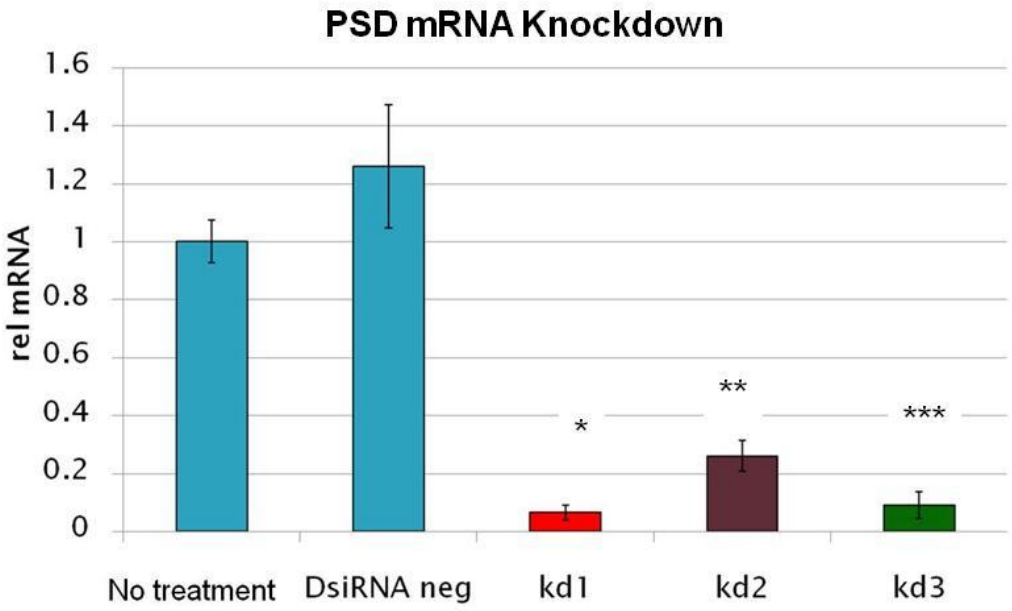

Fig. 7.27
The relative *Pisd* mRNA levels of cells which received no transfection, negative control cells, and three PSD KD cell lines called kd1, kd2, kd3 (each targeting a different region of the *Pisd* mRNA) are shown above. The negative control construct was a scrambled dsiRNA which does not target any known eukaryotic mRNAs. *Pisd* mRNA knockdowns were performed in three independent experiments with three dsiRNA constructs each time. In each experiment, triplicate dishes were transfected with each dsiRNA construct. The *Pisd* mRNA of each of the latter dishes was quantified in reaction triplicates with respect to mRNA encoding the housekeeper gene cyclophilin. P-values of *= 1.6×10^{-3}, **= 5.4×10^{-3}, and ***= 3.5×10^{-3}.

PSD KD Mitochondria Have Decreased PE

After *Pisd* mRNA was decreased by ~90%, the molar masses of PS, PE, and PC in PSD KD mitochondria were determined. Phosphorus analysis showed that PSD KD mitochondria had 35.9% and 30.5% less PE compared to non-transfected and negative control mitochondria respectively (Fig. 7.28B). The mitochondrial PS and PC levels of PSD KD cells were unchanged compared to the mitochondria of untreated cells (Fig. 7.28 A, C). However, the PS levels of negative control mitochondria were 52.1% higher than that of untreated cells. It is possible that the scrambled dsiRNA negative control up-regulated enzymes for PS synthesis. If this is indeed the case with future replicates, then a new dsiRNA negative control duplex would be required.

Just as PSD KD appears to not be able to reduce *Pisd* mRNA by greater than ~95%, reductions in mitochondrial PE of greater than 35% have not been observed in PSB-2, R-41, and PSD KD cells. Therefore, these two findings together suggest that the minimum level of mitochondrial PE required for life may be within in the range of ~80nmol/mg of mitochondrial protein.

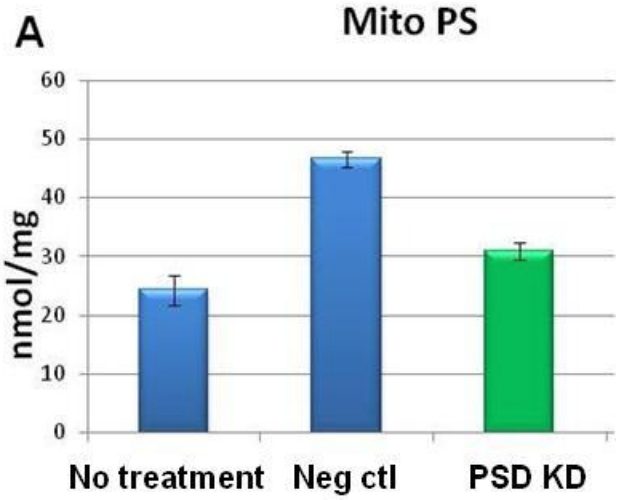
A
Mito PS
nmol/mg
60
50
40
30
20
10
0
No treatment
Neg ctl
PSD KD

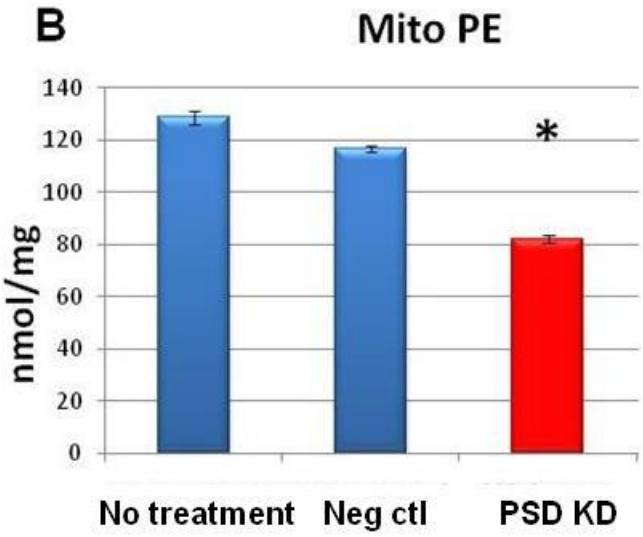
B
Mito PE
nmol/mg
140
120
100
80
60
40
20
0
*
No treatment
Neg ctl
PSD KD

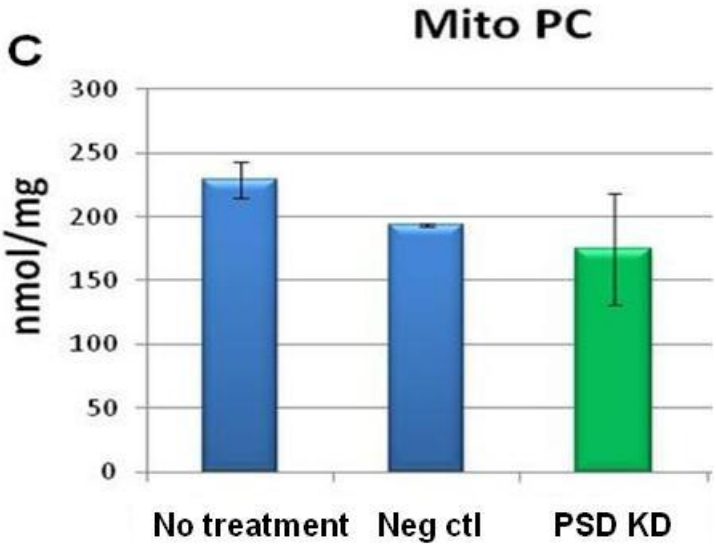
C
Mito PC
nmol/mg
300
250
200
150
100
50
0
No treatment
Neg ctl
PSD KD

Fig. 7.28
Pisd mRNA was reduced in CHO cells through transfecting three different dsiRNAs targeting different regions of the *Pisd* transcript. Mitochondrial PS (Panel A), PE (Panel B), and PC (Panel C) were measured for un-transfected cells, negative control cells, and PSD KD cells. The above data represent the average of three independent experiments. A different PSD knockdown construct was used for each experiment. The p-values of comparing PSD KD to non-treated and negative control mitochondria were 4.5×10^{-3} and 7.8×10^{-3} respectively (Panel B). All other differences had p-values >0.05 (Panel A and C).

Phospholipid Content in Homogenates of PSD KD Cells

The PS, PE, and PC levels in homogenates of untransfected cells, negative control cells, and PSD KD cells were measured through phosphorus analysis. There were no statistically significant differences between the phospholipids measured from PSD KD and negative control cells. This result suggests that PSD KD does not significantly affect whole cell PE levels and therefore, mitochondrial PE and cytoplasmic PE pools must spatially separate.

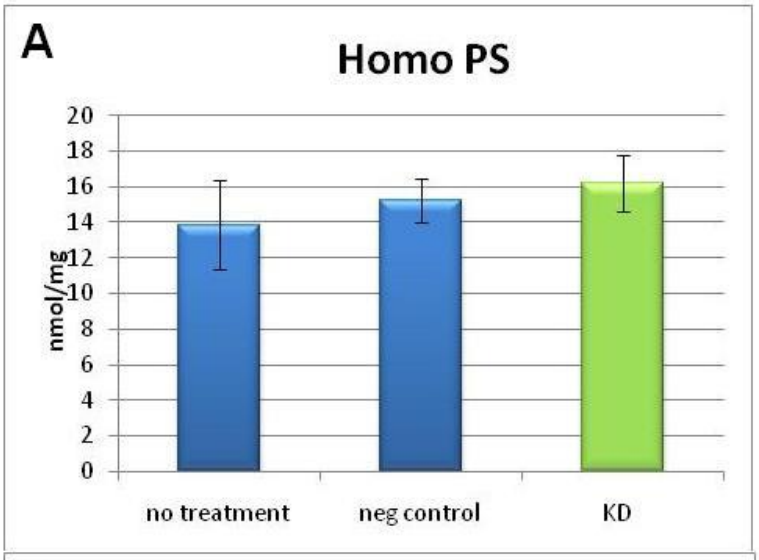
A
Homo PS
nmol/mg
20
18
16
14
12
10
8
6
4
2
0
no treatment
neg control
KD

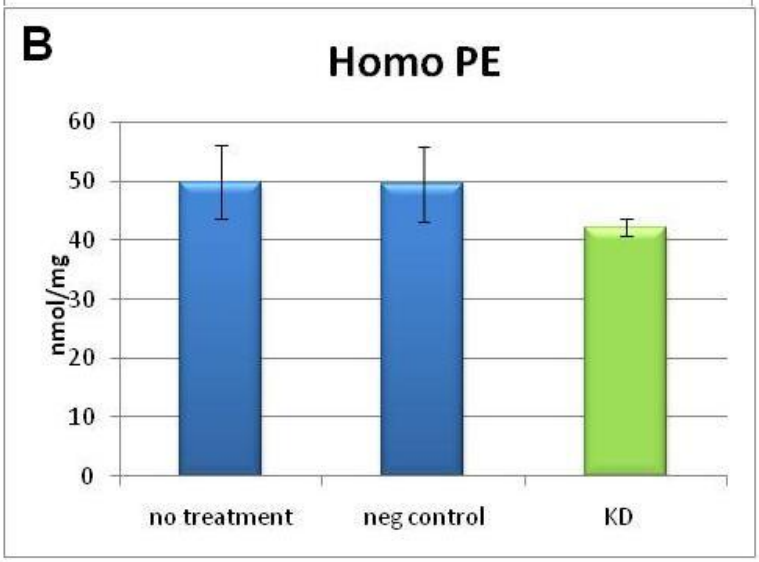
B
Homo PE
nmol/mg
60
50
40
30
20
10
0
no treatment
neg control
KD

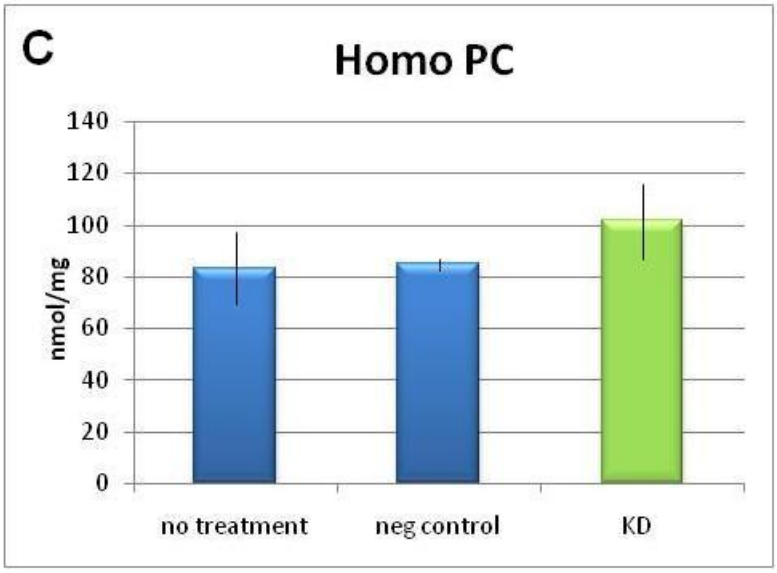
C
Homo PC
nmol/mg
140
120
100
80
60
40
20
0
no treatment
neg control
KD

Fig. 7.29
Pisd mRNA was reduced in CHO-K1 cells through dsiRNA transfection and the cellular PS, PE, and PC levels were measured using phosphorus analysis. Whole cell homogenate PS (Panel A), PE (Panel B), and PC (Panel C) levels are displayed above for cells which received no transfection, negative control cells, and PSD KD cells. The above data represent the average of three independent experiments. A different PSD knockdown construct targeting a different region of the *Pisd* gene was used for each experiment. All of the above differences had p-values >0.05 using the student's t-test.

Cardiolipin Content of PSD KD Mitochondria

Cardiolipin is a mitochondrial phospholipid which is essential to the function of mitochondrial ETC enzymes [155]. The cardiolipin levels of PSD KD mitochondria were compared to that of negative control mitochondria. Through phosphorus analysis of cardiolipin mass, it was determined that there were no statistically significant differences between mitochondria of PSD KD and negative control cells. This result is similar to previous PSB-2 and R-41 cardiolipin measurements in that none of the PSD pathway defective cells had altered levels of cardiolipin (Fig. 7.3 and 7.18). Indeed, this result is not surprising given that the PSD pathway for PE synthesis is not coupled to cardiolipin synthesis.

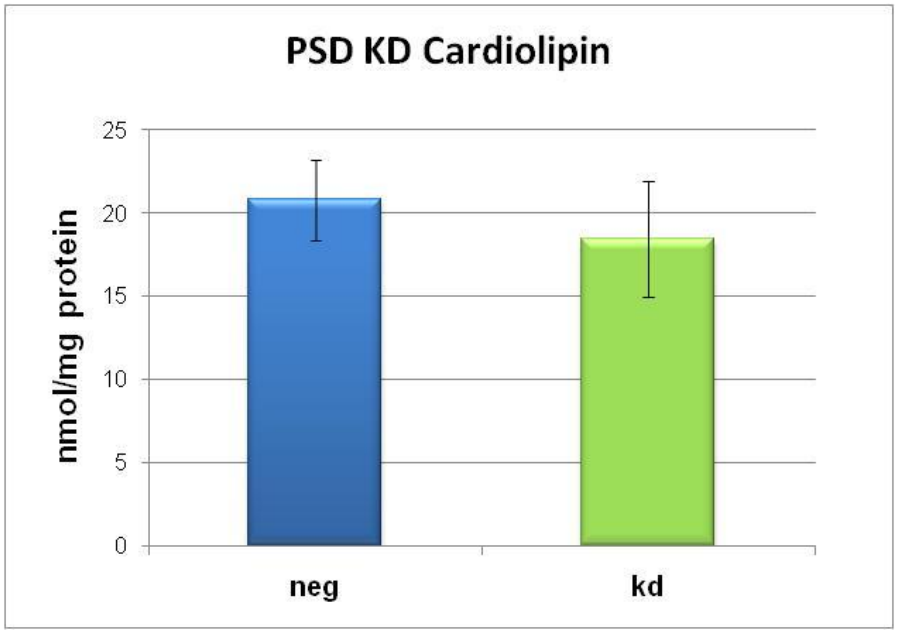

Fig. 7.30 Mitochondrial cardiolipin levels in nmol/mg of for cells transfected with negative control dsiRNA and cells transfected with PSD knockdown dsiRNA. Mitochondrial cardiolipin was quantified using three independent preparations of pure mitochondria from negative control cells and PSD knockdown cells. The statistical significance of the above data had a p-value > 0.05.

[^{3}H] Serine Incorporation into PS and PE in PSD KD Cells

Having determined that PSD KD mitochondria have decreased PE mass, the incorporation of [^{3}H] serine into PS and its subsequent decarboxylation to form PE were measured. After 1, 3, 5, and 10h of [^{3}H] serine incubation, PSD KD cells had 40.0% and 46.3% less [^{3}H] PE compared to negative control cells at 5 and 10 h time points. Hence, this latter difference in the radiolabeling of PE appears to increase with respect to time, suggesting that PSD KD mitochondrial PE levels are likely to decrease linearly after transfection for at least 10 hours. The difference in [^{3}H] PS incorporation between negative control and PSD KD cells was small, as PSD KD cells only 21.42% less [^{3}H] PS after 10 h of radiolabeling (Fig. 7.31).

The sum of [^{3}H] PS and [^{3}H] PE radioactivity represents the total incorporation of [^{3}H] serine into PS. When the combined radioactivity of [^{3}H] PS and [^{3}H] PE was calculated, PSD KD cells had 12.9%, 10.3%, 27.3%, and 32.8% less [^{3}H] serine incorporation than negative control cells at 1, 3, 5, and 10h time points. Therefore, the difference in [^{3}H] serine incorporation into phospholipids between PSD KD and negative control cells is approximately half of the difference previously observed in R-41 and wildtype cells. This result is not surprising given that PS transport is the rate limiting step of the PSD pathway and CHO cells are more likely to be sensitive to decreases in PS transport than PS decarboxylation.

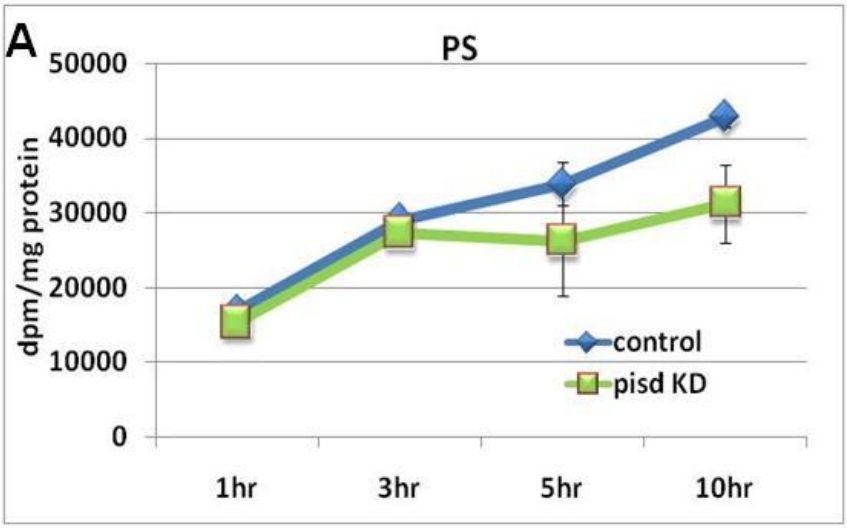
A
PS
50000
40000
30000
20000
10000
0
dpm/mg protein
control
pisd KD
1hr
3hr
5hr
10hr

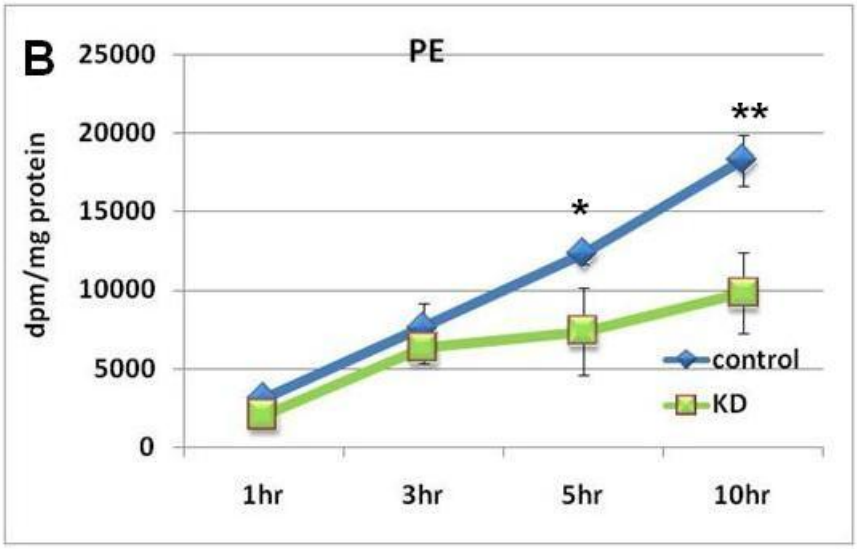
B
PE
25000
20000
15000
10000
5000
0
dpm/mg protein
**
*
control
KD
1hr
3hr
5hr
10hr

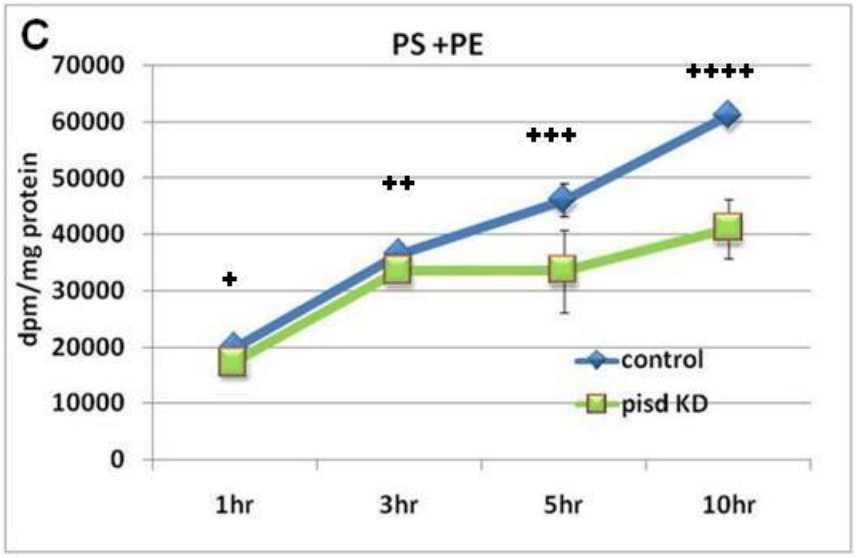
C
PS +PE
70000
60000
50000
40000
30000
20000
10000
0
dpm/mg protein
++++
+++
++
+
control
pisd KD
1hr
3hr
5hr
10hr

Fig. 7.31
PSD mRNA levels were reduced in CHO-K1 cells by dsiRNA transfection. The PSD KD cells were incubated with [^{3}H] serine for 1, 3, 5, and 10 h. The radioactivity of [^{3}H] PS and [^{3}H] PE at the indicated times were quantified in dpms per milligram of cellular protein for negative control and PSD knockdown cells (Panel A and Panel B respectively). The sum of [^{3}H] PS and [^{3}H] PE radioactivity per milligram protein, which represents total [^{3}H] serine incorporation into PS with respect to time, was calculated for negative control and PSD knockdown cells (Panel C). The incorporation of [^{3}H] serine into negative control cells and PSD knockdown cells was quantified using three independent experiments with biological triplicates each time. A representative experiment is shown above. The statistical significance of the above data was calculated to be *1.6 x10^{-2}, **3.6 x10^{-3}, $^{+}$3.5 x10^{-2}, $^{++}$0.35, $^{+++}$0.24, $^{++++}$6.9 x10^{-3} using the student's t-test.

7.12 PSD KD Cells Have Normal Doubling Times

Previously, PSB-2 cells which have decreased mitochondrial PS and PE were found to have reduced growth (Fig. 7.5). In contrast, R-41 cells which only have decreased mitochondrial PE retained normal growth (Fig. 7.20). Thus, the question of whether PSD KD cells have abnormal growth arises. The growth rate of PSD KD cells was compared to that in negative control cells through measuring changes in cell numbers on $1mm^2$ areas. It was found that PSD KD cells do not have statistically significant increased doubling time, which suggests that their phenotype is closer to that of R-41 cells than PSB-2 cells. Indeed, since both PSD KD cells and R-41 cells have reduced content of only PE, but not PS, it is likely that they have similar metabolic rates.

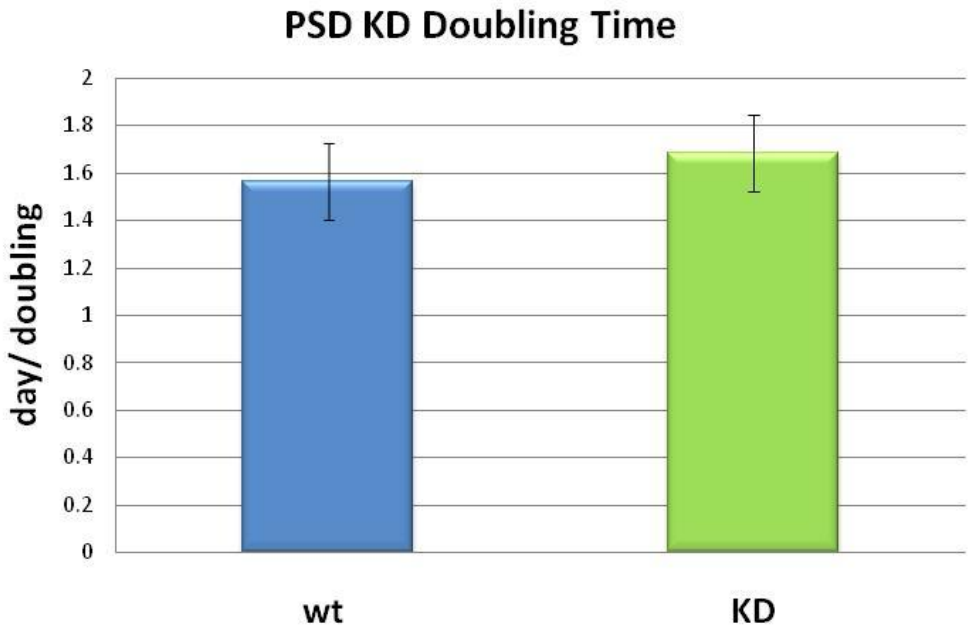

Fig. 7.32
A figure showing the doubling times of wildtype (wt) and PSD KD cells. Data are the averages of three independent experiments. In each experiment, the change in number of negative control and PSD KD cells in three 1mm x 1mm grids was

counted between 24 and 48 h after plating. The statistical significance was calculated to have a p-value >0.05 using the student's t-test.

7.13 PSD KD Mitochondrial Density

The sedimentation densities of negative control and PSD KD mitochondria were compared using Percoll gradient centrifugation. PSD KD mitochondria showed a higher sedimentation density in comparison to negative control mitochondria (Fig. 7.33). This abnormally high mitochondrial density is reminiscent of the increased densities found in PSB-2 and R-41 mitochondria. Thus, all three types of mitochondria are abnormally dense due to decreases in the phospholipid to protein ratio. Although the PS levels of negative control mitochondria were ~50% higher than PSD KD mitochondria, this finding does not negate the latter phospholipid to protein ratio theory as PS is a quantitatively minor mitochondrial phospholipid which represents only ~4% of total mitochondrial phospholipids.

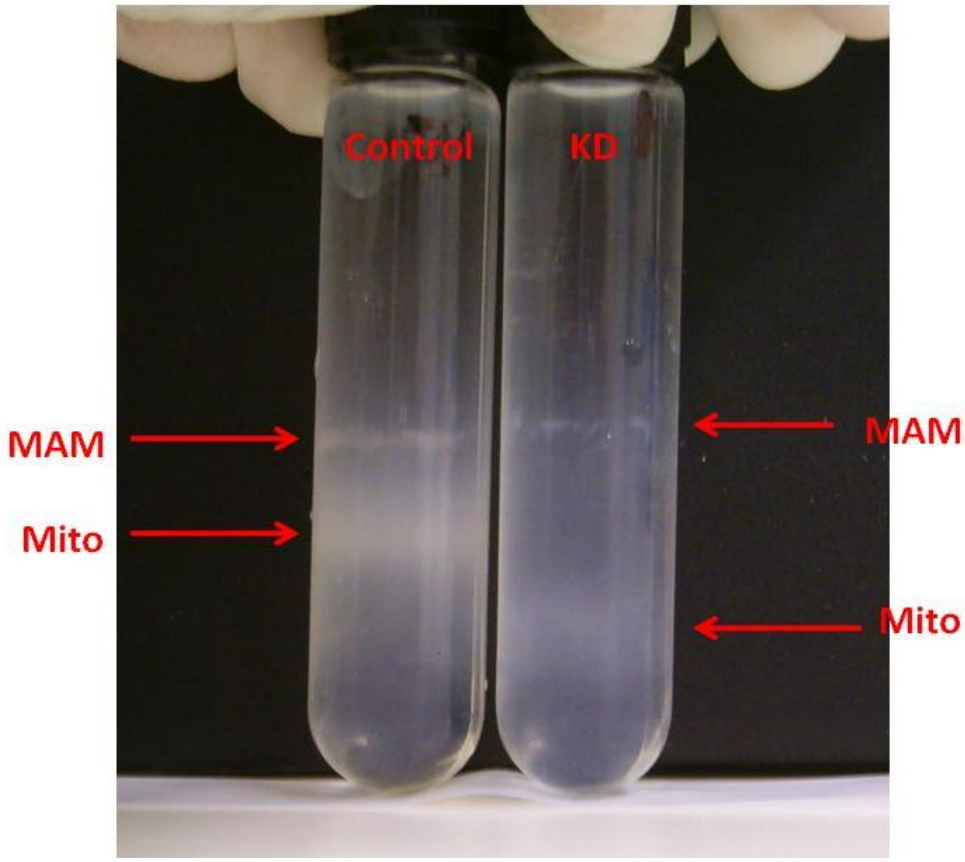

Fig. 7.33
Mitochondria and MAM from negative control cells and PSD knockdown cells after centrifugation on a 20% Percoll gradient. Pure mitochondria were isolated from negative control cells and PSD knockdown cells in three independent experiments.

7.13 Analysis of PSD KD Mitochondrial Physiology

As the terminal component to the mitochondrial ETC, COX is an indicator of cellular respiration activity. Given that normal COX function requires phospholipids, the activity of COX was measured in PSD KD mitochondria. In a result similar to that of R-41 mitochondria, PSD KD mitochondria had no statistically significant differences in COX activity compared to control cell (Fig. 7.34). This result suggests that COX activity is not affected by ~35% decreases in mitochondrial PE. However, results from PSB-2 mitochondria indicate that COX activity is modestly reduced when PS and PE are both reduced by ~35%. This result again, makes good biophysical sense because both PS and PE are inner leaflet phospholipids, and the simultaneous decrease of two inner leaflet phospholipids may be detrimental to membrane protein function.

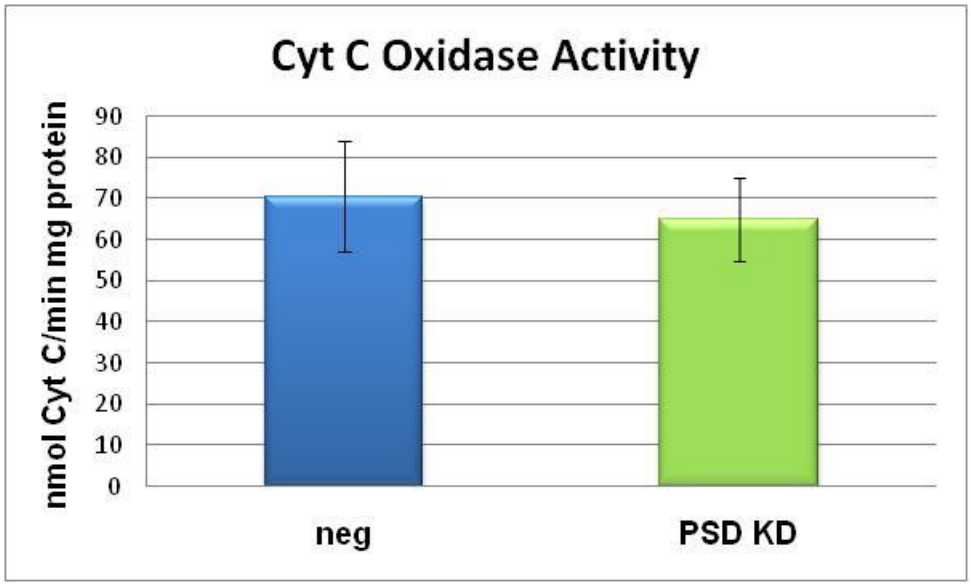

Fig. 7.34

Cytochrome c oxidase activity from the isolated mitochondria of negative control (neg) and PSD KD cells (PSD KD). Cytochrome c oxidase activity was assayed using three independent preparations of mitochondria in reaction triplicates from negative control cells and PSD knockdown cells. The statistical significance was calculated to have a p-value >0.05 using the student's t-test.

ATP Levels in PSD KD Cells

Since PSB-2 cells have increased ATP levels and R-41 cells have decreased ATP levels, the ATP levels of PSD KD cells came into question. PSB-2 mitochondria have decreased levels of PS and PE due to defective PS synthesis and R-41 mitochondria have decreased PE levels from defective PS transport (Fig. 1.2). Thus, logically, the ATP production of PSD KD cells should resemble R-41 cells in that their mitochondria both suffer from deficiencies in PE. Indeed, this was the case PSD KD cell lysates contained 33.80% less ATP than negative control cells (Fig. 7.35). The cause of the decrease in ATP in PSD KD cells is likely to be similar to that in R-41 cells. Since PSD KD cells and R-41 cells both had normal growth rates (Fig. 7.20 and Fig. 7.32), normal COX activities (Fig. 7.22 and Fig. 7.34), and their phospholipid deficiencies are similar (Fig. 7.15 and Fig. 7.28), it is likely that they both suffer from impaired ATP production. This proposed phenomenon is supported by the data showing that both types of cells have hyperpolarized mitochondria (Fig. 7.24 and Fig. 7.36). This hyperpolarization suggests that the mitochondrial ETCs changes of both cells are fully capable of producing sufficient $\Delta\Psi$ for ATP synthesis. Therefore, the most plausible explanation for this observation is that ATP synthesis is reduced in both R-41 and PSD KD cells. It is likely that the ATP synthase enzyme is inefficient due to the ~35% reduction in PE levels. This idea is supported by previous reports that ATP synthase *in vitro* requires specific phospholipids such as PC, phosphatidylglycerol, and cardiolipin for activity [169]. Thus, an important future experiment to confirm this spectulation would be to measure ATP synthase

activity *in vitro* with various concentrations of PE to determine the PE requirement of ATP synthase.

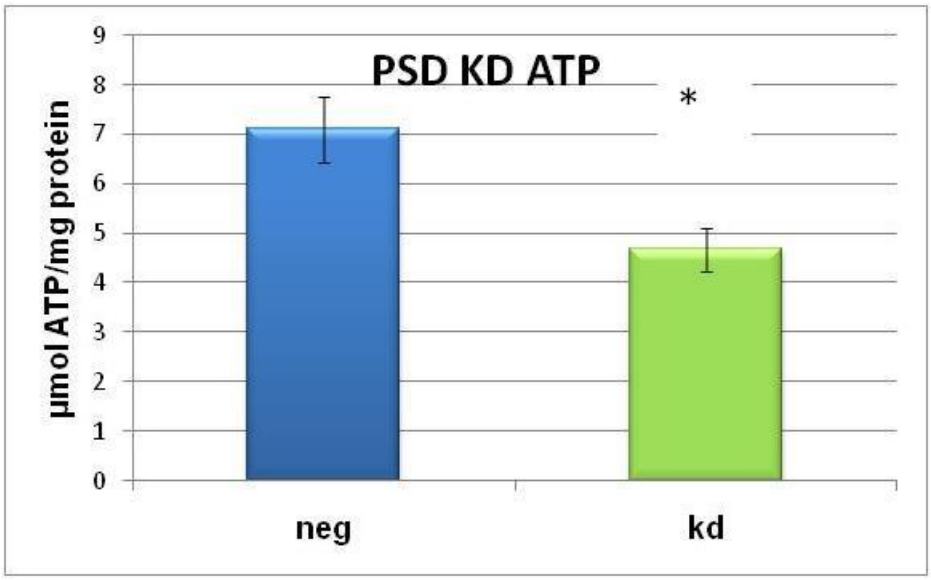

Fig. 7.35
ATP levels of cell lysates from negative control cells (neg) and PSD knockdown cells (kd). ATP was isolated through trichloroacetic acid TCA extraction and quantified through luciferase lumination analysis.
ATP was isolated and quantified from negative control cells and PSD knockdown cells in three independent experiments. In each experiment, ATP was quantified in triplicate luciferase reactions. P-value = 3.5×10^{-3}.

PSD KD Mitochondria Are Hyperpolarized

Having previously measured the $\Delta\Psi$ of PSB-2 and R-41 mitochondria, the $\Delta\Psi$ of PSD KD mitochondria was quantified and compared via TMRM fluorescence. Through using confocal microscopy imaging, it was found that PSD KD mitochondria had 25.5% more TMRM fluorescence than negative control cells (Fig. 7.36A). When TMRM fluorescence was normalized to MIM surface area using Mitotracker Green, PSD KD mitochondria had 51.2% more relative TMRM fluorescence than negative control cells (Fig. 7.36B). This 51.2% increase in normalized TMRM fluorescence observed in PSD KD mitochondria is less than the 68.5% difference observed in PSB-2 mitochondria but more than the 45.00% difference observed in R-41 mitochondria. At present, there is not enough evidence to establish a mechanism for this difference in mitochondrial hyperpolarization. Based on the current observations, one can however, propose that the different defects in the PSD pathway in the three types of cells can have different effects on $\Delta\Psi$.

The observation that R-41 cells and PSD KD cells both show reduced ATP levels and increased $\Delta\Psi$ supports the notion decreases in mitochondrial PE levels can decrease mitochondrial ATP production. As previously stated, it is possible that a decrease in ATP synthase activity due to decreased PE up-regulates mitochondrial ETC enzymes to compensate for decreased levels of ATP. In PSB-2 cells, this phenotype is likely masked by reductions in growth rates due to limitations of both mitochondrial PS and PE, which subsequently leads to a buildup of ATP pools in anticipation for cell division.

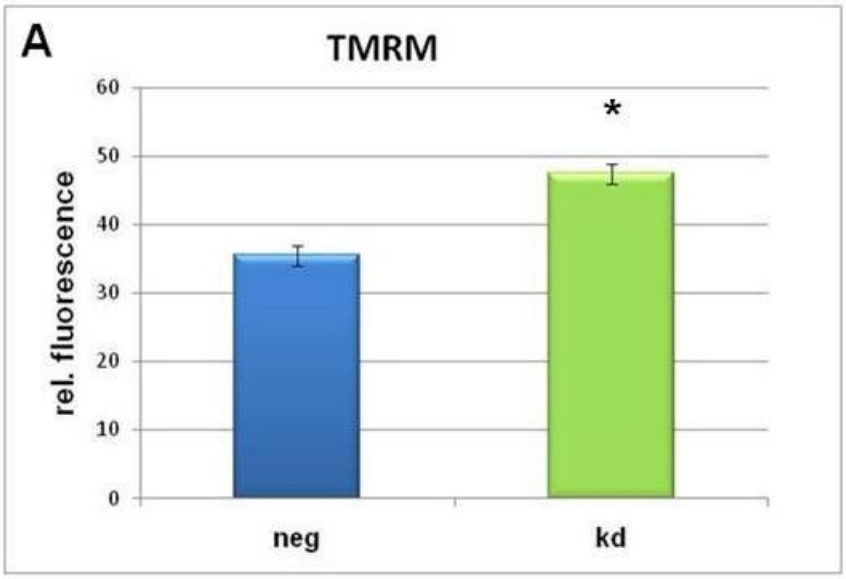
A
TMRM
rel. fluorescence
60
50
40
30
20
10
0
*
neg
kd

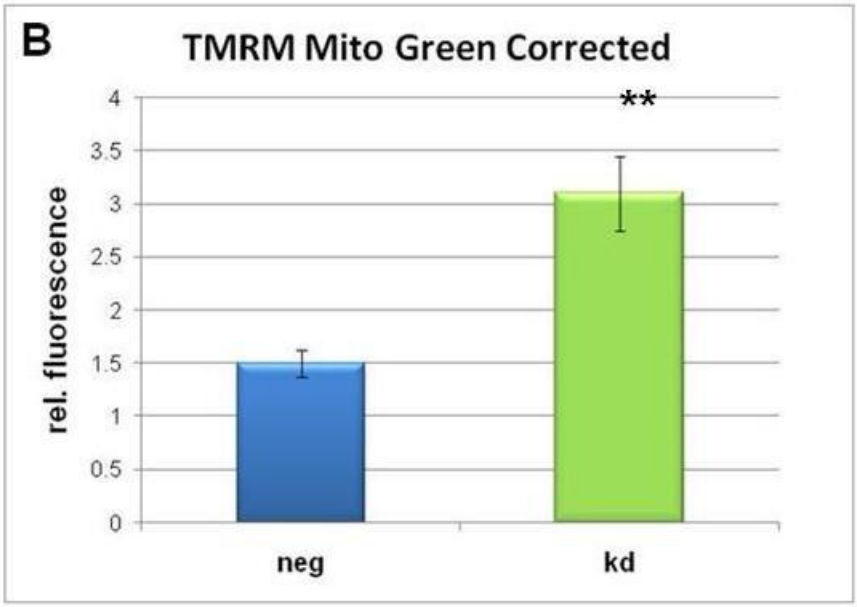
B
TMRM Mito Green Corrected
rel. fluorescence
4
3.5
3
2.5
2
1.5
1
0.5
0
**
neg
kd

Fig. 7.36
The $\Delta\Psi$ of negative control cells (neg) and PSD KD cells (kd) was measured using TMRM fluorescence (Panel A). $\Delta\Psi$ was also quantified with respect to mitochondrial MIM surface area using the ratio of TMRM fluorescence to Mitotracker Green fluorescence (Panel B). Negative control and PSD knockdown $\Delta\Psi$ were quantified from three independent experiments using triplicate dishes each time. In each dish, three images were taken, and fluorescence of 20 cells was measured per image. P-values of *=2.1×10^{-5} and **4.5×10^{-4} using the student's t-test.

7.15 PSDKD Mitochondrial Morphology and Motility

PSD KD Mitochondrial Morphology

PS and PE deficient mitochondria from PSB-2 cells have a punctate morphology (Fig. 7.13) and the PE deficient R-41 mitochondria are abnormally tubular (Fig. 7.25). The morphology of PE deficient PSD KD mitochondria was subsequently examined. After PSD KD mitochondria were stained with Mitotracker Red CMX-ROS and imaged via confocal microscopy, it was found that they were not visually abnormal compared to negative control mitochondria. However, PSD KD cells as a whole were larger than negative control cells (Fig. 7.38). Indeed, PSD KD cells appeared to have larger cellular footprints, more cytoplasm, and more mitochondria (Fig. 7.38). Thus, this observation of normal mitochondria in abnormal cells was surprising given that PSB-2 and R-41 mitochondria had abnormal morphologies. In addition, *Pisd*$^{-/-}$ mouse embryonic fibroblasts were also found to have abnormal shaped mitochondria. These observations together, suggest that changes in mitochondrial morphology in PSD KD cells may take longer than 48 hours after initial dsiRNA transfection to take effect. Given that the PE content, the $\Delta\Psi$, and the sedimentation densities of PSD KD mitochondria were changed 48 hours after transfection, it may be possible that changes in mitochondrial morphology will take longer. The rationale for this possibility is that the proteins which are involved in mitochondrial morphology may be surrounded in pools of PE which have not yet been depleted at 48 hours post transfection.

The observation that PSD KD cells were larger than negative control cells was also surprising given that PSD KD cells did not have reduced growth rates. A closer examination of *Pisd*$^{-/-}$ mouse embryonic fibroblasts, however, shows that they are similar to PSD KD cells in that they also have larger cellular footprints compared to *Pisd*$^{+/+}$ cells (Fig. 1.5). To quantify PSD KD cell size, confocal microscopy images of PSD KD cells were assessed using Area of Interest calculations to determine individual cell sizes. It was found that PSD KD cells were 21.5% larger than negative control cells (Fig. 7.39). This finding suggests that cytoplasmic turn over within PSD KD cells may be reduced leading to increased cell volume. As previously discussed in Chapter 4, PE synthesized via the PSD pathway is known to be utilized for autophagy. Indeed, reports from *Neubauer et al.* (2007) and *Hailey et al.* (2010) have both documented the importance of mitochondrial PE from the PSD pathway to the formation of autophagosomes for organelle degradation. It is likely that reduced autophagy leading decreased degradation of intracellular organelles and membranes within PSD KD cells are causing them have larger volumes. The question of why PSB-2 and R-41 cells do not have increased cytoplasmic volumes might be explained by their chronic PE deficiency. Although is likely that these latter two cell types do have reduced autophagy, it is also likely that this reduction is offset by the reduced synthesis of new membranes from a lack of PE. Therefore, unlike PSB-2 cells and R-41 cells, the transient reduction of PE in PSD KD cells may allow them to temporarily have enough PE for organelle division but not enough for subsequent autophagy.

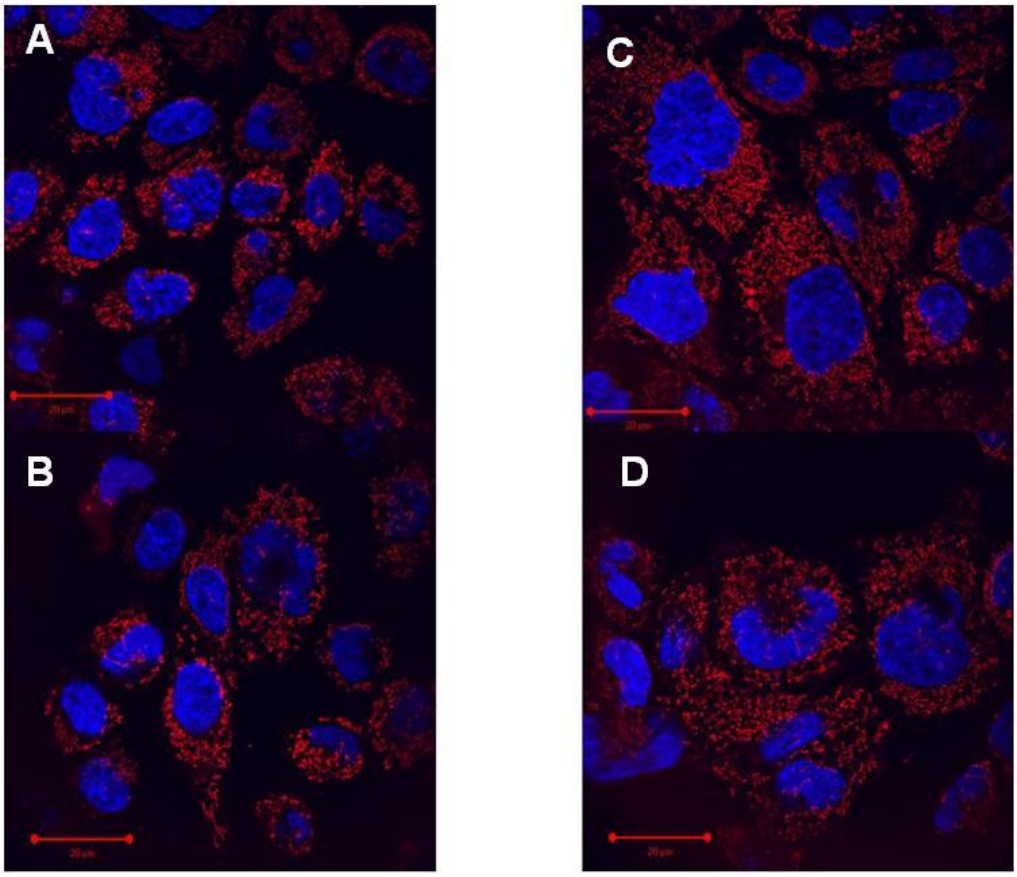

Fig. 7.38
Negative control cells (Panel A and B) and PSD knockdown cells two days after transfection (Panel B and C) were stained with 150nM Mitotracker Red CMX-ROS and 50nM Hoechst (blue) stains and imaged at 5000X. Red size bars represent 20µm. Three independent experiments were performed using two 2 dishes each. In each dish, three representative cells were chosen for imaging.

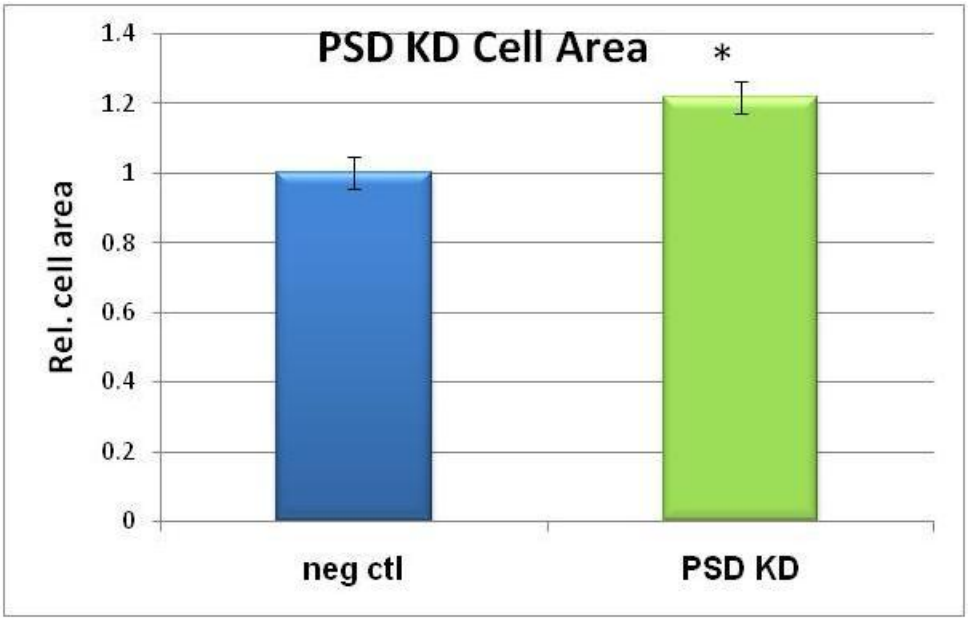

Fig. 7.39
A figure showing relative cellular foot print sizes of negative control (neg ctl) and PSD KD cells 48 h after transfection. Three dishes of cells from three independent experiments were used for analysis. Area calculations were performed on 20 cells per dish. The p-value was 6.48×10^{-4} using the student's t-test.

PSD KD Mitochondrial Have Normal Motility

Since PSB-2 and R-41 mitochondria both had reduced motility, it was hypothesized that PSD KD mitochondria would also have reduced motility. The velocity of PSD KD mitochondrial movement was visually compared to that of negative control mitochondria at 48 hours post-transfection. When cells stained with Mitotracker CMX-ROS were imaged using time lapse microscopy, it was found that PSD KD mitochondria had a similar motility compared to negative control mitochondria (Fig. 7.40). This result could be explained by the possibility that changes in mitochondrial motility and morphology may require longer reductions in *Pisd* mRNA. Indeed, PSB-2 and R-41 cells have nuclear mutations which result in prolonged phospholipid deficiencies whereas the PE level of PSD KD cells is only transiently reduced. Thus, the mitochondrial morphology and motility of PSD KD cells may need to be examined at time points longer than 48 hours post-transfection. Some solutions to maintaining prolonged PE reductions might include generating stably knocked down PSD cells and possibly even titrating back PSD expression to cells lacking PSD.

Although mitochondrial movement and morphology were unchanged in PSD KD cells compared to negative control cells, PSD KD cells were larger and contained more mitochondria (Fig. 7.38). The motility of mitochondria did not appear to be affected by the larger cytoplasmic volume of PSD KD cells. Since it is likely that PSD KD cells have increased cytoplasmic volumes due to decreased autophagy, it may be worthwhile to examine PSD mitochondrial motility in cells

which have chronic PSD deficiencies, as over time, a decrease in mitochondrial recycling may mean an overall reduction in mitochondrial motility.

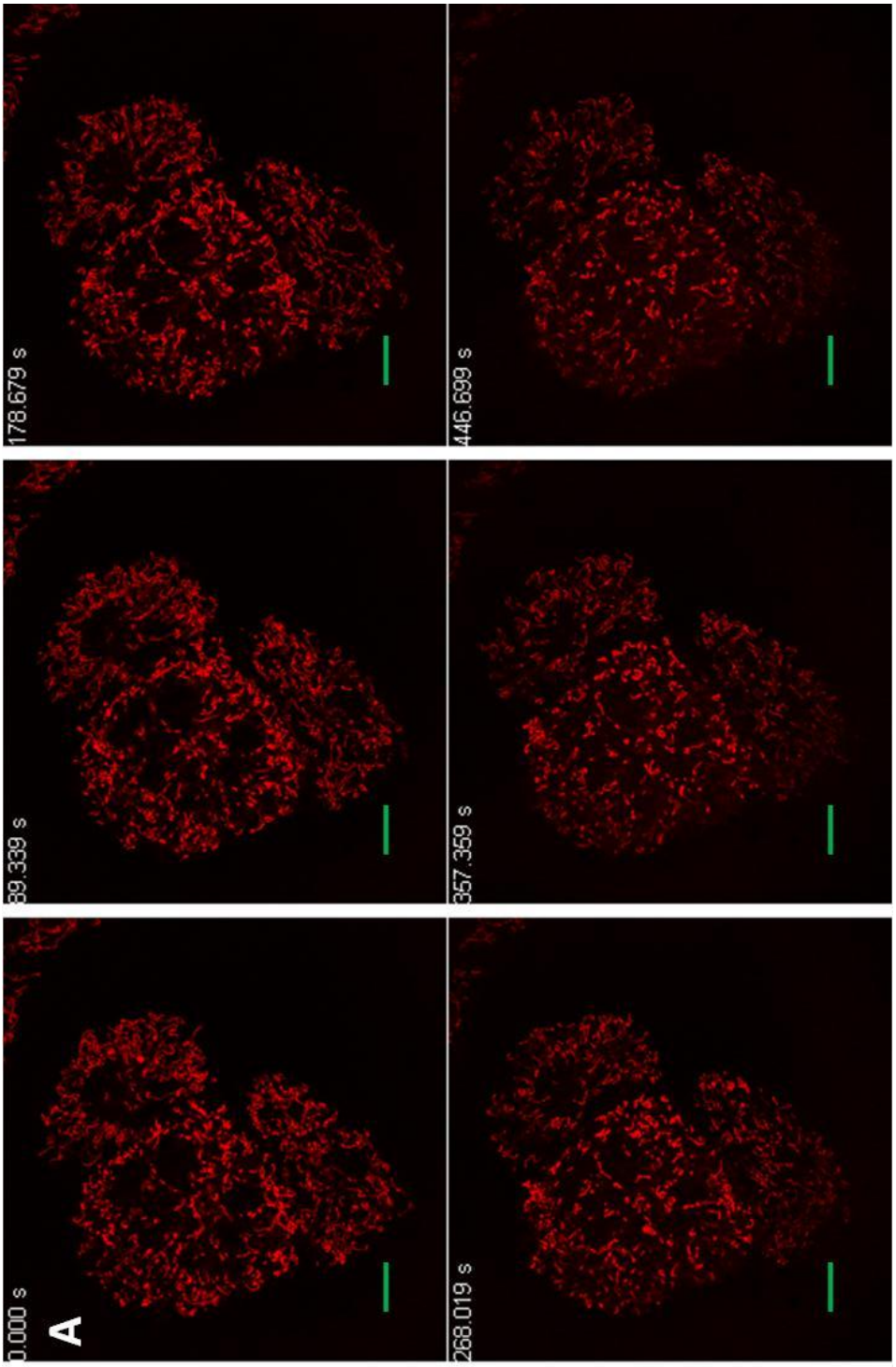

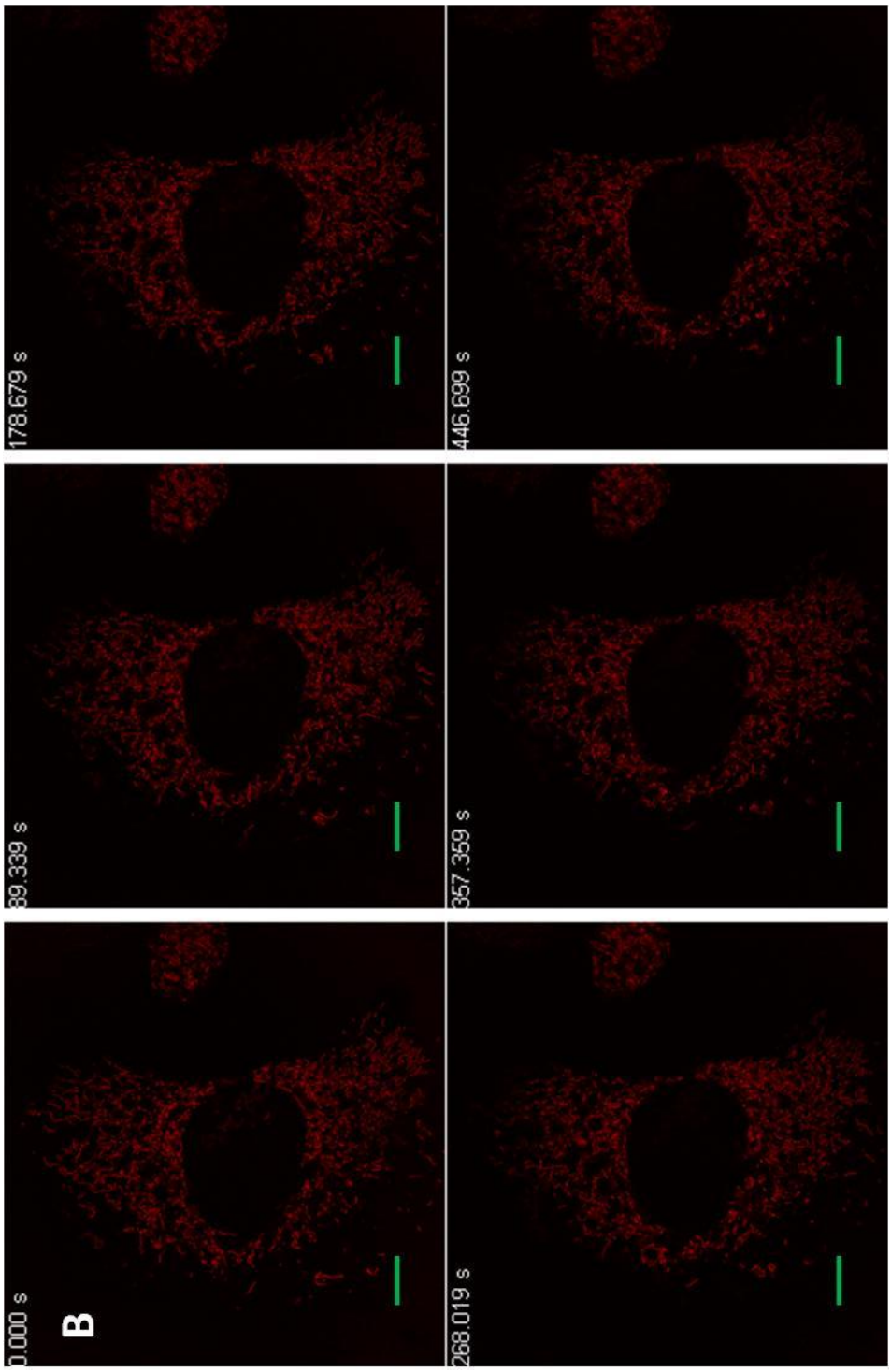

Fig. 7.40
Mitochondria from negative control cells (Panel A) and PSD knockdown cells (Panel B) were stained with Mitotracker Red CMX-ROS and imaged using timelapse video capture for approximately 7.5 minutes at 2500X magnfication. Six images representing 90 second increments are shown above for each of the

cells respectively. Green size bars represent 10μm. Three independent experiments were performed using duplicate dishes of cells and three representative cells were imaged per dish.

CHAPTER 8:

CONCLUSION

Conclusion

In mammalian cells, mitochondria not only generate the majority of cellular energy, but also regulate cellular signaling, cell growth, and apoptosis. Thus, it is important for cells to provide mitochondria with sufficient amounts of nutrients and metabolites to maintain their symbiotic survival. The PSD pathway for PE synthesis is a metabolic pathway which exemplifies the interdependence of cells and their mitochondria (Fig. 1.2). In the PSD pathway, PS is synthesized on a special domain of the ER called MAM and is transported to mitochondria for decarboxylation into mitochondrial PE, an important phospholipid for the survival of cells and their mitochondria. This investigation examined the PSD pathway in detail in three types of cells with different PSD pathway defects (Fig. 1.2). The PSB-2 cells have a defect in the synthesis of PS, a substrate for the PE synthesis, the R-41 cells have a defect in the transport of PS to the mitochondrion for decarboxylation by PSD, and the PSD KD cells have decreased expression of PSD via mRNA KD. As a result, each of these cells contained a different set of mitochondrial defects. In the following, a summary of the defects in PSB-2 cells, R-41 cells, and PSD KD cells will be provided along with implications of these abnormalities.

8.1 PSB-2 Cells

PS, which comprises ~10% of cellular membranes and 4% of mitochondrial membranes is utilized for the synthesis of PE via the PSD pathway. The synthesis of PS in PSB-2 cells was reduced by ~95% through chemically mutagenizing genes which encode its PSS I and PSS II enzymes. In this

investigation, PSB-2 cells which had a ~35% decrease in mitochondrial PS and PE levels exhibited a number of abnormalities.

Firstly, PSB-2 cells had 39.5% longer doubling times compared to wildtype cells. This decrease in growth rate indicates that mitochondrial PS and PE together are important for mammalian cell growth. The mitochondria of PSB-2 cells were also found to have abnormally high sedimentation densities compared to wildtype mitochondria. This result supports earlier findings by *Schumacher et al.* who have proposed that mitochondrial sedimentation densities can increase due to decreases phospholipid to protein ratios, as proteins are generally denser than phospholipids. Therefore, this finding suggests that phospholipid deficiencies in mitochondria can lead to decreases in matrix volume and possibly changes in mitochondrial function.

Decreased mitochondrial PS and PE levels were also found to have affected COX activity. COX is the final component of the mitochondrial ETC and an indicator of cellular respiration. The COX activity of PSB-2 cells was found to be reduced by 21.9% compared to wildtype cells. Ethanolamine supplementation, which normalized PSB-2 PS and PE levels, was found to rescue PSB-2 cells of their decreased COX activity. Together, these results provide strong evidence that PS and PE are involved in mitochondrial ETC function.

Interestingly, PSB-2 cells contained a 39.3% higher level of ATP than wildtype cells. Although the exact mechanism for this increase is currently unclear, observations from mitochondrial isolations suggest a decrease in PSB-2 MAM might be a likely cause. It is possible that a decrease in MAM mass may

lead to ER and mitochondrion disconnection. The ER is an organelle which utilizes energy for many processes such as protein synthesis and lipid synthesis. Thus, it is possible that a disconnection between MAM and mitochondria in PSB-2 cells led to a buildup of mitochondrial ATP. Indeed, given the present evidence, this is a likely scenario as PSB-2 cells were found to have inhibited growth rates.

When the membrane potential of PSB-2 mitochondria was measured, it was found that they showed 52.3% more TMRM fluorescence than wildtype mitochondria. This increase was found to be 16.2% higher when TMRM fluorescence was normalized with respect to MIM surface area using Mitotracker Green, suggesting that PSB-2 mitochondria may be hyperpolarized due to a decrease in the ratio of MIM to ETC enzymes. Ethanolamine supplementation, which rescued PSB-2 mitochondria of their PS and PE deficiencies, was found to normalize mitochondrial hyperpolarization. This is an important result because it provides evidence to show that phospholipid deficiency induced mitochondrial hyperpolarization can be rescued through phospholipid-precursor supplementation. Mitochondrial membrane hyperpolarization is also a hallmark of malignant cancers. At present, there is no link between phospholipid decreases and cancer phenotypes. However, further characterization PSB-2 cells may provide a valuable model for the understanding of cancer growth and development.

The morphology and motility of PS and PE deficient PSB-2 mitochondria were examined through confocal microscopy. PSB-2 mitochondria were observed to be strikingly different from wildtype mitochondria in that they were highly

punctate. Since PE is known to be involved in the fusion of membranes, it is possible that PSB-2 mitochondria are punctate due to a decrease in fusion. To test this hypothesis, future experiments to examine the fusion activity of PSB-2 mitochondria will be useful. PSB-2 mitochondria were also observed to have decreased motility in comparison to wildtype mitochondria. This decrease in motility is likely due to an increase in ATP pools. Previously, *Bereiter-Hahn et al.* had reported that intracellular ATP microinjections can inhibit mitochondrial motility. It is therefore likely that an increase in surrounding ATP is causing PSB-2 mitochondria to be senescent, as they no longer need to travel to sites of high ATP demand.

The study of PS and PE deficiencies in PSB-2 mitochondria has yielded a wealth of knowledge about the relationship between phospholipids and mitochondrial function. This investigation has now brought forth new information about the importance of PS and PE to cellular metabolism, energy production, and organelle function. Nevertheless, a thorough study of PSB-2 cells can only elucidate one part of the PSD pathway, and therefore in the next two sections the consequences of other PSD pathway disruptions will be reviewed.

8.2 R-41 Cells

The transport of PS from the MAM to the mitochondrion is the rate limiting step of PE synthesis via the PSD pathway. This transport step was disrupted in CHO cells through chemical mutagenesis to provide a model for understanding non-vesicular intracellular PS transport. These PS transport

deficient cells, named R-41 cells were used in this investigation to understand the importance PSD synthesized PE for mitochondrial function.

R-41 mitochondria which were measured to have ~35% decreases in PE levels were found to have number of defects. Like PSB-2 mitochondria which have decreased PS and PE levels, R-41 mitochondria were also found to have an abnormally high sedimentation density. This increase in density is also believed to be caused by a decrease in phospholipid to protein ratios, as proteins are generally denser than phospholipids.

However, unlike PSB-2 mitochondria, R-41 mitochondria have normal COX activity and decreased ATP levels. Since R-41 mitochondria have decreased PE, but not decreased PS, these contrasting observations suggest that a combination of PS and PE deficiencies in PSB-2 mitochondria may be masking some of the effects of PE decreases. For example, it is likely the decreased PE levels are causing reduced ATP production in both PSB-2 and R-41 mitochondria, but a combination of PS and PE decreases are causing PSB-2 mitochondria to ineffectively efflux ATP through the MAM, which subsequently results in a buildup of ATP. This hypothesis is plausible because PSB-2 cells have decreased cell growth and R-41 cells have normal growth suggesting that R-41 cells are effectively obtaining and using ATP energy. In other words, a deficiency in PE may inhibit ATP synthase activity and a deficiency of both PS and PE may inhibit both ATP synthase and COX activity. Thus, for this theory to be tested, ATP synthase activity must be measured in both PSB-2 and R-41 mitochondria and compared to wildtype mitochondria.

The PE deficiency induced ATP synthase inhibition hypothesis is supported by the observation that PSB-2 and R-41 mitochondria both have hyperpolarized $\Delta\Psi$. Like PSB-2 mitochondria, R-41 mitochondria were observed to show a 45.00% increase in TMRM/Mitotracker Green fluorescence compared to wildtype mitochondria. Hence, it is possible that the mitochondrial ETC is creating a higher $\Delta\Psi$ in both cell types to compensate for inhibited ATP synthesis.

Morphologically speaking, R-41 mitochondria were also found to be different from PSB-2 mitochondria. In contrast to the punctate morphology of PSB-2 mitochondria, R-41 mitochondria were more tubular than wildtype mitochondria. Given that R-41 cells have a defect in MAM to mitochondrion interaction, it is likely that R-41 mitochondria are increasing their contact surface area with MAM through increasing tubulation. This phenotype can be clearly seen through confocal microscopy as R-41 mitochondria were observed to cluster around cell centers where the ER resides in contrast to wildtype mitochondria which were observed to be distributed throughout the cytoplasm (Fig. 25). This observation is further supported through the time lapse imagining of R-41 mitochondria. When R-41 mitochondria were monitored with respect to time, they were observed to be immotile and rarely ventured to the periphery of the cell cytoplasm.

The comparison of PSB-2 and R-41 mitochondria has yielded information about mitochondrial PS and PE requirements which neither of them alone could provide. At present, the observation data collected still requires mechanistic data supplementation. Thus, future experiments to study the enzymes responsible for

PSB-2 and R-41 mitochondrial abnormalities will need to be performed. In addition, the examination of other cell models which show similar phospholipid deficiencies may also be helpful for understanding the important of PS and PE.

8.3 PSD KD Cells

In mammalian cells, the synthesis of mitochondrial PE is catalyzed by the enzyme PSD. Previously, others from our laboratory have documented the importance of PSD to cell survival and mammalian life [19]. Here, the effects of PSD deficiencies were investigated through dsiRNA KD of PSD. After exhaustively trying various lipid transfection reagents and different dsiRNA and siRNA duplexes, it was found that the maximum achievable PSD KD was ~95% (Fig. 7.27). Therefore, it is likely that cells may require a minimum of 5% residual PSD mRNA to survive. Cells which have had PSD mRNA reduced by ~95% were found to have ~35% reductions in mitochondrial PE. Since neither PSB-2, R-41, nor PSD KD mitochondria were found to have more than ~35% reductions in PE levels, it is likely that mammalian mitochondria require a minimum of ~65% residual PE to maintain cell survival.

The characterization of PSD KD mitochondria revealed that they shared many similar abnormalities with R-41 mitochondria. This was not surprising given that they both shared a similar ~35% reduction in mitochondrial PE. Like R-41 mitochondria, PSD KD mitochondria were found to have unusually high sedimentation densities, normal COX activity, and hyperpolarized $\Delta\Psi$. Since mitochondria from both types of cells suffer from a similar reduction in PE, the mechanisms for the latter phenotypes are likely similar. For example, PSD KD

mitochondria likely have a higher sedimentation density due to a reduction in PE to protein ratio and they likely also have hyperpolarized $\Delta\Psi$ due to their need to compensate for decreased ATP production. These similar mitochondrial phenotypes suggest that the effects of PSD substrate reduction and PSD activity reduction are likely very similar. Indeed, the cellular physiology of R-41 and PSD KD cells were also similar in the they both had normal growth rates compared to control cells and they both had reduced levels of cellular ATP.

There are, however, differences between R-41 and PSD KD cells due to the methods by which they were generated. Where R-41 mitochondria have a chronic reduction in PE levels due to a genetic mutation, PSD KD mitochondria only suffer from acute PE reductions due to the transient nature of their KD transfection. This difference is most likely the cause of differences in morphology and motility between R-41 and PSD KD mitochondria. Where R-41 mitochondria are tubular and show reduced motility, PSD KD mitochondria appear to be outwardly normal. This finding suggests that there may be residual pools of PE within mitochondrial protein and membrane domains which were still un-depleted in PSD KD mitochondria. Indeed, mitochondrial enzymes such as COX have PE embedded within their tertiary structure and therefore the effects of PE reduction may depend on protein turnover.

On a macroscopic level, PSD KD cells were found to have a 21.53% larger cellular footprint than negative control cells. Since PE synthesized via the PSD pathway is required for organelle degradation through autophagy, it is possible that PSD KD cells had enough PE for synthesizing new organelles and

membranes but not enough PE for their subsequent degradation through autophagy. Thus, to have a complete understanding of the PSD pathway, one must also explore the temporal consequences of PSD disruption in addition to absolute enzyme activity.

8.4 Conclusion

The study of different disruptions to the PSD pathway has yielded a myriad of different previously uncharacterized phenotypes. The examination of mitochondria from PSB-2, R-41, and PSD KD cells has provided new insights into the possible roles of PS and PE for cellular growth, energy production, and autophagy as well as mitochondrial density, ETC function, membrane potential, morphology, and motility. It is the author's hope that through understanding the underlying causes of these phenotypes, new information regarding mitochondrial diseases will be elucidated, namely diseases such as myopathy, neurodegeneration, and cancer.

Conclusions

PSB-2 Cells	R-41 Cells	PSD KD Cells
↓ Mito PS and PE	↓ Mito PE	↓ Mito PE
↓ [^{3}H] Serine into PS and PE	↓ [^{3}H] Serine into PE	↓ [^{3}H] Serine into PE
↓ Growth	Norm. Growth	Norm. Growth
↑ Mito. Density	↑ Mito. Density	↑ Mito. Density
↓ Complex IV Activity	Norm. Complex IV Activity	Norm. Complex IV Activity
↑ ATP Levels	↓ ATP Levels	↓ ATP Levels
↑ Mito. Membrane Pot.	↑ Mito. Membrane Pot.	↑ Mito. Membrane Pot.
Puncate Mito Morph	Tubular Mito Morph	Norm. Mito Morph
↓ Mito Motility	↓ Mito Motility	Norm. Mito Motility
		↑ Cell Footprint

Fig. 8.1
A summary observed defects in PSB-2 cells, R-41 cells and PSD KD cells.

CHAPTER 9:

BIBLIOGRAPHY

1. Henze, K. and W. Martin, *Evolutionary biology: essence of mitochondria.* Nature, 2003. **426**(6963): p. 127-8.
2. Sarzi, E. and A. Rotig, *Mitochondrial genome instability and associated diseases.* Med Sci (Paris), 2010. **26**(2): p. 171-6.
3. Elliott, H.R., et al., *Pathogenic mitochondrial DNA mutations are common in the general population.* Am J Hum Genet, 2008. **83**(2): p. 254-60.
4. Voet, D., J.G. Voet, and C.W. Pratt, *Fundamentals of biochemistry : life at the molecular level*. 2006, Wiley: Hoboken, N.J. p. 547.
5. Green, D.R., *Apoptotic pathways: the roads to ruin.* Cell, 1998. **94**(6): p. 695-8.
6. McBride, H.M., M. Neuspiel, and S. Wasiak, *Mitochondria: more than just a powerhouse.* Curr Biol, 2006. **16**(14): p. R551-60.
7. Hajnoczky, G., et al., *Mitochondrial calcium signalling and cell death: approaches for assessing the role of mitochondrial Ca2+ uptake in apoptosis.* Cell Calcium, 2006. **40**(5-6): p. 553-60.
8. Schlame, M. and M. Ren, *The role of cardiolipin in the structural organization of mitochondrial membranes.* Biochim Biophys Acta, 2009. **1788**(10): p. 2080-3.
9. Macfarlane, M.G., *Phosphatidylglycerols and lipoamino acids.* Adv Lipid Res, 1964. **2**: p. 91-125.
10. Hatch, G.M., *Cell biology of cardiac mitochondrial phospholipids.* Biochem Cell Biol, 2004. **82**(1): p. 99-112.
11. Vance, D.E. and J.E. Vance, *Physiological consequences of disruption of mammalian phospholipid biosynthetic genes.* J Lipid Res, 2009. **50 Suppl**: p. S132-7.
12. Vance, D.E. and J.E. Vance, *Biochemistry of lipids, lipoproteins, and membranes*. 4th ed. New comprehensive biochemistry v. 36. 2002, Amsterdam ; Boston: Elsevier. xxiv, 607 p.
13. Kennedy, E.P. and S.B. Weiss, *The function of cytidine coenzymes in the biosynthesis of phospholipides.* J Biol Chem, 1956. **222**(1): p. 193-214.
14. Zborowski, J., A. Dygas, and L. Wojtczak, *Phosphatidylserine decarboxylase is located on the external side of the inner mitochondrial membrane.* FEBS Lett, 1983. **157**(1): p. 179-82.
15. Bleijerveld, O.B., et al., *The CDP-ethanolamine pathway and phosphatidylserine decarboxylation generate different phosphatidylethanolamine molecular species.* J Biol Chem, 2007. **282**(39): p. 28362-72.
16. Zelinski, T.A. and P.C. Choy, *Phosphatidylethanolamine biosynthesis in isolated hamster heart.* Can J Biochem, 1982. **60**(8): p. 817-23.
17. Lundberg, G.A., B. Jergil, and R. Sundler, *Subcellular localization and enzymatic properties of rat liver phosphatidylinositol-4-phosphate kinase.* Biochim Biophys Acta, 1985. **846**(3): p. 379-87.
18. Shiao, Y.J., G. Lupo, and J.E. Vance, *Evidence that phosphatidylserine is imported into mitochondria via a mitochondria-associated membrane and that the majority of mitochondrial phosphatidylethanolamine is derived from decarboxylation of phosphatidylserine.* J Biol Chem, 1995. **270**(19): p. 11190-8.
19. Steenbergen, R., et al., *Disruption of the phosphatidylserine decarboxylase gene in mice causes embryonic lethality and mitochondrial defects.* J Biol Chem, 2005. **280**(48): p. 40032-40.
20. Saito, K., M. Nishijima, and O. Kuge, *Genetic Evidence That Phosphatidylserine Synthase II Catalyzes the Conversion of Phosphatidylethanolamine to Phosphatidylserine in Chinese Hamster Ovary Cells.* Journal of Biological Chemistry, 1998. **273**(27): p. 17199-17205.
21. Emoto, K., et al., *Isolation of a Chinese hamster ovary cell mutant defective in intramitochondrial transport of phosphatidylserine.* Proc Natl Acad Sci U S A, 1999. **96**(22): p. 12400-5.
22. Dowhan, W. and M. Bogdanov, *Functional roles of lipids in membranes*, in *Biochemistry of Lipids, Lipoproteins and Membranes.*, Elsevier Science: Amsterdam, The Netherlands. p. 1–35.

23. Emoto, K. and M. Umeda, *Membrane lipid control of cytokinesis.* Cell Struct Funct, 2001. **26**(6): p. 659-65.
24. Li, Z., et al., *The ratio of phosphatidylcholine to phosphatidylethanolamine influences membrane integrity and steatohepatitis.* Cell Metab, 2006. **3**(5): p. 321-31.
25. Vance, J.E. and R. Steenbergen, *Metabolism and functions of phosphatidylserine.* Prog Lipid Res, 2005. **44**(4): p. 207-34.
26. Fadok, V.A., et al., *Exposure of phosphatidylserine on the surface of apoptotic lymphocytes triggers specific recognition and removal by macrophages.* J Immunol, 1992. **148**(7): p. 2207-16.
27. Frasch, S.C., et al., *Regulation of phospholipid scramblase activity during apoptosis and cell activation by protein kinase Cdelta.* J Biol Chem, 2000. **275**(30): p. 23065-73.
28. Bratton, D.L., et al., *Appearance of phosphatidylserine on apoptotic cells requires calcium-mediated nonspecific flip-flop and is enhanced by loss of the aminophospholipid translocase.* J Biol Chem, 1997. **272**(42): p. 26159-65.
29. Bevers, E.M., P. Comfurius, and R.F. Zwaal, *Changes in membrane phospholipid distribution during platelet activation.* Biochim Biophys Acta, 1983. **736**(1): p. 57-66.
30. Hemker, H.C., et al., *Platelet membrane involvement in blood coagulation.* Blood Cells, 1983. **9**(2): p. 303-17.
31. Lentz, B.R., *Exposure of platelet membrane phosphatidylserine regulates blood coagulation.* Prog Lipid Res, 2003. **42**(5): p. 423-38.
32. Weinreb, G.E., et al., *Cooperative roles of factor V(a) and phosphatidylserine-containing membranes as cofactors in prothrombin activation.* J Biol Chem, 2003. **278**(8): p. 5679-84.
33. Takai, Y., et al., *Unsaturated diacylglycerol as a possible messenger for the activation of calcium-activated, phospholipid-dependent protein kinase system.* Biochem Biophys Res Commun, 1979. **91**(4): p. 1218-24.
34. Takai, Y., et al., *Calcium-dependent activation of a multifunctional protein kinase by membrane phospholipids.* J Biol Chem, 1979. **254**(10): p. 3692-5.
35. Ghosh, S., et al., *The cysteine-rich region of raf-1 kinase contains zinc, translocates to liposomes, and is adjacent to a segment that binds GTP-ras.* J Biol Chem, 1994. **269**(13): p. 10000-7.
36. Nagai, Y., et al., *An alternative splicing form of phosphatidylserine-specific phospholipase A1 that exhibits lysophosphatidylserine-specific lysophospholipase activity in humans.* J Biol Chem, 1999. **274**(16): p. 11053-9.
37. Powell, K.A., et al., *Phosphorylation of dynamin I on Ser-795 by protein kinase C blocks its association with phospholipids.* J Biol Chem, 2000. **275**(16): p. 11610-7.
38. Hofmann, K., et al., *Cloning and characterization of the mammalian brain-specific, Mg2+-dependent neutral sphingomyelinase.* Proc Natl Acad Sci U S A, 2000. **97**(11): p. 5895-900.
39. Arispe, N., et al., *Hsc70 and Hsp70 interact with phosphatidylserine on the surface of PC12 cells resulting in a decrease of viability.* FASEB J, 2004. **18**(14): p. 1636-45.
40. Hope, M.J., D.C. Walker, and P.R. Cullis, *Ca2+ and pH induced fusion of small unilamellar vesicles consisting of phosphatidylethanolamine and negatively charged phospholipids: a freeze fracture study.* Biochem Biophys Res Commun, 1983. **110**(1): p. 15-22.
41. Morris, R.J., *Ionic control of the metastable inner leaflet of the plasma membrane: Fusions natural and artefactual.* FEBS Lett, 2010. **584**(9): p. 1665-9.
42. Emoto, K., et al., *Exposure of phosphatidylethanolamine on the surface of apoptotic cells.* Exp Cell Res, 1997. **232**(2): p. 430-4.
43. Kamitani, T., et al., *Complexity of ethanolamine phosphate addition in the biosynthesis of glycosylphosphatidylinositol anchors in mammalian cells.* J Biol Chem, 1992. **267**(34): p. 24611-9.
44. Menon, A.K. and V.L. Stevens, *Phosphatidylethanolamine is the donor of the ethanolamine residue linking a glycosylphosphatidylinositol anchor to protein.* J Biol Chem, 1992. **267**(22): p. 15277-80.

45. Nebauer, R., S. Rosenberger, and G. Daum, *Phosphatidylethanolamine, a limiting factor of autophagy in yeast strains bearing a defect in the carboxypeptidase Y pathway of vacuolar targeting.* J Biol Chem, 2007. **282**(23): p. 16736-43.
46. Hailey, D.W., et al., *Mitochondria supply membranes for autophagosome biogenesis during starvation.* Cell, 2010. **141**(4): p. 656-67.
47. Kuge, O. and M. Nishijima, *Phosphatidylserine synthase I and II of mammalian cells.* Biochim Biophys Acta, 1997. **1348**(1-2): p. 151-6.
48. Hubscher, G., R.R. Dils, and W.F. Pover, *Studies on the biosynthesis of phosphatidyl serine.* Biochim Biophys Acta, 1959. **36**: p. 518-28.
49. Borkenhagen, L.F., E.P. Kennedy, and L. Fielding, *Enzymatic Formation and Decarboxylation of Phosphatidylserine.* Journal of Biological Chemistry, 1961. **236**(6): p. 28-32.
50. Jelsema, C.L. and D.J. Morre, *Distribution of phospholipid biosynthetic enzymes among cell components of rat liver.* J Biol Chem, 1978. **253**(21): p. 7960-71.
51. Vance, J.E., *Phospholipid synthesis in a membrane fraction associated with mitochondria.* J Biol Chem, 1990. **265**(13): p. 7248-56.
52. van Golde, L.M., et al., *Biosynthesis of lipids in Golgi complex and other subcellular fractions from rat liver.* Biochim Biophys Acta, 1974. **360**(2): p. 179-92.
53. Saito, K., et al., *Immunochemical identification of the pssA gene product as phosphatidylserine synthase I of Chinese hamster ovary cells.* FEBS Lett, 1996. **395**(2-3): p. 262-6.
54. Kanfer, J.N., *The base exchange enzymes and phospholipase D of mammalian tissue.* Can J Biochem, 1980. **58**(12): p. 1370-80.
55. Suzuki, T.T. and J.N. Kanfer, *Purification and properties of an ethanolamine-serine base exchange enzyme of rat brain microsomes.* J Biol Chem, 1985. **260**(3): p. 1394-9.
56. Voelker, D.R. and J.L. Frazier, *Isolation and characterization of a Chinese hamster ovary cell line requiring ethanolamine or phosphatidylserine for growth and exhibiting defective phosphatidylserine synthase activity.* J Biol Chem, 1986. **261**(3): p. 1002-8.
57. Kuge, O., M. Nishijima, and Y. Akamatsu, *Isolation of a somatic-cell mutant defective in phosphatidylserine biosynthesis.* Proc Natl Acad Sci U S A, 1985. **82**(7): p. 1926-30.
58. Kuge, O., M. Nishijima, and Y. Akamatsu, *A Chinese hamster cDNA encoding a protein essential for phosphatidylserine synthase I activity.* J Biol Chem, 1991. **266**(35): p. 24184-9.
59. Kuge, O., K. Saito, and M. Nishijima, *Cloning of a Chinese hamster ovary (CHO) cDNA encoding phosphatidylserine synthase (PSS) II, overexpression of which suppresses the phosphatidylserine biosynthetic defect of a PSS I-lacking mutant of CHO-K1 cells.* J Biol Chem, 1997. **272**(31): p. 19133-9.
60. Stone, S.J., Z. Cui, and J.E. Vance, *Cloning and expression of mouse liver phosphatidylserine synthase-1 cDNA. Overexpression in rat hepatoma cells inhibits the CDP-ethanolamine pathway for phosphatidylethanolamine biosynthesis.* J Biol Chem, 1998. **273**(13): p. 7293-302.
61. Sturbois-Balcerzak, B., et al., *Structure and expression of the murine phosphatidylserine synthase-1 gene.* J Biol Chem, 2001. **276**(11): p. 8205-12.
62. Ohsawa, T., M. Nishijima, and O. Kuge, *Functional analysis of Chinese hamster phosphatidylserine synthase 1 through systematic alanine mutagenesis.* Biochem J, 2004. **381**(Pt 3): p. 853-9.
63. Schutze, M.P., P.A. Peterson, and M.R. Jackson, *An N-terminal double-arginine motif maintains type II membrane proteins in the endoplasmic reticulum.* EMBO J, 1994. **13**(7): p. 1696-705.
64. Stone, S.J. and J.E. Vance, *Cloning and expression of murine liver phosphatidylserine synthase (PSS)-2: differential regulation of phospholipid metabolism by PSS1 and PSS2.* Biochem J, 1999. **342 (Pt 1)**: p. 57-64.
65. Nishijima, M., O. Kuge, and Y. Akamatsu, *Phosphatidylserine biosynthesis in cultured Chinese hamster ovary cells. I. Inhibition of de novo phosphatidylserine biosynthesis by exogenous phosphatidylserine and its efficient incorporation.* J Biol Chem, 1986. **261**(13): p. 5784-9.

66. Hasegawa, K., et al., *Isolation and characterization of a Chinese hamster ovary cell mutant with altered regulation of phosphatidylserine biosynthesis.* J Biol Chem, 1989. **264**(33): p. 19887-92.
67. Kuge, O., et al., *Control of phosphatidylserine biosynthesis through phosphatidylserine-mediated inhibition of phosphatidylserine synthase I in Chinese hamster ovary cells.* Proc Natl Acad Sci U S A, 1998. **95**(8): p. 4199-203.
68. Kuge, O., *Phosphatidylserine metabolism and biosynthetic regulation in mammalian cells.* Seikagaku, 1999. **71**(1): p. 1-15.
69. Kuge, O., et al., *Purification and characterization of Chinese hamster phosphatidylserine synthase 2.* J Biol Chem, 2003. **278**(43): p. 42692-8.
70. Saito, K., M. Nishijima, and O. Kuge, *Genetic evidence that phosphatidylserine synthase II catalyzes the conversion of phosphatidylethanolamine to phosphatidylserine in Chinese hamster ovary cells.* J Biol Chem, 1998. **273**(27): p. 17199-205.
71. Bergo, M.O., et al., *Defining the importance of phosphatidylserine synthase 2 in mice.* J Biol Chem, 2002. **277**(49): p. 47701-8.
72. Arikketh, D., R. Nelson, and J.E. Vance, *Defining the importance of phosphatidylserine synthase-1 (PSS1): unexpected viability of PSS1-deficient mice.* J Biol Chem, 2008. **283**(19): p. 12888-97.
73. Daum, G. and J.E. Vance, *Import of lipids into mitochondria.* Prog Lipid Res, 1997. **36**(2-3): p. 103-30.
74. Simbeni, R., et al., *Import of phosphatidylserine into isolated yeast mitochondria.* Biochim Biophys Acta, 1993. **1145**(1): p. 1-7.
75. Ardail, D., et al., *Involvement of mitochondrial contact sites in the subcellular compartmentalization of phospholipid biosynthetic enzymes.* J Biol Chem, 1993. **268**(34): p. 25985-92.
76. Gasnier, F., et al., *Further evidence for both functional and structural microcompartmentation within the membranes of two associated organelles, mitochondrion and endoplasmic reticulum.* Biochem Biophys Res Commun, 1993. **195**(3): p. 1365-70.
77. Voelker, D.R., *Phosphatidylserine translocation to the mitochondrion is an ATP-dependent process in permeabilized animal cells.* Proc Natl Acad Sci U S A, 1989. **86**(24): p. 9921-5.
78. Achleitner, G., et al., *Synthesis and intracellular transport of aminoglycerophospholipids in permeabilized cells of the yeast, Saccharomyces cerevisiae.* J Biol Chem, 1995. **270**(50): p. 29836-42.
79. Vance, J.E., *Newly made phosphatidylserine and phosphatidylethanolamine are preferentially translocated between rat liver mitochondria and endoplasmic reticulum.* J Biol Chem, 1991. **266**(1): p. 89-97.
80. Achleitner, G., et al., *Association between the endoplasmic reticulum and mitochondria of yeast facilitates interorganelle transport of phospholipids through membrane contact.* Eur J Biochem, 1999. **264**(2): p. 545-53.
81. Hovius, R., et al., *On the mechanism of the mitochondrial decarboxylation of phosphatidylserine.* J Biol Chem, 1992. **267**(24): p. 16790-5.
82. Schumacher, M.M., J.Y. Choi, and D.R. Voelker, *Phosphatidylserine transport to the mitochondria is regulated by ubiquitination.* J Biol Chem, 2002. **277**(52): p. 51033-42.
83. Fisk, H.A. and M.P. Yaffe, *A role for ubiquitination in mitochondrial inheritance in Saccharomyces cerevisiae.* J Cell Biol, 1999. **145**(6): p. 1199-208.
84. Simbeni, R., F. Paltauf, and G. Daum, *Intramitochondrial transfer of phospholipids in the yeast, Saccharomyces cerevisiae.* J Biol Chem, 1990. **265**(1): p. 281-5.
85. Heikinheimo, L. and P. Somerharju, *Preferential decarboxylation of hydrophilic phosphatidylserine species in cultured cells. Implications on the mechanism of transport to mitochondria and cellular aminophospholipid species compositions.* J Biol Chem, 1998. **273**(6): p. 3327-35.
86. Borkenhagen, L.F., E.P. Kennedy, and L. Fielding, *Enzymatic Formation and Decarboxylation of Phosphatidylserine.* Journal of Biological Chemistry, 1961. **236**(6): p. PC28-PC30.

87. Rontein, D., et al., *Mitochondrial phosphatidylserine decarboxylase from higher plants. Functional complementation in yeast, localization in plants, and overexpression in Arabidopsis.* Plant Physiol, 2003. **132**(3): p. 1678-87.
88. Larsson, K.E., B. Nystrom, and C. Liljenberg, *A phosphatidylserine decarboxylase activity in root cells of oat (Avena sativa) is involved in altering membrane phospholipid composition during drought stress acclimation.* Plant Physiol Biochem, 2006. **44**(4): p. 211-9.
89. Hawrot, E. and E.P. Kennedy, *Biogenesis of membrane lipids: mutants of Escherichia coli with temperature-sensitive phosphatidylserine decarboxylase.* Proc Natl Acad Sci U S A, 1975. **72**(3): p. 1112-6.
90. Dennis, E.A. and E.P. Kennedy, *Intracellular sites of lipid synthesis and the biogenesis of mitochondria.* J Lipid Res, 1972. **13**(2): p. 263-7.
91. Dowhan, W., W.T. Wickner, and E.P. Kennedy, *Purification and properties of phosphatidylserine decarboxylase from Escherichia coli.* J Biol Chem, 1974. **249**(10): p. 3079-84.
92. Trotter, P.J., et al., *Phosphatidylserine decarboxylase 2 of Saccharomyces cerevisiae. Cloning and mapping of the gene, heterologous expression, and creation of the null allele.* J Biol Chem, 1995. **270**(11): p. 6071-80.
93. Trotter, P.J. and D.R. Voelker, *Identification of a non-mitochondrial phosphatidylserine decarboxylase activity (PSD2) in the yeast Saccharomyces cerevisiae.* J Biol Chem, 1995. **270**(11): p. 6062-70.
94. Nerlich, A., et al., *Deficiency in phosphatidylserine decarboxylase activity in the psd1 psd2 psd3 triple mutant of Arabidopsis affects phosphatidylethanolamine accumulation in mitochondria.* Plant Physiol, 2007. **144**(2): p. 904-14.
95. Baunaure, F., et al., *Characterization of a non-mitochondrial type I phosphatidylserine decarboxylase in Plasmodium falciparum.* Mol Microbiol, 2004. **51**(1): p. 33-46.
96. Schuiki, I. and G. Daum, *Phosphatidylserine decarboxylases, key enzymes of lipid metabolism.* IUBMB Life, 2009. **61**(2): p. 151-62.
97. Larkin, M.A., et al., *Clustal W and Clustal X version 2.0.* Bioinformatics, 2007. **23**(21): p. 2947-8.
98. Trotter, P.J., J. Pedretti, and D.R. Voelker, *Phosphatidylserine decarboxylase from Saccharomyces cerevisiae. Isolation of mutants, cloning of the gene, and creation of a null allele.* J Biol Chem, 1993. **268**(28): p. 21416-24.
99. Clancey, C.J., S.C. Chang, and W. Dowhan, *Cloning of a gene (PSD1) encoding phosphatidylserine decarboxylase from Saccharomyces cerevisiae by complementation of an Escherichia coli mutant.* J Biol Chem, 1993. **268**(33): p. 24580-90.
100. Kuge, O., M. Nishijima, and Y. Akamatsu, *A cloned gene encoding phosphatidylserine decarboxylase complements the phosphatidylserine biosynthetic defect of a Chinese hamster ovary cell mutant.* J Biol Chem, 1991. **266**(10): p. 6370-6.
101. Snell, E.E., *Pyruvate-containing enzymes.* Trends in Biochemical Sciences, 1977. **2**(6): p. 131-135.
102. van Poelje, P.D. and E.E. Snell, *Pyruvoyl-Dependent Enzymes.* Annual Review of Biochemistry, 1990. **59**(1): p. 29-59.
103. Voelker, D.R., *Phosphatidylserine decarboxylase.* Biochim Biophys Acta, 1997. **1348**(1-2): p. 236-44.
104. Kuge, O., et al., *Post-translational processing of the phosphatidylserine decarboxylase gene product in Chinese hamster ovary cells.* Biochem J, 1996. **319 (Pt 1)**: p. 33-8.
105. Igarashi, K., et al., *A novel phosphatidylserine-binding peptide motif defined by an anti-idiotypic monoclonal antibody. Localization of phosphatidylserine-specific binding sites on protein kinase C and phosphatidylserine decarboxylase.* J Biol Chem, 1995. **270**(49): p. 29075-8.
106. Kitamura, H., W.I. Wu, and D.R. Voelker, *The C2 domain of phosphatidylserine decarboxylase 2 is not required for catalysis but is essential for in vivo function.* J Biol Chem, 2002. **277**(37): p. 33720-6.

107. Li, Q.X. and W. Dowhan, *Studies on the mechanism of formation of the pyruvate prosthetic group of phosphatidylserine decarboxylase from Escherichia coli.* J Biol Chem, 1990. **265**(7): p. 4111-5.
108. Satre, M. and E.P. Kennedy, *Identification of bound pyruvate essential for the activity of phosphatidylserine decarboxylase of Escherichia coli.* J Biol Chem, 1978. **253**(2): p. 479-83.
109. Li, Q.X. and W. Dowhan, *Structural characterization of Escherichia coli phosphatidylserine decarboxylase.* J Biol Chem, 1988. **263**(23): p. 11516-22.
110. Warner, T.G. and E.A. Dennis, *Action of the highly purified, membrane-bound enzyme phosphatidylserine decarboxylase Escherichia coli toward phosphatidylserine in mixed micelles and erythrocyte ghosts in the presence of surfactant.* J Biol Chem, 1975. **250**(20): p. 8004-9.
111. Warner, T.G. and E.A. Dennis, *Phosphatidylserine decarboxylase: analysis of its action towards unsaturated and saturated phosphatidylserine and the effect of Triton X-100 on activity.* Arch Biochem Biophys, 1975. **167**(2): p. 761-8.
112. Kevala, J.H. and H.Y. Kim, *Determination of substrate preference in phosphatidylserine decarboxylation by liquid chromatography-electrospray ionization mass spectrometry.* Anal Biochem, 2001. **292**(1): p. 130-8.
113. Overmeyer, J.H. and C.J. Waechter, *Regulation of phosphatidylserine decarboxylase in Saccharomyces cerevisiae by inositol and choline: kinetics of repression and derepression.* Arch Biochem Biophys, 1991. **290**(2): p. 511-6.
114. Griac, P., *Regulation of yeast phospholipid biosynthetic genes in phosphatidylserine decarboxylase mutants.* J Bacteriol, 1997. **179**(18): p. 5843-8.
115. Burgermeister, M., et al., *Contribution of different pathways to the supply of phosphatidylethanolamine and phosphatidylcholine to mitochondrial membranes of the yeast Saccharomyces cerevisiae.* Biochim Biophys Acta, 2004. **1686**(1-2): p. 161-8.
116. Okada, M., et al., *Cloning, sequencing, and expression in Escherichia coli of the Bacillus subtilis gene for phosphatidylserine synthase.* J Bacteriol, 1994. **176**(24): p. 7456-61.
117. Birner, R., et al., *Roles of phosphatidylethanolamine and of its several biosynthetic pathways in Saccharomyces cerevisiae.* Mol Biol Cell, 2001. **12**(4): p. 997-1007.
118. Gamble, S.C., et al., *Prohibitin, a protein downregulated by androgens, represses androgen receptor activity.* Oncogene, 2007. **26**(12): p. 1757-68.
119. Tatsuta, T., K. Model, and T. Langer, *Formation of membrane-bound ring complexes by prohibitins in mitochondria.* Mol Biol Cell, 2005. **16**(1): p. 248-59.
120. Nebauer, R., et al., *The phosphatidylethanolamine level of yeast mitochondria is affected by the mitochondrial components Oxa1p and Yme1p.* FEBS J, 2007. **274**(23): p. 6180-90.
121. Gulshan, K., et al., *Evidence for the bifunctional nature of mitochondrial phosphatidylserine decarboxylase: role in Pdr3-dependent retrograde regulation of PDR5 expression.* Mol Cell Biol, 2008. **28**(19): p. 5851-64.
122. Shahi, P. and W.S. Moye-Rowley, *Coordinate control of lipid composition and drug transport activities is required for normal multidrug resistance in fungi.* Biochim Biophys Acta, 2009. **1794**(5): p. 852-9.
123. Balzi, E. and A. Goffeau, *Yeast multidrug resistance: the PDR network.* J Bioenerg Biomembr, 1995. **27**(1): p. 71-6.
124. Fullerton, M.D. and M. Bakovic, *Complementation of the metabolic defect in CTP:phosphoethanolamine cytidylyltransferase (Pcyt2)-deficient primary hepatocytes.* Metabolism, 2010.
125. Matsumoto, K., et al., *Cloning, sequencing, and disruption of the Bacillus subtilis psd gene coding for phosphatidylserine decarboxylase.* J Bacteriol, 1998. **180**(1): p. 100-6.
126. Hawrot, E. and E.P. Kennedy, *Phospholipid composition and membrane function in phosphatidylserine decarboxylase mutants of Escherichia coli.* J Biol Chem, 1978. **253**(22): p. 8213-20.
127. DeChavigny, A., P.N. Heacock, and W. Dowhan, *Sequence and inactivation of the pss gene of Escherichia coli. Phosphatidylethanolamine may not be essential for cell viability.* J Biol Chem, 1991. **266**(8): p. 5323-32.

128. Sundler, R., B. Akesson, and A. Nilsson, *Quantitative role of base exchange in phosphatidylethanolamine synthesis in isolated rat hepatocytes.* FEBS Lett, 1974. **43**(3): p. 303-7.
129. Riekhof, W.R. and D.R. Voelker, *Uptake and Utilization of Lyso-phosphatidylethanolamine by Saccharomyces cerevisiae.* Journal of Biological Chemistry, 2006. **281**(48): p. 36588-36596.
130. Stein, Y. and O. Stein, *Metabolism of labeled lysolecithin, lysophosphatidyl ethanolamine and lecithin in the rat.* Biochim Biophys Acta, 1966. **116**(1): p. 95-107.
131. Mathews, C.K., K.E. Van Holde, and K.G. Ahern, *Biochemistry*. 2000, Benjamin Cummings: San Francisco, Calif. p. 523.
132. Scheffler, I.E., *Mitochondria*. 2nd ed. 2008, Hoboken, N.J.: Wiley-Liss. xviii, 462 p., 12 p. of plates.
133. Yadava, N., et al., *Development and characterization of a conditional mitochondrial complex I assembly system.* J Biol Chem, 2004. **279**(13): p. 12406-13.
134. Yadava, N., et al., *Species-specific and mutant MWFE proteins. Their effect on the assembly of a functional mammalian mitochondrial complex I.* J Biol Chem, 2002. **277**(24): p. 21221-30.
135. Scheffler, I.E., N. Yadava, and P. Potluri, *Molecular genetics of complex I-deficient Chinese hamster cell lines.* Biochim Biophys Acta, 2004. **1659**(2-3): p. 160-71.
136. Friedrich, T., et al., *Redox components and structure of the respiratory NADH:ubiquinone oxidoreductase (complex I).* Biochim Biophys Acta, 1998. **1365**(1-2): p. 215-9.
137. Grigorieff, N., *Three-dimensional structure of bovine NADH:ubiquinone oxidoreductase (complex I) at 22 A in ice.* J Mol Biol, 1998. **277**(5): p. 1033-46.
138. Guenebaut, V., et al., *Consistent structure between bacterial and mitochondrial NADH:ubiquinone oxidoreductase (complex I).* J Mol Biol, 1998. **276**(1): p. 105-12.
139. Scheffler, I.E., *Molecular genetics of succinate:quinone oxidoreductase in eukaryotes.* Prog Nucleic Acid Res Mol Biol, 1998. **60**: p. 267-315.
140. Yankovskaya, V., et al., *Architecture of succinate dehydrogenase and reactive oxygen species generation.* Science, 2003. **299**(5607): p. 700-4.
141. Blaut, M., et al., *Fumarate reductase mutants of Escherichia coli that lack covalently bound flavin.* J Biol Chem, 1989. **264**(23): p. 13599-604.
142. Elbehti-Green, A., et al., *Characterization of the human SDHC gene encoding of the integral membrane proteins of succinate-quinone oxidoreductase in mitochondria.* Gene, 1998. **213**(1-2): p. 133-40.
143. Ditta, G., K. Soderberg, and I.E. Scheffler, *Chinese hamster cell mutant with defective mitochondrial protein synthesis.* Nature, 1977. **268**(5615): p. 64-7.
144. Soderberg, K.L., G.S. Ditta, and I.E. Scheffler, *Mammalian cells with defective mitochondrial functions: a Chinese hamster mutant cell line lacking succinate dehydrogenase activity.* Cell, 1977. **10**(4): p. 697-702.
145. Ozawa, T., M. Tanaka, and Y. Shimomura, *Crystallization of cytochrome bc1 complex.* Proc Natl Acad Sci U S A, 1983. **80**(4): p. 921-5.
146. Steffens, G. and G. Buse, *[Studies on cytochrome c oxidase, I. Purification and characterization of bovine myocardial enzyme and identification of peptide chains in the complex]*. Hoppe Seylers Z Physiol Chem, 1976. **357**(8): p. 1125-37.
147. Lenaz, G. and M.L. Genova, *Structure and organization of mitochondrial respiratory complexes: a new understanding of an old subject.* Antioxid Redox Signal, 2010. **12**(8): p. 961-1008.
148. Fry, M. and D.E. Green, *Cardiolipin requirement for electron transfer in complex I and III of the mitochondrial respiratory chain.* J Biol Chem, 1981. **256**(4): p. 1874-80.
149. Gomez, B., Jr. and N.C. Robinson, *Phospholipase digestion of bound cardiolipin reversibly inactivates bovine cytochrome bc1.* Biochemistry, 1999. **38**(28): p. 9031-8.
150. Mitchell, D.M., et al., *Site-directed mutagenesis of residues lining a putative proton transfer pathway in cytochrome c oxidase from Rhodobacter sphaeroides.* Biochemistry, 1996. **35**(40): p. 13089-93.

151. Ferguson-Miller, S., *Mammalian cytochrome c oxidase, a molecular monster subdued.* Science, 1996. **272**(5265): p. 1125.
152. Tsukihara, T., et al., *Structures of metal sites of oxidized bovine heart cytochrome c oxidase at 2.8 A.* Science, 1995. **269**(5227): p. 1069-74.
153. Diaz, F., *Cytochrome c oxidase deficiency: patients and animal models.* Biochim Biophys Acta, 2010. **1802**(1): p. 100-10.
154. Siletsky, S.A., et al., *Time-resolved O(H)-->E(H) transition of the aberrant ba(3) oxidase from Thermus thermophilus.* Biochim Biophys Acta, 2009.
155. Paradies, G., G. Petrosillo, and F.M. Ruggiero, *Cardiolipin-dependent decrease of cytochrome c oxidase activity in heart mitochondria from hypothyroid rats.* Biochim Biophys Acta, 1997. **1319**(1): p. 5-8.
156. Robinson, N.C., J. Zborowski, and L.H. Talbert, *Cardiolipin-depleted bovine heart cytochrome c oxidase: binding stoichiometry and affinity for cardiolipin derivatives.* Biochemistry, 1990. **29**(38): p. 8962-9.
157. Shinzawa-Itoh, K., et al., *Structures and physiological roles of 13 integral lipids of bovine heart cytochrome c oxidase.* EMBO J, 2007. **26**(6): p. 1713-25.
158. Leigh, D., *Subacute necrotizing encephalomyelopathy in an infant.* J Neurol Neurosurg Psychiatry, 1951. **14**(3): p. 216-21.
159. Antonicka, H., et al., *Identification and characterization of a common set of complex I assembly intermediates in mitochondria from patients with complex I deficiency.* J Biol Chem, 2003. **278**(44): p. 43081-8.
160. Antonicka, H., et al., *Mutations in COX10 result in a defect in mitochondrial heme A biosynthesis and account for multiple, early-onset clinical phenotypes associated with isolated COX deficiency.* Hum Mol Genet, 2003. **12**(20): p. 2693-702.
161. Merante, F., et al., *A biochemically distinct form of cytochrome oxidase (COX) deficiency in the Saguenay-Lac-Saint-Jean region of Quebec.* Am J Hum Genet, 1993. **53**(2): p. 481-7.
162. Hatefi, Y., et al., *Proteins, polypeptides, prosthetic groups, and enzymic properties of complexes I, II, III, IV, and V of the mitochondrial oxidative phosphorylation system.* Methods Enzymol, 1979. **56**: p. 577-602.
163. Stiggall, D.L., Y.M. Galante, and Y. Hatefi, *Preparation and properties of complex V.* Methods Enzymol, 1979. **55**: p. 308-15, 819-21.
164. Mathews, C.K., K.E. Van Holde, and K.G. Ahern, *Biochemistry*. 3rd ed. 2000, San Francisco, Calif.: Benjamin Cummings. xxviii, 1186 p.
165. Zhou, Y., T.M. Duncan, and R.L. Cross, *Subunit rotation in Escherichia coli FoF1-ATP synthase during oxidative phosphorylation.* Proc Natl Acad Sci U S A, 1997. **94**(20): p. 10583-7.
166. Mannella, C.A., *Structure and dynamics of the mitochondrial inner membrane cristae.* Biochim Biophys Acta, 2006. **1763**(5-6): p. 542-8.
167. Mannella, C.A., *The relevance of mitochondrial membrane topology to mitochondrial function.* Biochim Biophys Acta, 2006. **1762**(2): p. 140-7.
168. Strauss, M., et al., *Dimer ribbons of ATP synthase shape the inner mitochondrial membrane.* EMBO J, 2008. **27**(7): p. 1154-60.
169. Khalifat, N., et al., *Membrane deformation under local pH gradient: mimicking mitochondrial cristae dynamics.* Biophys J, 2008. **95**(10): p. 4924-33.
170. Mileykovskaya, E. and W. Dowhan, *Cardiolipin membrane domains in prokaryotes and eukaryotes.* Biochim Biophys Acta, 2009. **1788**(10): p. 2084-91.
171. Boyer, P.D., *A research journey with ATP synthase.* J Biol Chem, 2002. **277**(42): p. 39045-61.
172. Lardy, H.A. and H. Wellman, *Oxidative phosphorylations; role of inorganic phosphate and acceptor systems in control of metabolic rates.* J Biol Chem, 1952. **195**(1): p. 215-24.
173. Chance, B. and G.R. Williams, *Respiratory enzymes in oxidative phosphorylation. I. Kinetics of oxygen utilization.* J Biol Chem, 1955. **217**(1): p. 383-93.
174. Bonnet, S., et al., *A mitochondria-K+ channel axis is suppressed in cancer and its normalization promotes apoptosis and inhibits cancer growth.* Cancer Cell, 2007. **11**(1): p. 37-51.

175. Warburg, O., *On respiratory impairment in cancer cells.* Science, 1956. **124**(3215): p. 269-70.
176. Warburg, O., *On the origin of cancer cells.* Science, 1956. **123**(3191): p. 309-14.
177. Warburg, O., F. Wind, and E. Negelein, *The Metabolism of Tumors in the Body.* J Gen Physiol, 1927. **8**(6): p. 519-30.
178. Gatenby, R.A. and R.J. Gillies, *Why do cancers have high aerobic glycolysis?* Nat Rev Cancer, 2004. **4**(11): p. 891-9.
179. Gillies, R.J., et al., *pH imaging. A review of pH measurement methods and applications in cancers.* IEEE Eng Med Biol Mag, 2004. **23**(5): p. 57-64.
180. Gatenby, R.A. and B.R. Frieden, *Information dynamics in carcinogenesis and tumor growth.* Mutat Res, 2004. **568**(2): p. 259-73.
181. Plas, D.R. and C.B. Thompson, *Cell metabolism in the regulation of programmed cell death.* Trends Endocrinol Metab, 2002. **13**(2): p. 75-8.
182. Kim, J.W. and C.V. Dang, *Multifaceted roles of glycolytic enzymes.* Trends Biochem Sci, 2005. **30**(3): p. 142-50.
183. Elstrom, R.L., et al., *Akt stimulates aerobic glycolysis in cancer cells.* Cancer Res, 2004. **64**(11): p. 3892-9.
184. Roche, T.E. and Y. Hiromasa, *Pyruvate dehydrogenase kinase regulatory mechanisms and inhibition in treating diabetes, heart ischemia, and cancer.* Cell Mol Life Sci, 2007. **64**(7-8): p. 830-49.
185. Michelakis, E.D., L. Webster, and J.R. Mackey, *Dichloroacetate (DCA) as a potential metabolic-targeting therapy for cancer.* Br J Cancer, 2008. **99**(7): p. 989-94.
186. Archer, S.L., et al., *Preferential expression and function of voltage-gated, O2-sensitive K+ channels in resistance pulmonary arteries explains regional heterogeneity in hypoxic pulmonary vasoconstriction: ionic diversity in smooth muscle cells.* Circ Res, 2004. **95**(3): p. 308-18.
187. Clapham, D.E., *Calcium signaling.* Cell, 1995. **80**(2): p. 259-68.
188. Carafoli, E., et al., *Generation, control, and processing of cellular calcium signals.* Crit Rev Biochem Mol Biol, 2001. **36**(2): p. 107-260.
189. Tovey, S.C., et al., *Calcium-modulating cyclophilin ligand desensitizes hormone-evoked calcium release.* Biochem Biophys Res Commun, 2000. **276**(1): p. 97-100.
190. Gunter, T.E., et al., *Calcium and mitochondria.* FEBS Lett, 2004. **567**(1): p. 96-102.
191. Gunter, T.E., et al., *The Ca2+ transport mechanisms of mitochondria and Ca2+ uptake from physiological-type Ca2+ transients.* Biochim Biophys Acta, 1998. **1366**(1-2): p. 5-15.
192. Smaili, S.S., et al., *Mitochondria in Ca2+ signaling and apoptosis.* J Bioenerg Biomembr, 2000. **32**(1): p. 35-46.
193. Ichas, F., et al., *Mitochondrial calcium spiking: a transduction mechanism based on calcium-induced permeability transition involved in cell calcium signalling.* FEBS Lett, 1994. **348**(2): p. 211-5.
194. Armstrong, J.S., *Mitochondrial membrane permeabilization: the sine qua non for cell death.* Bioessays, 2006. **28**(3): p. 253-60.
195. Green, D.R. and J.C. Reed, *Mitochondria and apoptosis.* Science, 1998. **281**(5381): p. 1309-12.
196. Andreyev, A.Y., B. Fahy, and G. Fiskum, *Cytochrome c release from brain mitochondria is independent of the mitochondrial permeability transition.* FEBS Lett, 1998. **439**(3): p. 373-6.
197. Jurgensmeier, J.M., et al., *Bax directly induces release of cytochrome c from isolated mitochondria.* Proc Natl Acad Sci U S A, 1998. **95**(9): p. 4997-5002.
198. Izzotti, A., A. Bagnis, and S.C. Sacca, *The role of oxidative stress in glaucoma.* Mutat Res, 2006. **612**(2): p. 105-14.
199. Lin, M.T. and M.F. Beal, *Mitochondrial dysfunction and oxidative stress in neurodegenerative diseases.* Nature, 2006. **443**(7113): p. 787-95.
200. Rohdich, F., et al., *Studies on the nonmevalonate terpene biosynthetic pathway: metabolic role of IspH (LytB) protein.* Proc Natl Acad Sci U S A, 2002. **99**(3): p. 1158-63.

201. Vance, J.E., *Molecular and cell biology of phosphatidylserine and phosphatidylethanolamine metabolism.* Prog Nucleic Acid Res Mol Biol, 2003. **75**: p. 69-111.
202. Voelker, D.R., *Bridging gaps in phospholipid transport.* Trends Biochem Sci, 2005. **30**(7): p. 396-404.
203. Rizzuto, R., M.R. Duchen, and T. Pozzan, *Flirting in little space: the ER/mitochondria Ca2+ liaison.* Sci STKE, 2004. **2004**(215): p. re1.
204. Sharma, K., et al., *Involvement of transforming growth factor-beta in regulation of calcium transients in diabetic vascular smooth muscle cells.* Am J Physiol Renal Physiol, 2003. **285**(6): p. F1258-70.
205. Csordas, G., et al., *Structural and functional features and significance of the physical linkage between ER and mitochondria.* J Cell Biol, 2006. **174**(7): p. 915-21.
206. Soltys, B.J. and R.S. Gupta, *Interrelationships of endoplasmic reticulum, mitochondria, intermediate filaments, and microtubules--a quadruple fluorescence labeling study.* Biochem Cell Biol, 1992. **70**(10-11): p. 1174-86.
207. Wang, H.J., et al., *Calcium regulates the association between mitochondria and a smooth subdomain of the endoplasmic reticulum.* J Cell Biol, 2000. **150**(6): p. 1489-98.
208. Mikoshiba, K., *The IP3 receptor/Ca2+ channel and its cellular function.* Biochem Soc Symp, 2007(74): p. 9-22.
209. Duchen, M.R., *Ca(2+)-dependent changes in the mitochondrial energetics in single dissociated mouse sensory neurons.* Biochem J, 1992. **283 (Pt 1)**: p. 41-50.
210. Simmen, T., et al., *PACS-2 controls endoplasmic reticulum-mitochondria communication and Bid-mediated apoptosis.* EMBO J, 2005. **24**(4): p. 717-29.
211. Hayashi, T., et al., *MAM: more than just a housekeeper.* Trends Cell Biol, 2009. **19**(2): p. 81-8.
212. Mannella, C.A., M. Marko, and K. Buttle, *Reconsidering mitochondrial structure: new views of an old organelle.* Trends Biochem Sci, 1997. **22**(2): p. 37-8.
213. Frey, T.G. and C.A. Mannella, *The internal structure of mitochondria.* Trends Biochem Sci, 2000. **25**(7): p. 319-24.
214. Okamoto, K. and J.M. Shaw, *Mitochondrial morphology and dynamics in yeast and multicellular eukaryotes.* Annu Rev Genet, 2005. **39**: p. 503-36.
215. Bleazard, W., et al., *The dynamin-related GTPase Dnm1 regulates mitochondrial fission in yeast.* Nat Cell Biol, 1999. **1**(5): p. 298-304.
216. Kelly, R.B., *Endocytosis. Ringing necks with dynamin.* Nature, 1995. **374**(6518): p. 116-7.
217. Schrader, M., *Shared components of mitochondrial and peroxisomal division.* Biochim Biophys Acta, 2006. **1763**(5-6): p. 531-41.
218. Song, B.D. and S.L. Schmid, *A molecular motor or a regulator? Dynamin's in a class of its own.* Biochemistry, 2003. **42**(6): p. 1369-76.
219. Pucadyil, T.J. and S.L. Schmid, *Real-time visualization of dynamin-catalyzed membrane fission and vesicle release.* Cell, 2008. **135**(7): p. 1263-75.
220. Cereghetti, G.M., et al., *Dephosphorylation by calcineurin regulates translocation of Drp1 to mitochondria.* Proc Natl Acad Sci U S A, 2008. **105**(41): p. 15803-8.
221. Harder, Z., R. Zunino, and H. McBride, *Sumo1 conjugates mitochondrial substrates and participates in mitochondrial fission.* Curr Biol, 2004. **14**(4): p. 340-5.
222. Ishihara, N., et al., *Regulation of mitochondrial morphology by membrane potential, and DRP1-dependent division and FZO1-dependent fusion reaction in mammalian cells.* Biochem Biophys Res Commun, 2003. **301**(4): p. 891-8.
223. Eura, Y., et al., *Two mitofusin proteins, mammalian homologues of FZO, with distinct functions are both required for mitochondrial fusion.* J Biochem, 2003. **134**(3): p. 333-44.
224. Amutha, B., et al., *A novel role of Mgm1p, a dynamin-related GTPase, in ATP synthase assembly and cristae formation/maintenance.* Biochem J, 2004. **381**(Pt 1): p. 19-23.
225. Delettre, C., et al., *Nuclear gene OPA1, encoding a mitochondrial dynamin-related protein, is mutated in dominant optic atrophy.* Nat Genet, 2000. **26**(2): p. 207-10.

226. Ishihara, N., Y. Eura, and K. Mihara, *Mitofusin 1 and 2 play distinct roles in mitochondrial fusion reactions via GTPase activity.* J Cell Sci, 2004. **117**(Pt 26): p. 6535-46.
227. Spinazzi, M., et al., *A novel deletion in the GTPase domain of OPA1 causes defects in mitochondrial morphology and distribution, but not in function.* Hum Mol Genet, 2008. **17**(21): p. 3291-302.
228. Olichon, A., et al., *Loss of OPA1 perturbates the mitochondrial inner membrane structure and integrity, leading to cytochrome c release and apoptosis.* J Biol Chem, 2003. **278**(10): p. 7743-6.
229. Bereiter-Hahn, J., *Behavior of mitochondria in the living cell.* Int Rev Cytol, 1990. **122**: p. 1-63.
230. Chen, H. and D.C. Chan, *Critical dependence of neurons on mitochondrial dynamics.* Curr Opin Cell Biol, 2006. **18**(4): p. 453-9.
231. Bereiter-Hahn, J. and M. Voth, *Dynamics of mitochondria in living cells: shape changes, dislocations, fusion, and fission of mitochondria.* Microsc Res Tech, 1994. **27**(3): p. 198-219.
232. Pathak, D., K.J. Sepp, and P.J. Hollenbeck, *Evidence that Myosin activity opposes microtubule-based axonal transport of mitochondria.* J Neurosci, 2010. **30**(26): p. 8984-92.
233. Hollenbeck, P.J. and W.M. Saxton, *The axonal transport of mitochondria.* J Cell Sci, 2005. **118**(Pt 23): p. 5411-9.
234. Chada, S.R. and P.J. Hollenbeck, *Mitochondrial movement and positioning in axons: the role of growth factor signaling.* J Exp Biol, 2003. **206**(Pt 12): p. 1985-92.
235. Hollenbeck, P.J., *The pattern and mechanism of mitochondrial transport in axons.* Front Biosci, 1996. **1**: p. d91-102.
236. Morris, R.L. and P.J. Hollenbeck, *Axonal transport of mitochondria along microtubules and F-actin in living vertebrate neurons.* J Cell Biol, 1995. **131**(5): p. 1315-26.
237. Miller, K.E. and M.P. Sheetz, *Axonal mitochondrial transport and potential are correlated.* J Cell Sci, 2004. **117**(Pt 13): p. 2791-804.
238. Amarzguioui, M., J.J. Rossi, and D. Kim, *Approaches for chemically synthesized siRNA and vector-mediated RNAi.* FEBS Lett, 2005. **579**(26): p. 5974-81.
239. Rio, D.C., et al., *Purification of RNA using TRIzol (TRI reagent).* Cold Spring Harb Protoc, 2010. **2010**(6): p. pdb prot5439.
240. German, C.L. and C.L. Howe, *Preparation of biologically active subcellular fractions using the Balch homogenizer.* Anal Biochem, 2009. **394**(1): p. 117-24.
241. Croze, E.M. and D.J. Morre, *Isolation of plasma membrane, golgi apparatus, and endoplasmic reticulum fractions from single homogenates of mouse liver.* J Cell Physiol, 1984. **119**(1): p. 46-57.
242. Smith, L., *Spectrophotometric assay of cytochrome c oxidase.* Methods Biochem Anal, 1955. **2**: p. 427-34.
243. Smith, P.K., et al., *Measurement of protein using bicinchoninic acid.* Anal Biochem, 1985. **150**(1): p. 76-85.
244. Folch, J., M. Lees, and G.H. Sloane Stanley, *A simple method for the isolation and purification of total lipides from animal tissues.* J Biol Chem, 1957. **226**(1): p. 497-509.
245. Rouser, G., A.N. Siakotos, and S. Fleischer, *Quantitative analysis of phospholipids by thin-layer chromatography and phosphorus analysis of spots.* Lipids, 1966. **1**(1): p. 85-6.
246. Stanley, P.E., *Extraction of adenosine triphosphate from microbial and somatic cells.* Methods Enzymol, 1986. **133**: p. 14-22.
247. Gunter, T.E., et al., *The interaction of mitochondria with pulses of calcium.* Biofactors, 1998. **8**(3-4): p. 205-7.